SIMULATION AND ANALYSIS OF MATRIX CONVERTER

A DISSERTATION

Submitted in partial fulfillment of the requirements for the award of the degree of

MASTER OF TECHNOLOGY

in

ELECTRICAL ENGINEERING

(With Specialization in Power Apparatus and Electric Drives)

By

MITESHKUMAR NANDLAL POPAT

DEPARTMENT OF ELECTRICAL ENGINEERING
INDIAN INSTITUTE OF TECHNOLOGY ROORKEE
ROORKEE-247 667 (INDIA)

JUNE, 2006

ID NO. MT-321|2006-16|MNP-PA

Candidate's Declaration

I here by declare that the work which is being presented in the Dissertation Thesis entitled **"Simulation and Analysis of Matrix Converter"** in partial fulfillment of the requirements for the award of the degree **Master of Technology** in **Electrical Engineering** with specialization in **Power Apparatus and Electric Drives,** submitted in the **Department of Electrical Engineering, Indian Institute of Technology, Roorkee, India – 247 667.** This is an authentic record of my own work carried out in the period of last two semesters from Aug 2005 to May 2006, under the supervision of **Dr. Pramod Agarwal,** Professor, Department of Electrical Engineering, Indian Institute of Technology, Roorkee, INDIA – 247 667.

The matter embodied in this Dissertation Thesis has not been submitted by me for the award of any other degree or diploma.

Date: 22|06|2006

Place: Roorkee

(Miteshkumar Nandlal Popat)

This is to certify that the above statements made by the candidate are correct to the best of my knowledge.

(Dr. Pramod Agarwal)

Professor,
Department of Electrical Engineering
Indian Institute of Technology,
Roorkee-247 667,
India.

Acknowledgement

I wish to place on record my deep sense of gratitude and in debt ness to my guide **Dr. Pramod Agarwal**, Professor, Department of Electrical Engineering, Indian Institute of Technology Roorkee, Roorkee for his whole heartedness and high dedication with which he involved in this work. I am grateful for hours he spent in discussing and explaining even the minute details of the work in spite of their hectic schedule of work in the department. He listened patiently and authoritatively as they guided me and made their valuable suggestions.

I am very much thankful to **Dr. S. P. Gupta**, Professor and Head, Department of Electrical Engineering, IIT Roorkee for providing me all the support and facilities during my work.

I am grateful to all my teachers of the PAED group for their suggestions and constant encouragement. I am also grateful to all Research Scholars of the PAED group for their suggestions and constant encouragement.

Timely assistance and help from the laboratory staff of Drives Lab, Stores, and Workshop is sincerely acknowledged.

I gratefully acknowledge my sincere thanks to all my family members and friends for their inspirational impetus and moral support during the course of this work. I owe everything to them.

Finally, I would like express my deepest gratitude to God for His blessings.

Abstract

Power electronics is an emerging technology. New power circuits are invented and have to be introduced into the power electronics curriculum. One of the interesting new circuits is the matrix converter. The matrix converter is an array of controlled semiconductor switches that connects directly the three-phase source to the three-phase load without using any DC link or large energy storage elements, and therefore it is called the all-silicon solution. This converter has several attractive features such as: sinusoidal input and output currents, operation with unity power factor for any load, regeneration capability. In the last few years, an increase in research work has been observed, bringing this topology closer to the industrial application.

There are various control strategies used for matrix converter like venturini modulation method, space vector modulation scheme and indirect modulation method. In this thesis the 3-phase to 3-phase matrix converter is implemented using venturini modulation method. A Simulation model of 3-phase to 3-phase matrix converter is developed in MATLAB simulink. A prototype model of 3-phase to 3-phase Matrix converter is designed and developed in the laboratory for experimentation purpose. Both simulation and experimental results are presented. Venturini control scheme is implemented through programming. The complete program has been explained through flow charts and implemented on Pentium MMX Processor based PC using interfacing cards. The program is written in 'C-Language'.

List of Figures

Contents

Chapter-1

Introduction

1.1 AC / AC Conversion

Many parts of industrial application request ac/ac power conversion and ac/ac converter take power from one ac system and deliver it to another with waveforms of different amplitude and frequency. The ac/ac converters are commonly classified into indirect converter which utilizes a dc link between the two ac systems and direct converter that provides direct conversion. Indirect converter consists of two converter stages and energy storage element, which convert input ac to dc and then reconverting dc back to output ac with variable amplitude and frequency as shown in *fig.1.1*. The operation of these converter stages is decoupled on an instantaneous basis by means of energy storage element and controlled independently, so long as the average energy flow is equal. Therefore, the instantaneous power flow does not have to equal the instantaneous power output. The difference between the instantaneous input and output power must be absorbed or delivered by an energy storage element within the converter. The energy storage element can be either a capacitor or an inductor.

However, the energy storage element is not needed in direct converter as shown in *fig.1.2*. In General, direct converter can be identified as three distinct topological approaches. The first and simplest topology can be used to change the amplitude of an ac waveform. It is known as an ac controller and functions by simply chopping symmetric notches out of the input waveform. The second can be utilized if the output frequency is much lower than input source frequency. This topology is called a cycloconverter, and it approximates the desired output waveform by synthesizing it from piece of the input waveform.

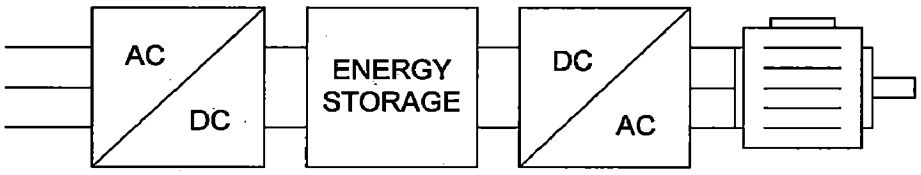

Figure 1.1: Indirect ac / ac converter

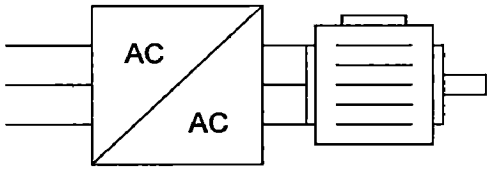

Figure 1.2: Direct ac / ac converter

1.2 Cycloconverter

In a cycloconverter, the ac power at one frequency is converted directly to an ac power at another frequency without any intermediate dc stage. The technique of cycloconversion was known in Germany in the 1930's, when Mercury-arc rectifiers were used to convert power from 50 Hz to 16-2/3 Hz for railway transportation. After the development of thyristors in the late 1950's, the first new cycloconverter applications were in the variable speed constant-frequency supply systems for aircraft. The variable-frequency induction motor drives were the next important applications.

Naturally commutated cycloconverters have limitations on output frequency range, input power factor, and distortion of input and output waveforms. An ac-ac matrix converter can overcome many of these limitations. The matrix converter can provide increased output frequency range and low distortion of input and output currents.

1.3 Matrix Converter

One of the most interesting families of ac/ac converters is that of the so-called matrix converters. The matrix converter is an array of bidirectional switches functioning as the main power elements. It interconnects directly the three-phase power supply to a three phase load, without using any DC link or large energy storage elements, and therefore it is called the all-silicon solution. The most important characteristics of the matrix converter are: (1) simple and compact power circuit; (2) generation of load voltage with arbitrary amplitude and frequency; (3) sinusoidal input and output currents; (4) operation with unity power factor; and (5) regeneration capability. These highly attractive characteristics are the reason for the present tremendous interest in this topology. The real development of matrix converters starts with the work of Venturini and Alesina published in 1980 [3], [4]. They presented the power circuit of the converter as a matrix of bidirectional power switches and they introduced the name "matrix converter." One of their main contributions is the development of a rigorous mathematical analysis to describe the low-frequency behavior of

the converter, introducing the "low-frequency modulation matrix" concept. In their modulation method, also known as the direct transfer function approach [28], the output voltages are obtained by the multiplication of the modulation (also called transfer) matrix with the input voltages.

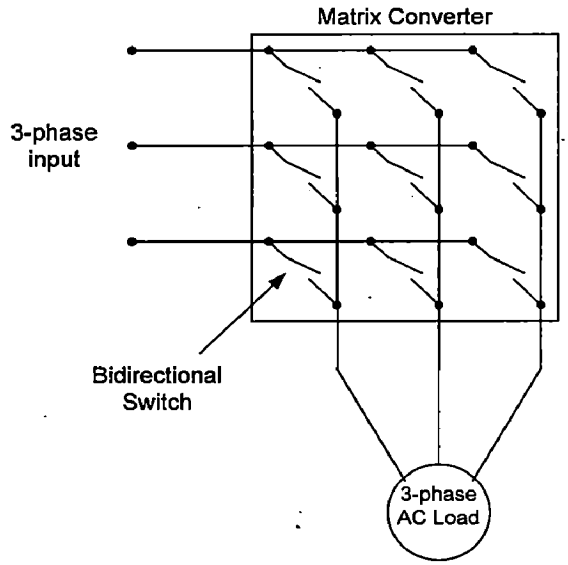

Figure 1.3: Three phase to three phase matrix converter

1.4 Literature Survey

The key element in a matrix converter is the fully controlled four-quadrant bidirectional switch, which allows high-frequency operation. The early work dedicated to unrestricted frequency changers used thyristors with external forced commutation circuits to implement the bidirectional controlled switch [1]. With this solution, the power circuit was bulky and the performance was poor. The introduction of power transistors for implementing the bidirectional switches made the matrix converter topology more attractive [2].

The Real development of this converter starts with the early work of Venturini and Alesina [3],[4]. They presented the power circuit of the converter as a matrix of bidirectional power switches and they introduced the name 'matrix converter'. Another major contribution of these authors is the development of a rigorous mathematical analysis to describe the low frequency behavior of the converter. In their modulation method, also known as the direct transfer function approach, the output voltages are obtained by the multiplication of the modulation matrix with the input voltages.

A conceptually different control technique based on the "fictitious dc link" idea was introduced by Rodriguez in 1983 [5]. In this method, the switching is arranged so that each output line is switched between the most positive and most negative input lines using a pulse width modulation (PWM) technique, as conventionally used in standard voltage-source inverters (VSIs). This concept is also known as the "indirect transfer function" approach [6].

In 1985–1986, Ziogas *et al.* published [7] and [8], which expanded on the "fictitious dc link" idea of Rodriguez and provided a rigorous mathematical explanation. In 1983, Braun [9], introduced the use of space vectors in the analysis and control of matrix converters.

In 1989, Huber *et al.* Published the first of a series of papers [10]-[14] in which Analysis, design, and implementation of the space vector modulated three-phase to three-phase matrix converter with input power factor correction are presented. The majority of published research results on the matrix converter control is given an overview, and the one, which employs simultaneous output-voltage and input-current space vector modulation, is systematically reviewed. The modulation algorithm is theoretically derived from the desired average transfer functions, using the indirect transfer function approach. The algorithm is verified through implementation of a 2-kVA experimental matrix converter driving a standard induction motor as a load. The switching frequency is 20 kHz. The modulator is implemented with a digital signal processor. The resultant output voltages and input currents are sinusoidal, practically without low-frequency harmonics. The input power factor is above 0.99 in the whole operating range.

It was experimentally confirmed by Neft and Schauder in 1992 [15] that a matrix converter with only nine switches can be effectively used in the vector control of an induction motor with high quality input and output currents. However, the simultaneous commutation of controlled bidirectional switches used in matrix converters is very difficult to achieve without generating over current or over voltage spikes that can destroy the power semiconductors. This fact limited the practical implementation and negatively affected the interest in matrix converters. Fortunately, this major problem has been solved with the development of several multistep commutation strategies that allow safe operation of the switches.

In 1989, Burany [16] introduced the later-named "semi-soft current commutation" technique. In this paper a radical solution for the commutation problem is proposed. The solution concerns four quadrant switches (4QSWs) where separated internal conduction

paths exist in the two possible directions of the load current. It is shown that the switching of these conduction paths must not be simultaneous but has to take place in the well defined four-stepped switching order. The actual switching policy depends on the direction of the commutated current. The given description deals mainly with the switching policy for two 4QSWs. Some hints for the extension of the switching policy for general polyphase matrix converter schemes are given.

Clare and wheeler published the papers [17],[18]. This paper deals with the problem of snubberless commutation in matrix converters. A novel method employs current detection within intelligent gate drive circuits for each bidirectional cell which communicate with the gate drives of other cells. The problems with other methods at low currents are overcome. Experimental results verifying the method are presented. Other interesting commutation strategies were introduced by Ziegler *et al.* [19], [20].

P. Nielsen, F. Blaabjerg, J. K. Pedersen, in their publication titled [21], "Novel solution for protection of matrix converter to three phase induction machine", presents the design of snubber/clamp circuit protection for a matrix converter for induction motor and it will propose two new component minimized protection circuits which have half the number of diodes.

J. Mahlein, M. Braun, in their publication titled [22], "A matrix converter without diode clamped over-voltage protection" presents the design and testing of a new protection strategy for a matrix converter feeding an induction motor is described. The new protection strategy with excellent over-voltage protection allows to remove the large and expensive diode clamp

C. Klumpner, P. Nielsen, I. Boldea, F. Blaabjerg, in their publication titled [23], "New steps towards a low cost power electronic building block for matrix converters" analyzes some aspects of integrating the matrix converter bi-directional switches into a power module. The analysis produces two optimal topologies for a power module: one for low-power and another for high-power matrix converters. The configuration of a power electronic building block for matrix converters is proposed. This includes the commutation control logic and the over current protection, provides safe-operation and eliminates the problem of operating with bi-directional switches. A new power module topology for a low power three-phase to three-phase matrix converter is proposed. By using the bootstrap circuits to feed the gate-drivers, the proposed configuration requires only three insulated power supplies. A new input filter topology is proposed, using only two choke cores and providing the size reduction. The experimental results validate the solution by comparing

the input current waveforms with the standard configuration. The two proposals constitute a solution recommended in the low power range, where low-cost and low-volume are the main objectives.

J. K. Kang, H. Hara., E. Yamamoto, E. Watanabe, A. M. Hava, and T. J. Kume, in their publication titled [24] "The matrix converter drive performance under abnormal input voltage conditions", presents, the behavior of the matrix converter drive under abnormal input line voltage conditions has been investigated. A technique to eliminate the input current distortion due to the input voltage unbalance has been developed and its feasibility proven via computer simulations and laboratory experiments. The power line failure behavior has also been investigated and the rapid re-starting capability of the matrix converter drive has been demonstrated via laboratory experiments.

P. Wheeler, H. Zhang, D. A. Grant, in their publication titled [25] "A theoretical and practical consideration of optimized input filter design for a low loss matrix converter" presents the problems associated with input current filtering to comply with existing and possible future European EMC regulations are investigated. The paper compares disturbance voltage results from mathematical theory, computer simulation, and practical measurements from a power level converter under microprocessor control. Possible designs for an input filter to meet the European standards are considered. The relationship between the converter switching frequency and the cost of the input filter is explored.

Watthanasarn C., Zhang L, D T W Liang, in their publication titled [26] "Analysis and DSP based Implementation Modulation Algorithms for AC-AC Matrix converters" presents comparison of two control strategies for direct AC-AC matrix converters: namely, the Venturini method and the space vector modulation (SVM) method. The relative performances is made with regard to operation under unbalanced/distorted supply voltage, output voltage and input current harmonics, and converter losses.

P.Wheeler, J.Rodri guez, J. Clare, L. Empringham and A. Weinstein in their publication titled [27] " Matrix Converters: A technology review" presents the state-of-the-art view in the development of this converter, starting with a brief historical review. An important part of the paper is dedicated to a discussion of the most important modulation and control strategies developed recently.Special attention is given to present modern methods developed to solve the commutation problem.

J. Rodriguez, E. Silva, F. Blaabjerg, P. Wheeler, J. Clare and J. Pontt, in their publication titled [28] "Matrix converter controlled with the direct transfer function approach: analysis, modelling and simulation" presents the working principle of the Matrix

Converter controlled with the direct transfer function approach. The modulation strategy and the most important equations are clearly presented.

1.5 Dissertation Outline

The contents of this dissertation are organized in six chapters in the following manner. Chapter 1 introduces ac/ac conversion and matrix converter as an advanced direct ac/ac converter. Then, a review of the previous work in the area of matrix converter is addressed.

In Chapter 2, The working principle of matrix converter is explained in initial section. The practical implementation of bidirectional switches for matrix converter is explained. Various Current commutation methods for Reliable current commutation between switches in the matrix converter are discussed. In last section, some practical issues related to the practical application of this technology, like over voltage protection, input filter and semiconductor losses are discussed.

Chapter 3 presents different modulation strategy like Venturini modulation method, Space vector modulation scheme and Indirect modulation method for the matrix converter.

In Chapter 4, a simulation model of 3-phase to 3-phase matrix converter using venturini modulation method is developed in MATLAB simulink. Simulation results are obtained for different output frequencies with R-L load. Simulation studies carried out by suddenly changing ouptput frequency.

Chapter 5 presents hardware requirement for the realization of the 3-phase to 3-phase matrix converter and hardware circuits are explained in detail. In software development section flow charts and PC interfacing with hardware are discussed briefly.

Chapter 6 presents experimental results carried out on prototype 3-phase to 3-phase matrix converter developed in laboratory. Firing pulses to MOSFETs, output voltage at different frequencies and their FFT have shown clearly.

In Chapter 7, Conclusion is drawn from the work done and presented. Future scope for improvements in the same field to improve the performance and to handle the problems associated are briefly studied and presented to carry out in upcoming projects.

Matrix Converter

2.1 Introduction

The transformation and control of energy is one of the most important processes in electrical engineering. In recent years, this work has been done with the use of power semiconductors and energy storage elements such as capacitors and inductances. Several converter families have been developed: rectifiers, inverters, choppers, cycloconverters, etc. Each of these families has its own advantages and limitations. The main advantage of all static converters over other energy processors is the high efficiency that can be achieved. One of the most interesting families of converters is that of the so-called matrix converters (MCs). The matrix converter is an array of bidirectional switches functioning as the main power elements. It interconnects directly the three-phase power supply to a three phase load, without using any DC link or large energy storage elements, and therefore it is called the all-silicon solution [6]. The most important characteristics of the matrix converter are : (1) simple and compact power circuit; (2) generation of load voltage with arbitrary amplitude and frequency; (3) sinusoidal input and output currents; (4) operation with unity power factor; and (5) regeneration capability. These highly attractive characteristics are the reason for the present tremendous interest in this topology. The development of this converter starts with the early work of Venturini and Alesina [3],[4]. They presented the power circuit of the converter as a matrix of bidirectional power switches and they introduced the name 'matrix converter'.

2.1 Power Circuit and Working Principle of the Matrix Converter

In general, the matrix converter is a single stage converter with m x n bidirectional power switches, designed to connect an m-phase voltage source to an n-phase load. The matrix converter of 3 X 3 switches, shown in *fig. 2.1* is the most important converter from a practical point of view, because it connects a three phase source to a three phase load, typically a motor.

Normally, the matrix converter is fed by a voltage source and for this reason the input terminals should not be short circuited. On the other hand, the load has typically an inductive nature and, for this reason, an output phase must never be opened.

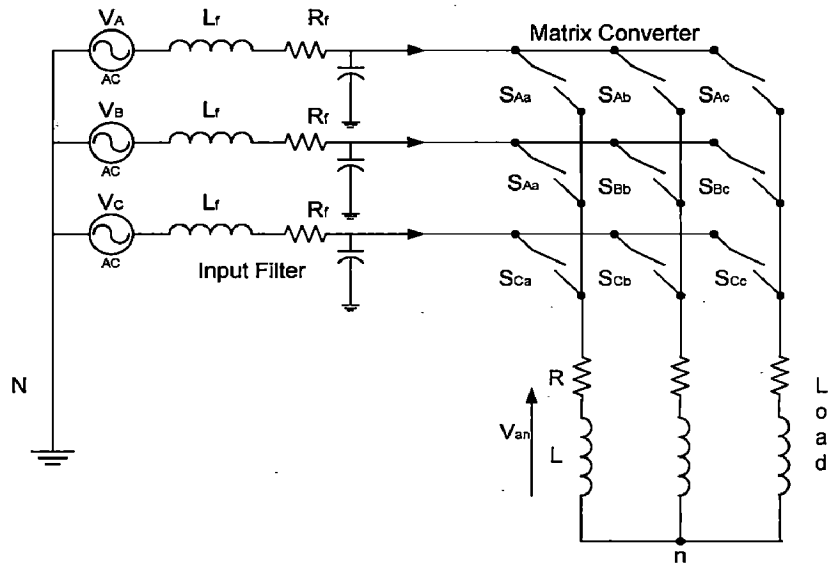

Figure 2.1: Basic power circuit of matrix converter

In the basic topology of the matrix converter shown in Fig.2.1, V_{si}, i={A, B, C}, are the source voltages, i_{si}, i={A, B, C}, are the source currents, V_{jn}, j={a, b, c}, are the load voltages with respect to the neutral point of the load n, and i_j, j={a, b, c}, are the load currents. Additionally, other auxiliary variables have been defined to be used as a basis of the modulation and control strategies: V_i, i={A, B, C}, are the matrix converter input voltages, i_i, i={A, B, C}, are the matrix converter input currents and V_{jN}, j={a, b, c}, are the load voltages with respect to the neutral point N of the grid.

The filter (Cf, L_f, R_f) located at the input of the converter has two main purposes [25]:

1) It filters the high-frequency component of the matrix converter input current (i_A, i_B, i_C), generating almost sinusoidal source currents (i_{SA} , i_{SB} , i_{SC}).

2) It avoids the generation of overvoltage produced by the fast commutation of currents i_A, i_B, i_C, due to the presence of the short-circuit reactance of any real power supply.

It should be noted that R_f is the internal resistance of inductor L_f, not an additional resistor.

Each switch S_{ij}, i={A, B, C}, j={a, b, c}, can connect or disconnect phase i of the input stage to phase j of the load and, with a proper combination to the conduction states of these switches, arbitrary output voltages V_{jN} can be synthesized. Each switch is characterized by a switching function, defined as follows:

$$S_{ij}(t)= 0 \text{ if switch } S_{ij} \text{ is open.}$$
$$S_{ij}(t)= 1 \text{ if switch } S_{ij} \text{ is closed.} \qquad (2.1)$$

Due to the presence of capacitors at the input of the matrix converter, only one switch of each column can be closed. Furthermore, the inductive nature of the load makes it impossible to interrupt the load current suddenly and, therefore, at least one switch of each column must be closed. Consequently, it is necessary that one and only one switch per column is closed at each instant. This condition can be stated in a more compact form as follows [28]:

$$\sum_{i=A,B,C} S_{ij}(t) = 1; j = \{a,b,c\}, \forall t \tag{2.2}$$

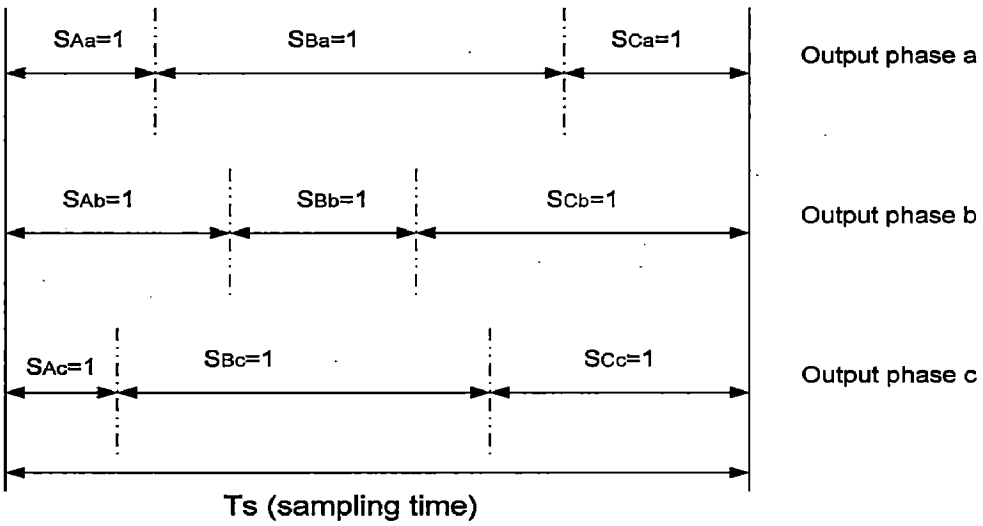

Figure 2.2: General form of switching pattern

Equation 2.2 imposes several restriction on the way in which the switches are turned on or off. With these restrictions, the 3 X 3 matrix converter has 27 possible switching states.

In order to develop a modulation strategy for the matrix converter, it is necessary to develop a mathematical model, which can be derived directly from *fig 2.1*, as follows [28]:

- Applying Kirchhoff's voltage law to the switch array, it can be easily found that

$$\begin{bmatrix} V_{aN}(t) \\ V_{bN}(t) \\ V_{cN}(t) \end{bmatrix} = \begin{bmatrix} S_{Aa}(t) & S_{Ba}(t) & S_{Ca}(t) \\ S_{Ab}(t) & S_{Bb}(t) & S_{Cb}(t) \\ S_{Ac}(t) & S_{Bc}(t) & S_{Cc}(t) \end{bmatrix} \begin{bmatrix} V_A(t) \\ V_B(t) \\ V_C(t) \end{bmatrix} \tag{2.3}$$

It is worth noting that equation (2.3) is only valid if equation (2.2) holds. Otherwise, these equations are inconsistent with the physical element distribution of *fig 2.1.*

- Applying Kirchhoff's current law to the switch array [28], it can be found that

$$\begin{bmatrix} i_A(t) \\ i_B(t) \\ i_C(t) \end{bmatrix} = \begin{bmatrix} S_{Aa}(t) & S_{Ab}(t) & S_{Ac}(t) \\ S_{Ba}(t) & S_{Bb}(t) & S_{Bc}(t) \\ S_{Ca}(t) & S_{Cb}(t) & S_{Cc}(t) \end{bmatrix} \begin{bmatrix} i_a(t) \\ i_b(t) \\ i_c(t) \end{bmatrix} \tag{2.4}$$

Equations (2.3) and (2.4) are the basis of all modulation methods which consist in selecting appropriate combinations of open and closed switches to generate the desired output voltages. It is important to note that the output voltages (V_{jN}, j={a, b, c}) are synthesized using the three input voltages (V_i, i={A, B, C}) and that the input currents (i_i, i={A, B, C}) are synthesized using the three output currents (i_j, j={a, b, c}) which are sinusoidal if the load has a low-pass frequency response.

2.2 Bidirectional Switch

The matrix converter requires a bi-directional switch capable of blocking voltage and conducting current in both directions. Unfortunately there are no such devices currently available that fulfill the needs: so discrete devices need to be used to construct suitable bi-directional cells [2]. In the discussion below it has been assumed that the switching devices would be an insulated gate bipolar transistor (IGBT), but other devices such as metal-oxide semiconductor field effect transistors (MOSFETs), MOS-controlled thyristors (MCTs) and insulated gate-commutated thyristors (IGCTs) can be used in the same way.

2.2.1 Diode Bridge Bi-directional Switch Cell

The diode bridge bidirectional switch cell arrangement consists of an IGBT at the center of a single phase diode bridge [19], arrangement as shown in *fig 2.3*. The main advantage is that both current directions are carried by the same switching device, therefore, only one gate driver is required per switch cell. Device losses are relatively high since there are three devices in each conduction path. The direction of current through the switch cell can not be controlled. This is a disadvantage, as many of the advanced commutation methods described later require this.

2.2.2 Common Emitter Anti-parallel IGBT, Diode Pair

This bi-directional switch arrangement consists of two diodes and two IGBTs connected in anti-parallel as shown in *fig. 2.4(a)*. The diodes are included to provide the

reverse blocking capability. It should be noted that it is possible to independently control the direction of the current in the bi-directional switch. Each bi-directional switch requires an isolated power supply for the gate drives, but both devices can be driven with respect to the same voltage-the common emitter point.

2.2.3 Common Collector Anti-parallel IGBT, Diode Pair

This arrangement is similar to the previous one but the IGBTs are arranged in a common collector configuration as shown in *fig. 2.4(b)*. The conduction losses are the same as the common emitter configuration. The advantage of this method is that only six isolated power supplies are needed to supply the gate drive signals. However this arrangement is often not feasible in a large practical system since inductance between commutation cells cause problems. Therefore the common emitter configuration is often preferred for creating the matrix converter bi-directional switch cells.

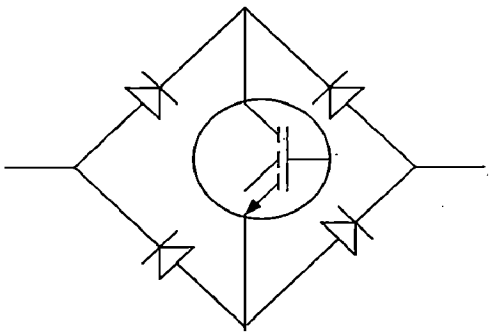

Figure 2.3: Diode bridge bidirectional switch

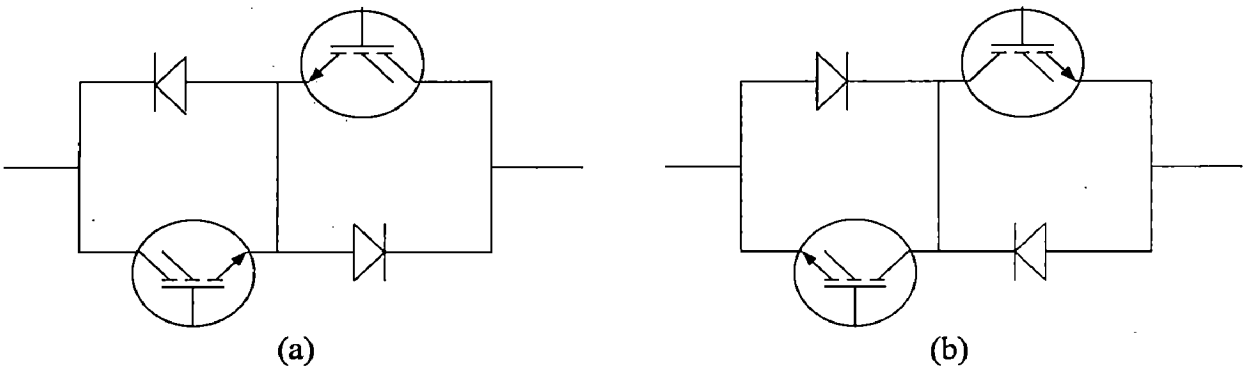

Figure 2.4: (a) Common emitter bidirectional switch
(b) Common collector bidirectional switch

If the switching devices used for the bi-directional switch have a reverse voltage blocking capability then it is possible to build the bi-directional switches by simply placing two

devices in anti-parallel. This arrangement leads to a very compact converter with the potential for substantial improvements in efficiency.

2.2.4 Integrated Power Module

It is possible to construct the common emitter bidirectional switch cell from discrete components, but it is also possible to build a complete matrix converter in the package style used for standard six-pack IGBT modules [23],[27]. This technology can be used to develop a full matrix converter power circuit in a single package, as shown in *fig.2.5*. This has been done by Eupec using devices connected in the common collector configuration as shown in *fig 2.6.* It is now available commercially. This type of packaging will have important benefits in terms of circuit layout as the stray inductance in the current commutation paths can be minimized.

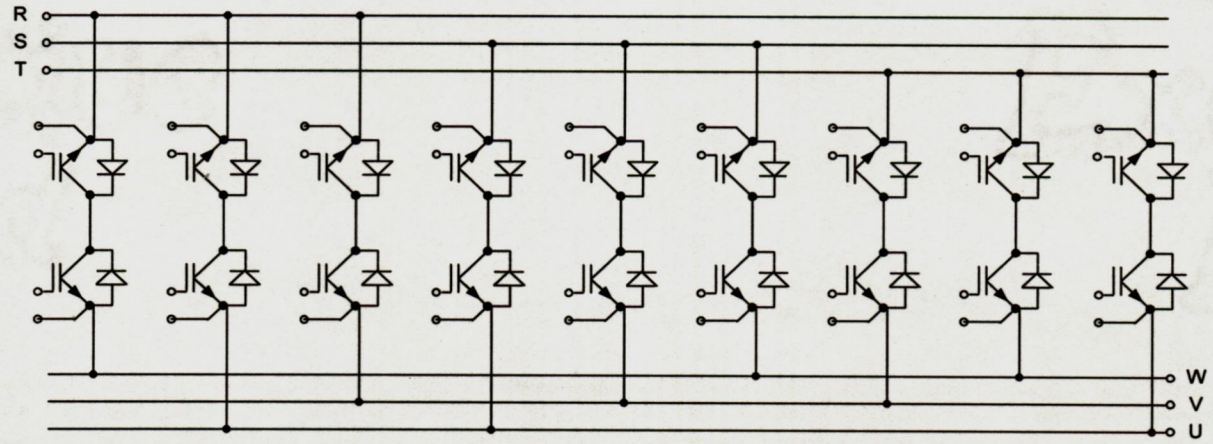

Figure2.5: Power stage of a matrix converter.

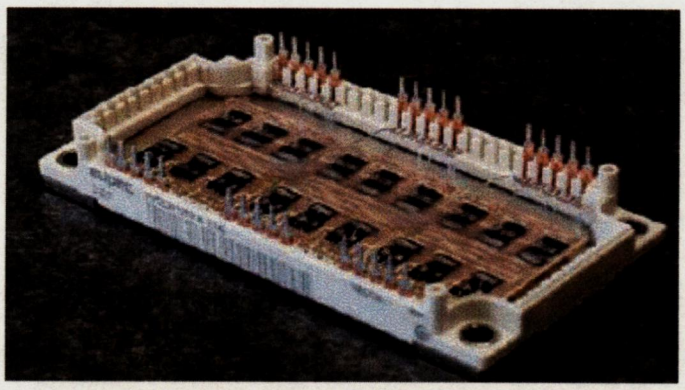

Figure 2.6: The Eupec ECONOMAC matrix module [27].

2.3 Current Commutation

Reliable current commutation between switches in matrix converters is more difficult to achieve than in conventional voltage source inverters since there are no natural freewheeling path [15],[20]. The commutation has to be actively controlled at all times with respect to two basic rules [17]. These rules can be visualized by considering just two switch cells on one output phase of the matrix converter. It is important that no two bidirectional switches are switched on at any instant, as shown pictorially in *fig 2.7(a)*. This would result in line-to-line short circuits and the destruction of the converter due to over currents. Also, the bidirectional switches for each output phase should not all be turned off at any instant, as shown in *fig 2.7(b)*. This would result in the absence of a path for the inductive load current, causing large over voltages. These two considerations cause a conflict since semiconductor devices cannot be switched instantaneously due to propagation delays and finite switching times. Various methods have been proposed to avoid this difficulty and to ensure successful commutation.

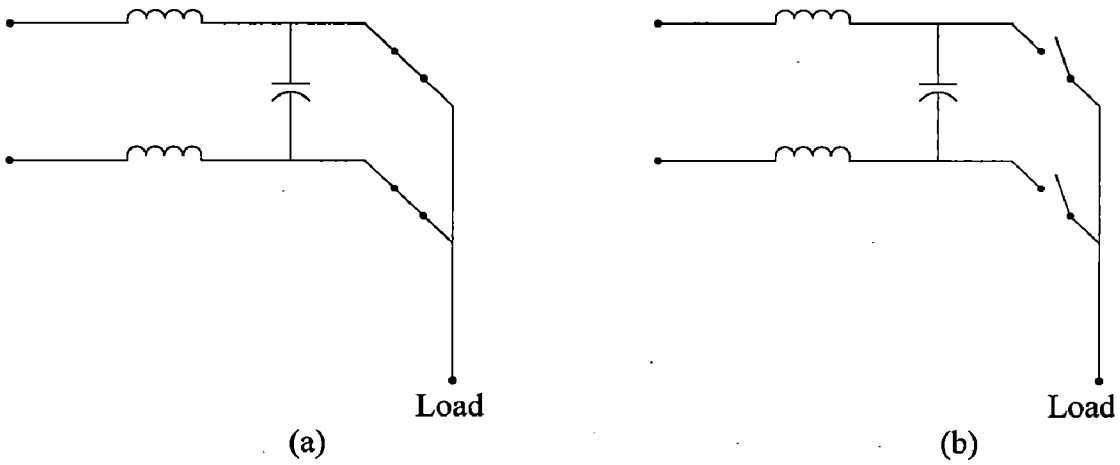

Figure 2.7(a) Avoid short circuits on the matrix converter input lines
(b) Avoid open circuits on the matrix converter output lines

2.3.1 Overlap Time Current Commutation

The two simplest forms of commutation strategy intentionally break the rules given above and need extra circuitry to avoid destruction of the converter. In overlap current commutation, the incoming cell is fired before the outgoing cell is switched off. This would normally cause a line-to-line short circuit but extra line inductance slows the rise in current so that safe commutation is achieved. This is not a desirable method since the inductors

used are large. The switching time for each commutation is also greatly increased which may cause control problems.

2.3.2 Dead Time Current Commutation

Dead-time commutation uses a period where no devices are gated, causing a momentary open circuit of the load. Snubbers or clamping devices are then needed across the switch cells to provide a path for the load current. This method is undesirable since energy is lost during every commutation and the bidirectional nature of the switch cells further complicates the snubber design. The clamping devices and the power loss associated with them also results in increased converter volume.

2.3.3 Semi Soft Current Commutation

Overlap can be used to commutate the load current from one switch to the next without creating, a short circuit if the incoming and outgoing halves of the two bidirectional switches involved in the commutation process are independently controlled. This method of current control will allow zero current switching of the IGBTs if the outgoing device is reverse biased by the turning on of the incoming device. This situation will occur when the voltage on the input line of the incoming switch is greater than the voltage on the input line of the outgoing switch in the conduction path. There is a 50% chance of reverse bias occurring. For this reason an appropriate term for this type of current control is 'semisoft current commutation' (half the switching operations are achieved by natural or soft commutation) [16].

2.3.3.1 Four Step Semi-Soft Current Commutation

A more reliable method of current commutation, which obeys the rules, uses a four-step commutation strategy in which the direction of current flow through the commutation cells can be controlled. To implement this strategy, the bidirectional switch cell must be designed in such a way as to allow the direction of the current flow in each switch cell to be controlled. *Fig.2.8* shows a schematic of a two phase to single phase matrix converter. In steady state, both of the devices in the active bidirectional switch cell are gated to allow both directions of current flow. The following explanation assumes that the load current is in the direction shown and that the upper bidirectional switch S1 is closed. When a commutation to S2 is required, the current direction is used to determine which device in

the active switch is not conducting. This device is then turned off. In this case device S1b is turned off. The device that will conduct the current in incoming switch is then gated, S2a in this example. The load current transfers to the incoming device either at this point or when

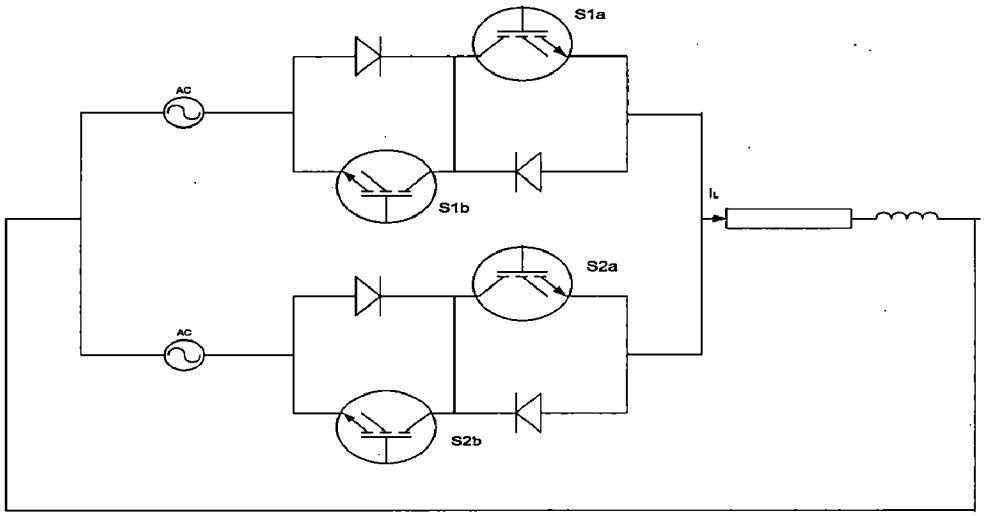

Figure 2.8: Two phase to single phase matrix converter

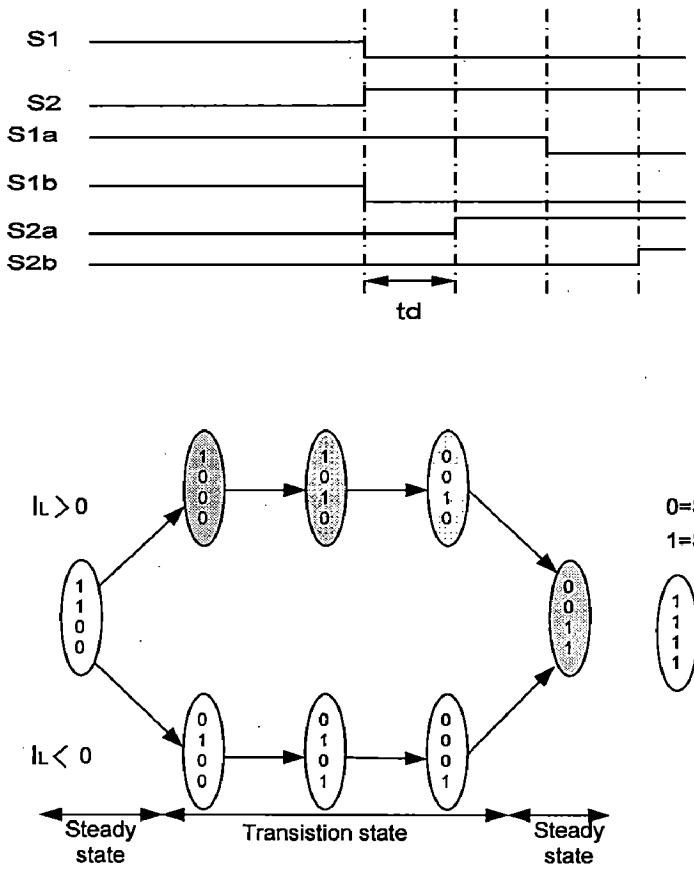

Figure 2.9: Four step semi-soft current commutation between two bidirectional switch

the outgoing device S1a is turned off. The remaining device in the incoming switch S2b is turned on to allow current reversals. This process is shown as a timing diagram in *fig 2.9.* The delay between each switching event is determined by the device characteristics.

This method allows the current to commutate from one switch cell to another without causing a line-to-line short circuit or a load open circuit. One advantage of all these techniques is that the switching losses in the silicon devices are reduced by 50% because half of the commutation process is soft switching and, hence, this method is often called "semi-soft current commutation".

2.3.3.2 Two-Step Semi-Soft Current Commutation

One popular variation in four step current commutation concept is to only gate the conduction device in the active switch cell, which creates a two-step current commutation strategy [19],[20]. In this method only the correct device in the conducting cell is gated. This simplifies the commutation to a 2 step process since only the correct device in the incoming cell is switched on and the outgoing device is switched off. Current reversal is catered for by gating both devices in the conducting cell when the current level falls below a threshold level. The non-conducting device is then turned off when the current has risen

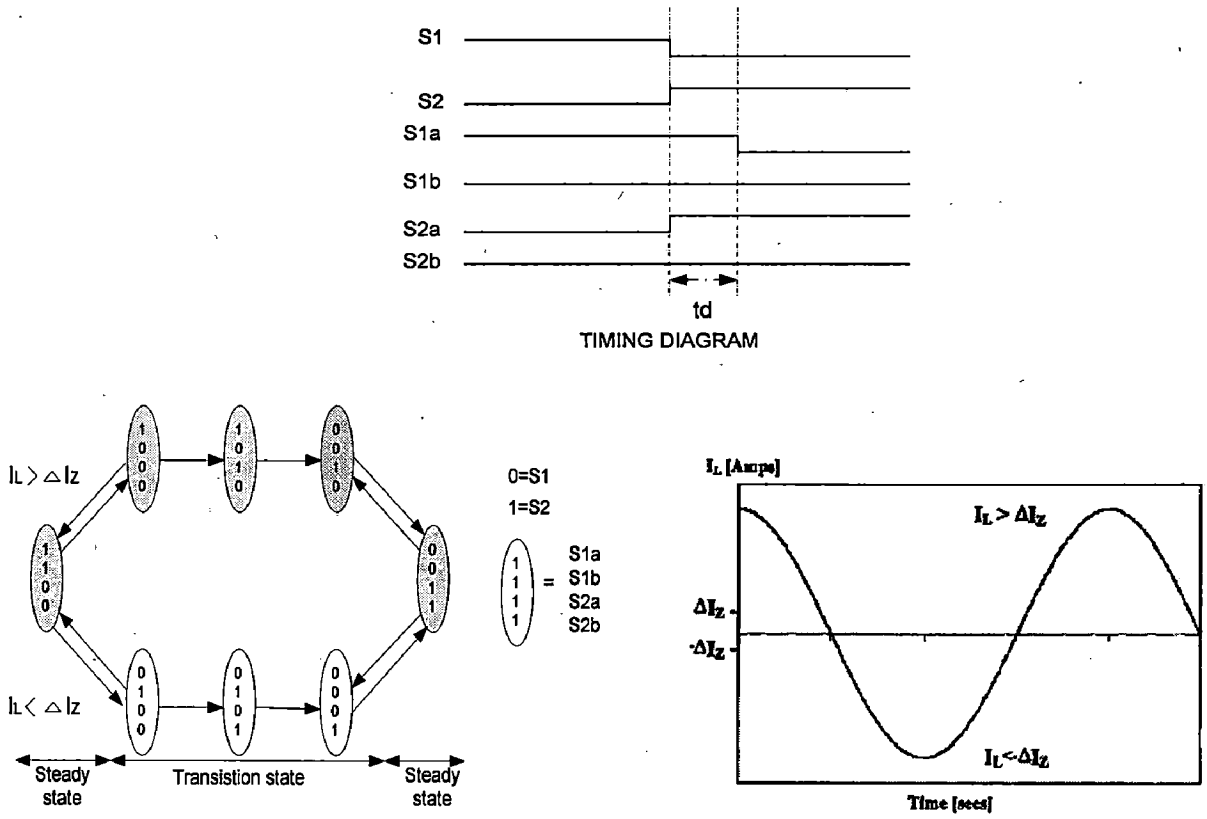

Figure 2.10: Two step semi soft current commutation between two bidirectional switch cell

sufficiently in the opposite direction. The problem with this method is that a commutation between cells cannot occur during a current reversal. Since the direction of current is unknown, the current outgoing device cannot be determined. This method would also be unsuitable if the target output current was to be within the threshold level.

All the current commutation techniques in this category rely on knowledge of the output line current direction. This can be difficult to reliably determine in a switching power converter, especially at low current levels in high-power applications where traditional current sensors such as Hall-effect probes are prone to producing uncertain result. One method that has been used to avoid these potential hazard conditions is to create a "near-zero" current zone where commutation is not allowed to take place, as shown for a two-step strategy in the state representation diagram in *fig.2.10*. However, this method will give rise to control problems at low current levels and at startup.

2.4 Current Direction Detection.

To avoid these current measurement problems, a technique for using the voltage across the bidirectional switch to determine the current direction has been developed [18],[20]. This method allows very accurate current direction detection with no external sensors. The voltages V_A and V_B are measured. Assuming current I_L is in the direction shown in *fig 2.11*, S1 will be conducting and S2 will be reversed biased. This results in V_A being around 1.2V (depending on devices used) and V_B being around -0.7V. When current is in the opposite direction the reverse situation exists. Assuming that the correct device is gated, the direction of current in the cell can be deduced. This detection circuit and associated control logic are integrated into the gate drive for each cell. To make the current direction information reliable only one of the devices in a cell is gated at any one time. This means that the current is either zero or flows in the designated direction.

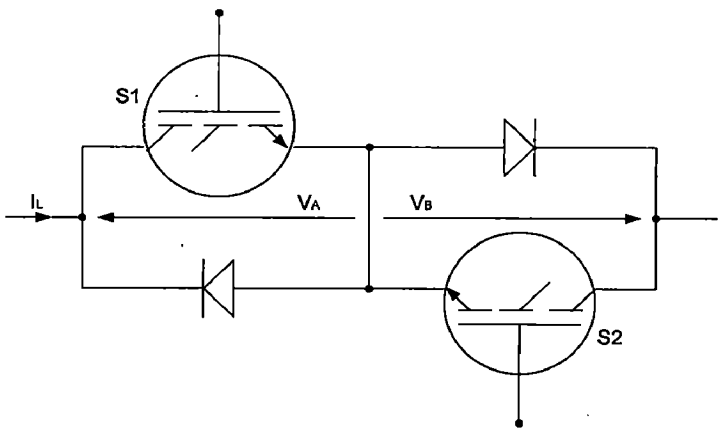

Figure 2.11: Bi-directional switch cell.

2.5 Practical Issues

Some practical issues related to the practical application of this technology, like overvoltage protection, input filter and semiconductor losses are discussed below.

2.5.1 Power Circuit Protection

A critical feature of the matrix converter is that current is always commutated from one controlled switch to another. This is in direct contrast to a conventional voltage source inverter where commutation is always from a controlled device to a complementary freewheeling diode or vice-versa. In a conventional inverter a time delay can be introduced between the drive signals for complementary devices (in order to avoid simultaneous conduction) safe in the knowledge that the inductive load current will be taken over by a freewheeling diode [22]. There is no such freewheeling path in the matrix converter but it is still necessary to introduce a delay between drive signals to avoid a short circuit of the input lines. During this delay time the inductive load current is taken over by a snubber circuit which must be chosen to limit the device voltage to an appropriate level. In the prototype a simple R-C snubber connected across the bidirectional switch is used. To avoid excessive snubber losses it is important to match the snubber design and delay time setting very carefully.

The absence of freewheeling paths also causes difficulty in protecting the power circuit against fault conditions. For instance, if the devices are turned-off in response to a fault condition, such as over current, severe overvoltage and destruction of the power circuit results because of the inductive nature of the load. The prototype converter overcomes this problem by employing a clamp arrangement connected to the matrix converter output [21]. The clamp consists of six pulse diode bridge feeding a capacitor which absorbs the excess load energy when all the converter devices are gated off. This clamp performs essentially the same function as the snubber circuits but in practice it has been found that small snubbers are still required to mitigate against the effects of wiring inductance.

When overvoltage occurs, the diode conducts and the RC circuit maintains the voltage level at a safe value. In normal operation, the diodes are off and the clamp circuit has no influence on the matrix converter operation. It is important to note that the power level is very low for the clamp circuit.

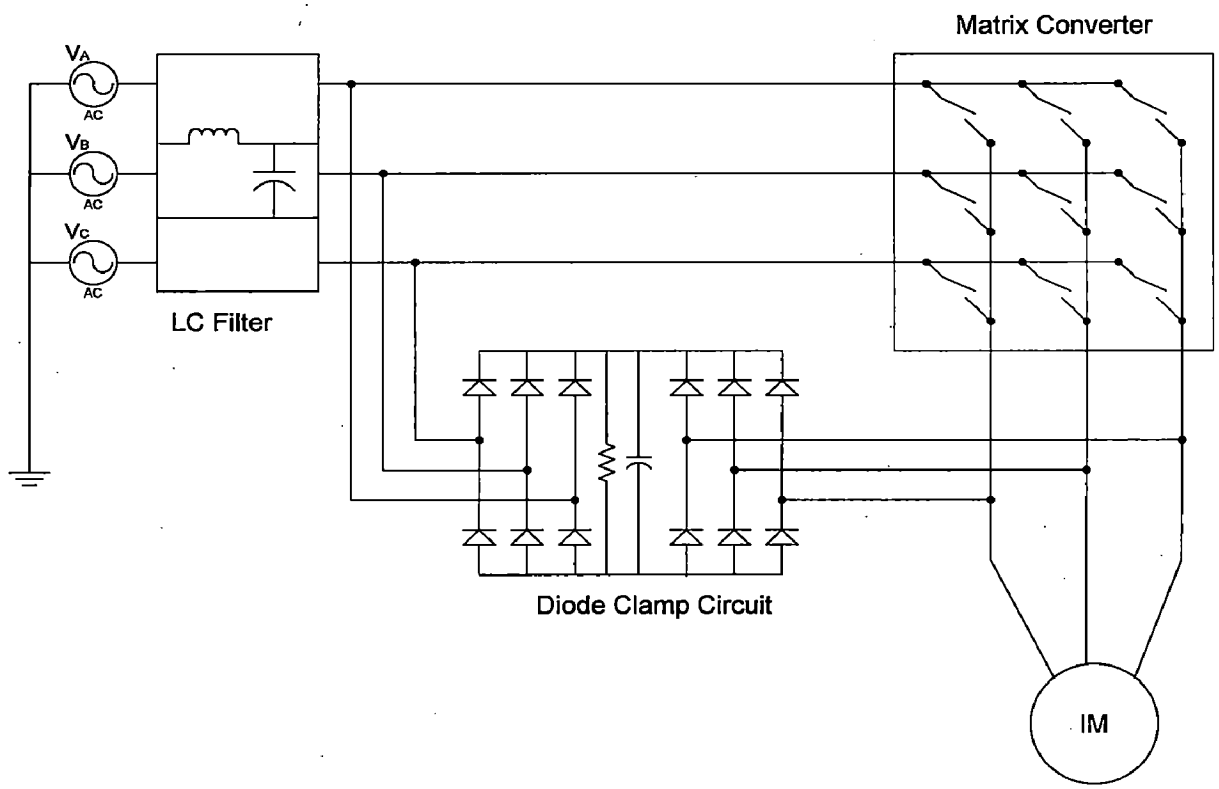

Figure 2.12: Matrix converter with clamp

2.5.2 Input Filter

Filters must be used at the input of the matrix converters to reduce the switching frequency harmonics present in the input current. The requirements for the filter are as follows [25]:

1) to have a cutoff frequency lower than the switching frequency of the converter;

2) to minimize its reactive power at the grid frequency;

3) to minimize the volume and weight for capacitors and chokes;

4) to minimize the filter inductance voltage drop at rated current in order to avoid a reduction in the voltage transfer ratio.

It must be noticed that this filter does not need to store energy coming from the load. Several filter configurations like simple *LC* and multistage *LC* have been investigated [25].

2.5.3 Semiconductor Losses

Since a suitable bidirectional semiconductor switch has not yet been developed, so the matrix converter can be realized using a switch constructed from discrete components. The back to back IGBT arrangements are preferred as it allows independent control of the

current in both directions within each switch. This control would not be possible if the diode bridge circuit was used. The diode bridge circuit also has a greater conduction loss since there are two diodes in series with the IGBT. The losses in a matrix converter consist of conduction losses and switching losses. The conduction losses are proportional to the forward voltage drop across the device and the current carried by the device. The conduction loss per switch is calculated as the sum of the conduction losses in the IGBT and in the associated diode. The conduction loss in a matrix converter is therefore slightly greater than in an inverter in which either the IGBT or the diode would carry the load current. The switching losses in the IGBT are due to the finite time taken for the device to change state. The switching losses are also proportional to the switching frequency at which the converter is operating.

2.5.4 Conclusion

The working principle of the matrix converter controlled with the direct transfer function approach, has been presented. The most important equations are clearly presented. In addition, an intelligent commutation strategy is explained, which avoids the generation of overvoltages and overcurrents. Some new arrays of power bidirectional switches integrated in a single module are also presented. Finally, some practical issues related to the practical application of this technology, like overvoltage protection, use of filters, and semiconductor losses are explained.

Chapter-3

Modulation Techniques

3.1 Introduction

The AC-AC matrix converter, an alternative to an AC-DC-AC converter for voltage and frequency transformation, has two major advantages: it requires no DC-link reactive components and it allows bidirectional power flow. Since its first description [l], the matrix converter has been the subject of intensive ongoing research and an aspect which attracts much of the research effort is the pulse-width modulation (PWM) control technique. For matrix converters used in variable-speed drive applications the ideal PWM algorithm should: provide independent control of the magnitude and frequency of the generated output voltages; give sinusoidal input currents with adjustable phase shift; achieve the maximum possible range of output to input voltage ratio; satisfy the conflicting requirements of minimum low order harmonics and minimum switching losses; and be computationally efficient.

There has been much published work in the area of modulation strategies for matrix converters. Apart from the basic Venturini solution there are essentially two other forms of matrix converter modulation algorithms. These are the fictitious DC link method [5],[7], [8] and the Space Vector modulation [10], [11]. The fictitious DC link method has implementations that claim to increase the voltage transfer ratio of over 100%, but this is done at the expense of low frequency harmonics in the input and output waveforms and is therefore sub optimal for many applications. The voltage transfer ratio limitation of 86% has often been cited as a major disadvantage of the matrix converter, but this is only really a problem if you need to use a standard machine from a standard supply. If the application allows you to specify the machine voltage (or the supply voltage) then the voltage ratio limitation is not a problem. The only situation where this can be seen as a major hurdle to the use of matrix converters is when the converter is retrofitted to an existing motor.

3.2 Venturini Modulation Method

Modulation is the procedure used to generate the appropriate firing pulses to each of the nine bidirectional switches in order to generate the desired output voltage. In this case, the primary objective of the modulation is to generate variable-frequency and variable-

amplitude sinusoidal output voltage (V_{jN}) from the fixed-frequency and fixed-amplitude input voltage (V_i). The easiest way of doing this is to consider time windows in which the instantaneous values of the desired output voltages are sampled and the instantaneous input voltages are used to synthesize a signal whose low frequency component is the desired output voltage.

If t_{ij} is defined as the time during which switch S_{ij} ON and T as the sampling interval (width of the time window), the synthesis principle described above can be expressed as [28]

$$\bar{V}_{jN}(t) = \frac{t_{Aj}V_A(t) + t_{Bj}V_B(t) + t_{Cj}V_C(t)}{T}; \qquad j=\{a, b, c\} \tag{3.1}$$

Where $\bar{V}_{jN}(t)$ is the low frequency component (mean value calculated over one sampling interval) of the j^{th} output pulse and changes in each sampling interval. With this strategy, a high frequency switched output voltage is generated, but the fundamental component of the voltage has the desired waveform.

Obviously, $T= t_{Aj} + t_{Bj} + t_{Cj} \quad \forall j$ and therefore the following duty cycles can be defined:

$$m_{Aj}(t) = \frac{t_{Aj}}{T}, \qquad m_{Bj}(t) = \frac{t_{Bj}}{T}, \qquad m_{Cj}(t) = \frac{t_{Cj}}{T} \tag{3.2}$$

Extending equation (3.1) to each output phase, and using equation (3.2), the following relationship between the input and output voltage and that of the output and input current can be derived [3],[4]:

$$\begin{bmatrix} \bar{V}_{aN}(t) \\ \bar{V}_{bN}(t) \\ \bar{V}_{cN}(t) \end{bmatrix} = \begin{bmatrix} m_{Aa}(t) & m_{Ba}(t) & m_{Ca}(t) \\ m_{Ab}(t) & m_{Bb}(t) & m_{Cb}(t) \\ m_{Ac}(t) & m_{Bc}(t) & m_{Cc}(t) \end{bmatrix} \begin{bmatrix} V_A(t) \\ V_B(t) \\ V_C(t) \end{bmatrix}$$

$$\Leftrightarrow \bar{V}_o(t) = M(t) \cdot v_i(t) \tag{3.3}$$

Where $\bar{V}_o(t)$ is the low frequency output voltage vector, $V_i(t)$ is the instantaneous input voltage vector and M(t) is the low frequency transfer matrix of the matrix converter.

$$i_i(t) = M^T(t) \cdot i_o(t) \tag{3.4}$$

Where $\bar{i}_i(t) = [\bar{i}_A(t) \quad \bar{i}_B(t) \quad \bar{i}_C(t)]^T$ is the low frequency component input current vector, $\bar{i}_o(t) = [i_a(t) \quad i_b(t) \quad i_c(t)]^T$ is the instantaneous output current vector and $M^T(t)$ is the transpose of M(t).

Equation (3.3) and (3.4) are the basis of the venturini modulation method [3],[4] and allows us to conclude that the low frequency components of the output voltages are

synthesized with the instantaneous values of the input voltages and that the low-frequency components of the input currents are synthesized with the instantaneous values of the output currents [28].

Suppose that the input voltages are given by

$$V_i(t) = \begin{bmatrix} V_A(t) \\ V_B(t) \\ V_C(t) \end{bmatrix} = \begin{bmatrix} V_i \cos(w_i t) \\ V_i \cos(w_i t + 2\pi/3) \\ V_i \cos(w_i t + 4\pi/3) \end{bmatrix} \tag{3.5}$$

And that due to the low-pass characteristic of the load the output currents are sinusoidal and can be expressed as

$$i_o(t) = \begin{bmatrix} i_a(t) \\ i_b(t) \\ i_c(t) \end{bmatrix} = \begin{bmatrix} I_o \cos(w_o t + \phi_o) \\ I_o \cos(w_o t + 2\pi/3 + \phi_o) \\ I_o \cos(w_o t + 4\pi/3 + \phi_o) \end{bmatrix} \tag{3.6}$$

Find a modulation matrix M(t) such that

$$\overline{V}_o(t) = \begin{bmatrix} \overline{V}_{aN}(t) \\ \overline{V}_{bN}(t) \\ \overline{V}_{cN}(t) \end{bmatrix} = \begin{bmatrix} qV_i \cos(w_o t) \\ qV_i \cos(w_o t + 2\pi/3) \\ qV_i \cos(w_o t + 4\pi/3) \end{bmatrix} \tag{3.7}$$

$$\overline{i}_i(t) = \begin{bmatrix} \overline{i}_A(t) \\ \overline{i}_B(t) \\ \overline{i}_C(t) \end{bmatrix} = \begin{bmatrix} qI_i \cos(w_i t + \phi_i) \\ qI_i \cos(w_i t + 2\pi/3 + \phi_i) \\ qI_i \cos(w_i t + 4\pi/3 + \phi_i) \end{bmatrix} \tag{3.8}$$

In equation (3.8), q is the voltage gain between the output and input voltages.

There are two basic solutions as shown in equation (3.9) and (3.10). The solution in equation (3.9) yields $\phi_i = \phi_o$ giving the same phase displacement at the input and output ports, whereas the solution in equation (3.10) yields $\phi_i = -\phi_o$, giving reversed phase displacement. Combining the two solutions provides the means for input displacement factor control.

This basic solution represents a direct transfer function approach and is characterized by the fact that, during each switch sequence time (T), the average output voltage is equal to the demand (target) voltage. For this to be possible, it is clear that the target voltages must fit within the input voltage envelope for any output frequency. This leads to a limitation on the maximum voltage ratio.

$$M1=\frac{1}{3}\begin{bmatrix} 1+2q\cos(w_m t) & 1+2q\cos(w_m t-\frac{2\pi}{3}) & 1+2q\cos(w_m t-\frac{4\pi}{3}) \\ 1+2q\cos(w_m t-\frac{4\pi}{3}) & 1+2q\cos(w_m t) & 1+2q\cos(w_m t-\frac{2\pi}{3}) \\ 1+2q\cos(w_m t-\frac{2\pi}{3}) & 1+2q\cos(w_m t-\frac{4\pi}{3}) & 1+2q\cos(w_m t) \end{bmatrix} \quad (3.9)$$

With $w_m = (w_o - w_i)$

$$M2=\frac{1}{3}\begin{bmatrix} 1+2q\cos(w_m t) & 1+2q\cos(w_m t-\frac{2\pi}{3}) & 1+2q\cos(w_m t-\frac{4\pi}{3}) \\ 1+2q\cos(w_m t-\frac{2\pi}{3}) & 1+2q\cos(w_m t-\frac{4\pi}{3}) & 1+2q\cos(w_m t) \\ 1+2q\cos(w_m t-\frac{4\pi}{3}) & 1+2q\cos(w_m t) & 1+2q\cos(w_m t-\frac{2\pi}{3}) \end{bmatrix} \quad (3.10)$$

With $w_m = -(w_o + w_i)$

However, calculating the switch timings directly from these equations is cumbersome for a practical implementation. They are more conveniently expressed directly in terms of the input voltages and the target output voltages (assuming unity displacement factor) in the following form [27].

$$m_{ij}(t)=\frac{1}{3}\left[1+2\frac{V_i(t)\bar{V}_{jN}(t)}{V_i^2}\right] \quad (3.11)$$

Where i = {A, B, C} and j = {a, b, c}.

It is worth noting that the derivation of M(t) supposes no sampling of the desired output voltages (reference), because it is a continuous time solution. In order to implement a digital simulation of the matrix converter or to develop an experimental set up, it is necessary to consider a sampled version of equation (3.11):

$$m_{ij}(kt)=\frac{1}{3}\left[1+2\frac{V_i(kt)\bar{V}_{jN}(kt)}{V_i^2}\right] \quad (3.12)$$

Where i = { A, B, C } and j = {a, b, c }, $k \in Z$ and T is the sampling interval. If T is small enough, the differences between equation (3.11) and (3.12) will be negligible.

3.2.1 Voltage Ratio Limitation and Optimization

The modulation solutions in equation (3.12) have a maximum voltage ratio (q) of 50% as illustrated in *fig 3.1*. An improvement in the achievable voltage ratio to $\sqrt{3}/2$ (or 87%) is possible by adding common-mode voltages to the target outputs as shown in equation (3.13).

$$V_o = qV_i \cdot \begin{bmatrix} COS(W_o t) - \frac{1}{6}COS(3W_o t) + \frac{1}{2\sqrt{3}}COS(3W_i t) \\ COS(W_o t + \frac{2\pi}{3}) - \frac{1}{6}COS(3W_o t) + \frac{1}{2\sqrt{3}}COS(3W_i t) \\ COS(W_o t + \frac{4\pi}{3}) - \frac{1}{6}COS(3W_o t) + \frac{1}{2\sqrt{3}}COS(3W_i t) \end{bmatrix} \quad (3.13)$$

The common-mode voltages have no effect on the output line-to-line voltages, but allow the target outputs to fit within the input voltage envelope with a value of up to 87% as illustrated in *fig 3.2.* in this case modulation function can be expressed as

$$m_{ij} = \frac{1}{3}\left[1 + \frac{2v_i v_j}{V_i^2} + \frac{4q}{3\sqrt{3}}\sin(w_i t + \beta_i)\sin(3w_i t)\right] \quad (3.14)$$

Where βi=0, 2π /3, 4π /3 for i=A, B, C respectively.

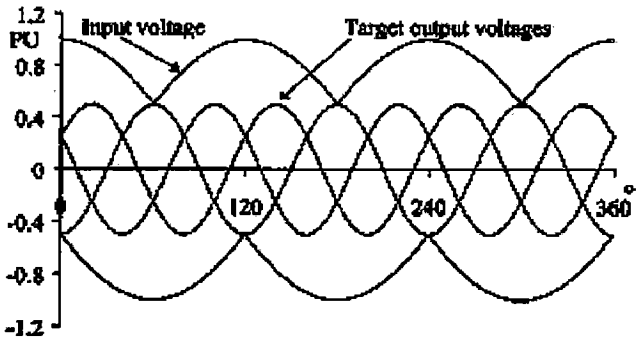

Figure 3.1: Illustrating maximum voltage ratio of 50% [27].

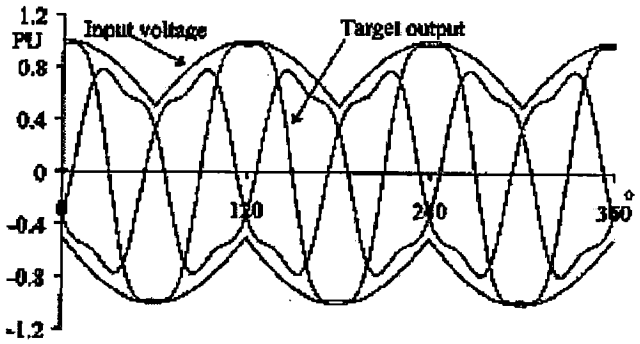

Figure 3.2: Illustrating voltage ratio improvement to 86.6% [27].

3.3 Space Vector Modulation Technique

In this modulation approach, the target output voltages and the target input line current directions are expressed as space vectors:

$$\overline{V}_o = V_o e^{j(w_o t)} \tag{3.15}$$

$$\overline{I}_i = I_i e^{j(w_i t - \phi_i)} \tag{3.16}$$

Where V_o represent the magnitude of the voltage vector and w_o defines angular velocity of the vector likewise I_i and w_i represent the magnitude and rotating velocity of the current vector respectively.

The principle of the space vector modulation (SVM) method can be summarized as follows:

For a sufficiently small time interval, the reference voltage vector can be approximated by a set of stationary vectors generated by a matrix converter. If this time interval is the sample time for converter control then, at the next sample instant when the reference voltage vector rotates to a new angular position, it may correspond to a new set of stationary voltage vectors. Carrying this process onwards by sampling entire waveform of the desired voltage vector being synthesized in sequence, the average output voltage would closely emulate the reference voltage. Meanwhile, the selected stationary vectors can also give the desirable phase shift between input voltage and current. The modulation process thus required consists of two main parts: selection of the switching vectors and computation of the vector time intervals.

The SVM is well known and established in conventional PWM inverters. Its application to matrix converters is conceptually the same, but is more complex [11]-[14]. With a matrix converter, the SVM can be applied to output voltage and input current control. A comprehensive discussion of the SVM and its relationship to other methods is provided in. Here, we just consider output voltage control to establish the basic principles. The voltage space vector of the target matrix converter output voltages is defined in terms of the line-to-line voltages by equation (3.17).

$$V_o(t) = \frac{2}{3}(v_{ab} + a v_{bc} + a^2 v_{ca}) \qquad \text{where} \quad a = \exp(j2\pi/3) \tag{3.17}$$

In the complex plane, $V_o(t)$ is a vector of constant length ($\sqrt{3}qV_{im}$) rotating at angular frequency w_o. In the SVM, is synthesized by time averaging from a selection of adjacent vectors in the set of converter output vectors in each sampling period. For a matrix

converter, the selection of vectors is by no means unique and a number of possibilities exist which are not discussed in detail here.

The 27 possible output vectors for a three-phase matrix converter can be classified into three groups with the following characteristics [14].

• *Group I:* Each output line is connected to a different input line. Output space vectors are constant in amplitude, rotating (in either direction) at the supply angular frequency.

• *Group II:* Two output lines are connected to a common input line; the remaining output line is connected to one of the other input lines. Output space vectors have varying amplitude and fixed direction occupying one of six positions regularly spaced 60° apart. The maximum length of these vectors is $2/3V_{env}$ where V_{env} is the instantaneous value of the rectified input voltage envelope.

• *Group III:* All output lines are connected to a common input line. Output space vectors have zero amplitude (i.e., located at the origin).

In the SVM, the Group I vectors are not used. The desired output is synthesized from the Group II active vectors and the Group III zero vectors. The hexagon of possible output vectors is shown in *fig 3.3*, where the Group II vectors are further subdivided dependent on which output line-to-line voltage is zero.

Fig. 3.4 shows an example of how $V_o(t)$ could be synthesized when it lies in the sextant between vector 1 and vector 6. $V_o(t)$ is generated through time averaging by choosing the time spent in vector 1 (t_1) and vector 6 (t_6) during the switching sequence. Here, it is assumed that the maximum length vectors are used, although that does not have to be the case. From *fig. 3.4*, the relationship in equation (3.18) is found

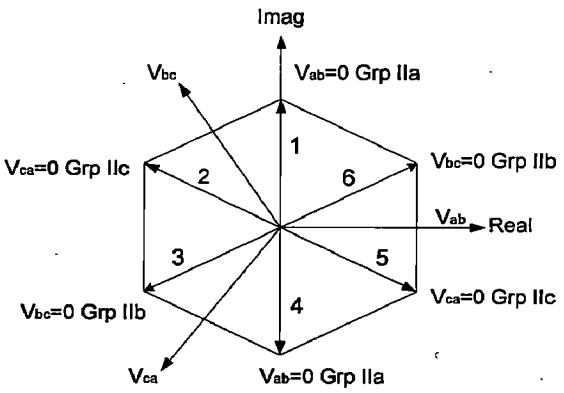

Figure 3.3: Output voltage space vectors

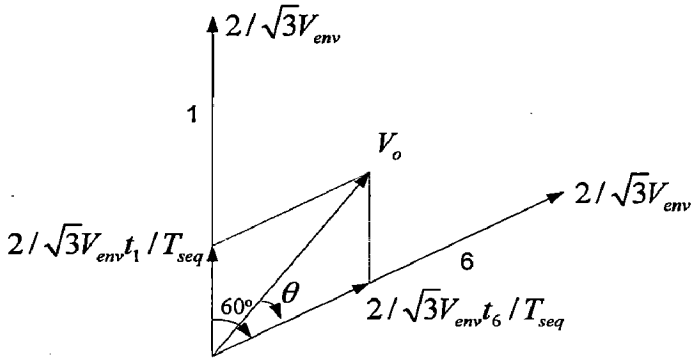

Figure 3.4: Example of output voltage space-vector synthesis.

$$t_1 = \frac{|V_o|}{V_{env}} T_{seq} \sin(\theta)$$

$$t_6 = \frac{|V_o|}{V_{env}} T_{seq} \sin(60 - \theta)$$

$$t_0 = T_{seq} - (t_1 + t_6) \tag{3.18}$$

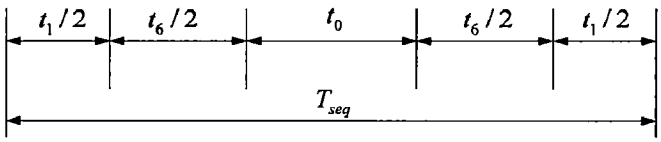

Figure 3.5: Possible way of allocating states within switching sequence.

where t_0 is the time spent in the zero vector (at the origin). There is no unique way for distributing the times (t_1, t_6, t_0) within the switching sequence. One possible method is shown T_{seq} in *fig 3.5*. For good harmonic performance at the input and output ports, it is necessary to apply the SVM to input current control and output voltage control. This generally requires four active vectors in each switching sequence, but the concept is the same. Under balanced input and output conditions, the SVM technique yields similar results to the other methods mentioned earlier. However, the increased flexibility in choice of switching vectors for both input current and output voltage control can yield useful advantages under unbalanced conditions.

3.4 Indirect Modulation Method

The indirect space vector modulation (indirect SVM) was first proposed by Borojevic et al in 1989 [10] where matrix converter was described to an equivalent circuit combining current source rectifier and voltage source inverter connected through

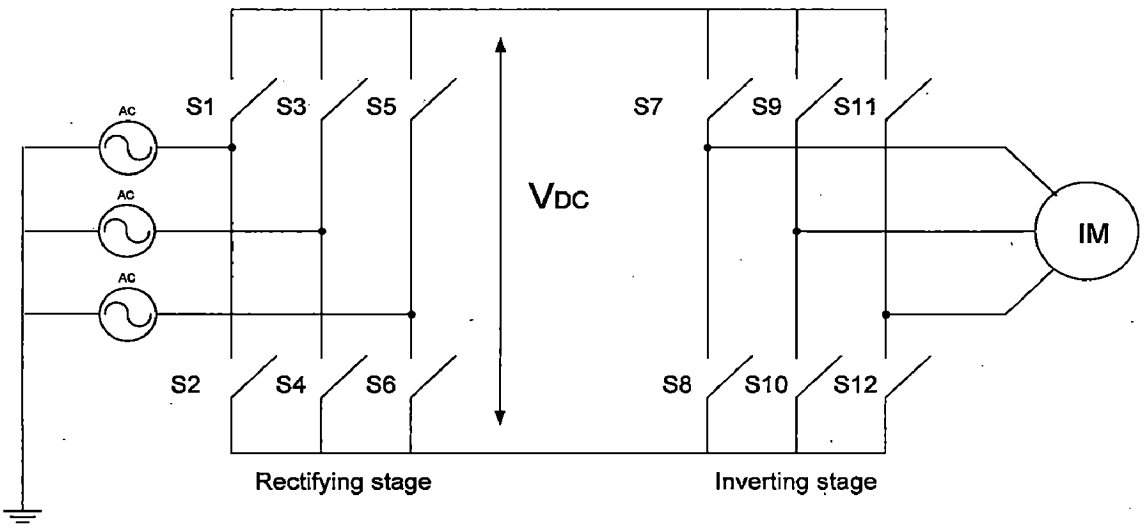

Figure 3.6: The equivalent circuit for indirect modulation

virtual dc link as shown in *fig 3.3*. Inverter stage has a standard 3-phase voltage source inverter topology consisting of six switches, *S7 ~ S12* and rectifier stage has the same power topology with another six switches, *S1 ~ S6*. Both power stages are directly connected through virtual dc-link and inherently provide bidirectional power flow capability because of its symmetrical topology.

These methods aim to increase the maximum voltage ratio above the 86.6% limit of other methods [8],[9]. To do this, the modulation process defined in equation (3.3) is split into two steps as indicated in equation (3.19).

$$V_o=(AV_i)B \tag{3.19}$$

In equation (3.19), premultiplication of the input voltages by **A** generates a "fictitious dc link"[10] and postmultiplication by **B** generates the desired output by modulating the "fictitious dc link." **A** is generally referred to as the "rectifier transformation" and **B** as the "inverter transformation" due to the similarity in concept with a traditional rectifier/dc link/inverter system. **A** is given by equation (3.20).

$$A = K_A \begin{bmatrix} \cos(w_i t) \\ \cos(w_i t + \frac{2\pi}{3}) \\ \cos(w_i t + \frac{4\pi}{3}) \end{bmatrix}^T \tag{3.20}$$

Hence,

$$AV_i = K_A V_{im} \begin{bmatrix} \cos(w_i t) \\ \cos(w_i t + \frac{2\pi}{3}) \\ \cos(w_i t + \frac{4\pi}{3}) \end{bmatrix}^T \begin{bmatrix} \cos(w_i t) \\ \cos(w_i t + \frac{2\pi}{3}) \\ \cos(w_i t + \frac{4\pi}{3}) \end{bmatrix} \tag{3.21}$$

$$= \frac{3K_A V_{im}}{2} \tag{3.22}$$

B is given by equation (3.23)

$$B = K_B \begin{bmatrix} \cos(w_o t) \\ \cos(w_o t + \frac{2\pi}{3}) \\ \cos(w_o t + \frac{4\pi}{3}) \end{bmatrix} \tag{3.23}$$

Hence,

$$V_o = (AV_i)B = \frac{3K_A K_B V_{im}}{2} \begin{bmatrix} \cos(w_o t) \\ \cos(w_o t + \frac{2\pi}{3}) \\ \cos(w_o t + \frac{4\pi}{3}) \end{bmatrix} \tag{3.24}$$

The voltage ratio $q=3K_AK_B/2$. Clearly, the **A** and **B** modulation steps are not continuous in time as shown above, but must be implemented by a suitable choice of the switching states. There are many ways of doing this, which are discussed in detail in [8] and [9]. To maximize the voltage ratio, the step in **A** is implemented so that the most positive and most negative input voltages are selected continuously. This yields $K_A = 2\sqrt{3}/\pi$ with a "fictitious dc link" of $3\sqrt{3}Vim/\pi$ (the same as a six-pulse diode bridge with resistive load). K_B represents the modulation index of a PWM process and has the maximum value (square-

wave modulation) of $2/\pi$. The overall voltage ratio q therefore has the maximum value of $2/\pi \; 6\sqrt{3}/\pi^2 = 105.3\%$ [8].

The voltage ratio obtainable is obviously greater than that of other methods but the improvement is only obtained at the expense of the quality of the input currents, the output voltages or both. For values of $q \rangle 0.866$, the mean output voltage no longer equals the target output voltage in each switching interval. This inevitably leads to low frequency distortion in the output voltage and/or the input current compared to other methods with $q \langle 0.866$. For $q \langle 0.866$, the indirect method yields very similar results to the direct methods. *Fig 3.4* shows typical line-to-line output voltage and current waveforms obtained with the indirect method generating an output voltage with a frequency of 50 Hz [27].

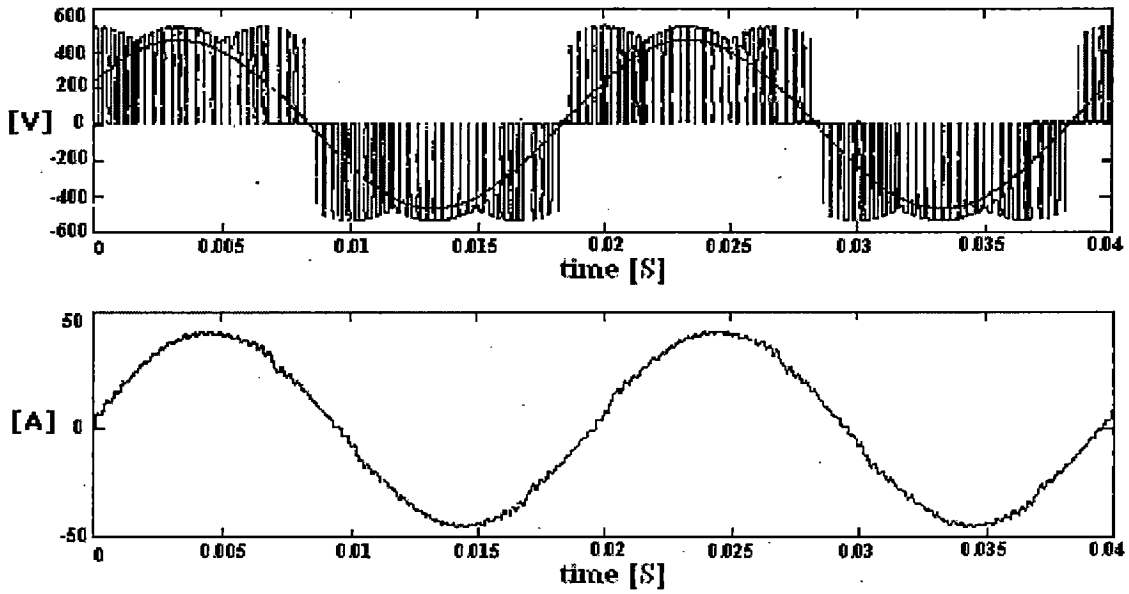

Figure 3.7: Line-to-line voltage and current in the load with the indirect method output frequency of 50 Hz [27].

3.5 Conclusion

There are various control strategy used for matrix converter. This chapter discusses three control strategies; Venturini modulation method, Space vector modulation method and Indirect modulation method. In this thesis Venturini modulation strategy has been implemented for 3-phase to 3-phase matrix converter.

Simulation Study

4.1 Introduction

Extensive simulation is carried out to investigate the performance of the 3-phase to 3-phase Matrix converter for different output frequencies. A simulation of the 3-Phase Matrix Converter is developed using MATLAB™ and its Power system blockset in SIMULINK. The model developed in MATLAB is shown in *fig 4.1.* Simulation results are obtained using Venturini modulation method for 3-phase to 3-phase matrix converter with R-L Load. In power system block set we can find different variety of blocks which represent switching devices, passive elements and measurements. The different components which are used to develop the model are below: Power Supply, 3-phase to 3-phase matrix

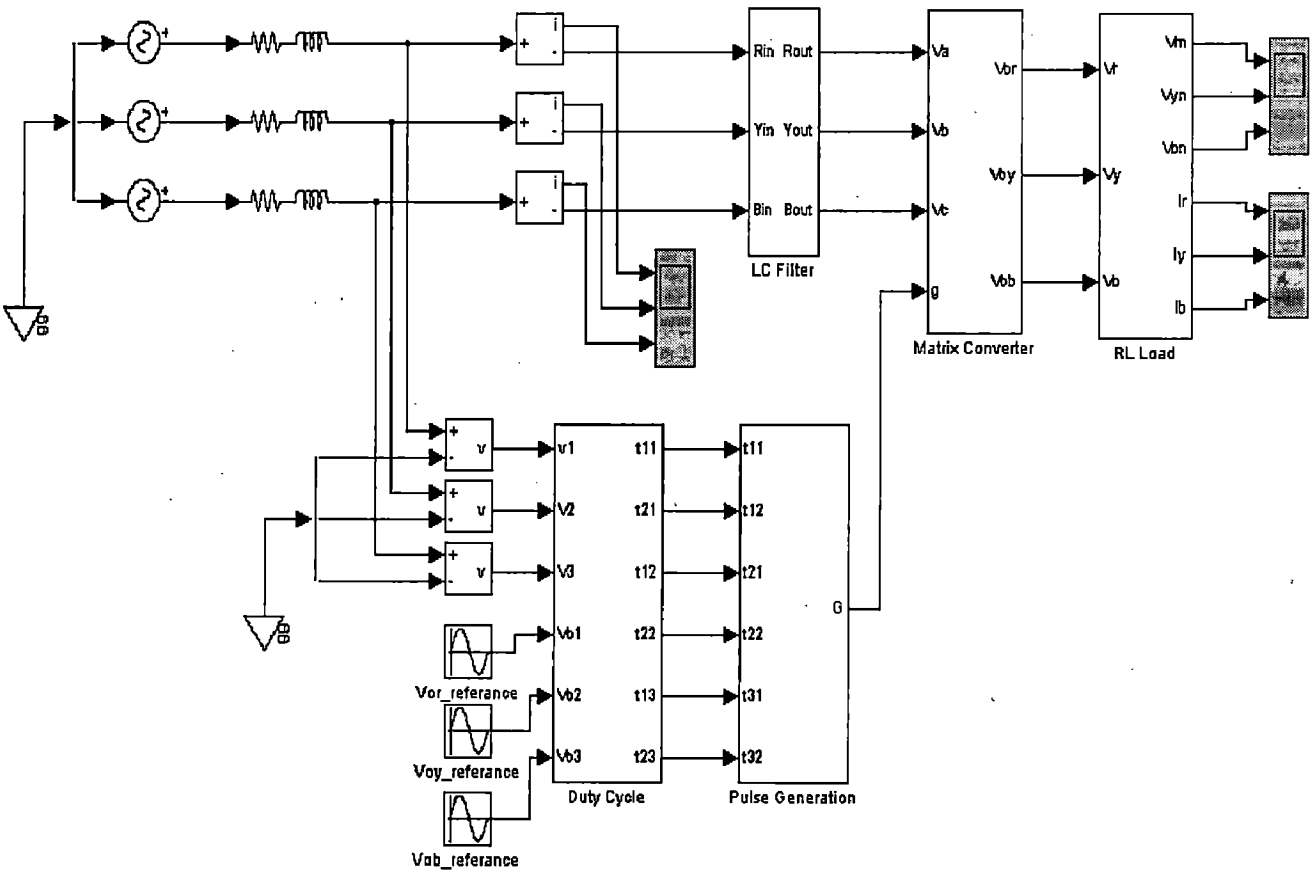

Figure 4.1: Simulation model developed in MATLAB using simulink

converter using MOSFETs, Current Measurement, Voltage Measurement, Capacitor, Inductor, Comparator, Multiplexers/ De-Multiplexers, Scope. For different output frequencies quantities like Output voltage, output current and input currents have been observed for 3-phase to 3-phase matrix converter.

4.2 Simulation Model Explanation

The model developed in MATLAB is shown in *fig 4.1*; it shows L-C filter block, 3-phase to 3-phase matrix converter block which contains nine bidirectional switches, Duty cycle generation block for bidirectional switches which uses venturini modulation method as discussed in chapter 3, pulse generation block and R-L load. Some important blocks are explained below.

4.2.1 Matrix Converter Power Circuit

The three phase matrix converter block consists of a nine bidirectional switch connected in 3 X 3 matrix form. Each bi-directional switch consists of two fast recovery

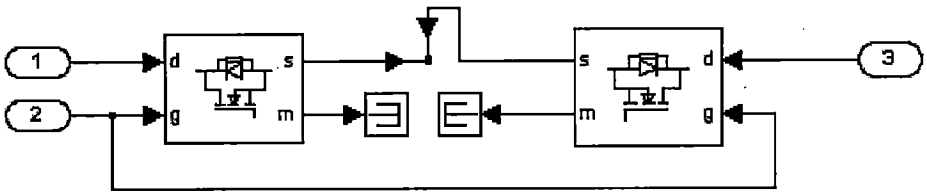

Figure 4.2: One bidirectional switch of 3-phase to 3-phase matrix converter

diodes and two switch devices such as MOSFET. One bidirectional switch of matrix converter is shown in *fig 4.2.*

4.2.2 Duty Cycle Generation

Fig 4.3 shows the general structure of the module that generates the components m_{ij} of matrix M(t), taking as inputs the current samples of the Matrix converter input voltage (V_i) and of the desired output voltages ($V_{jN}=V_{jREF}$)

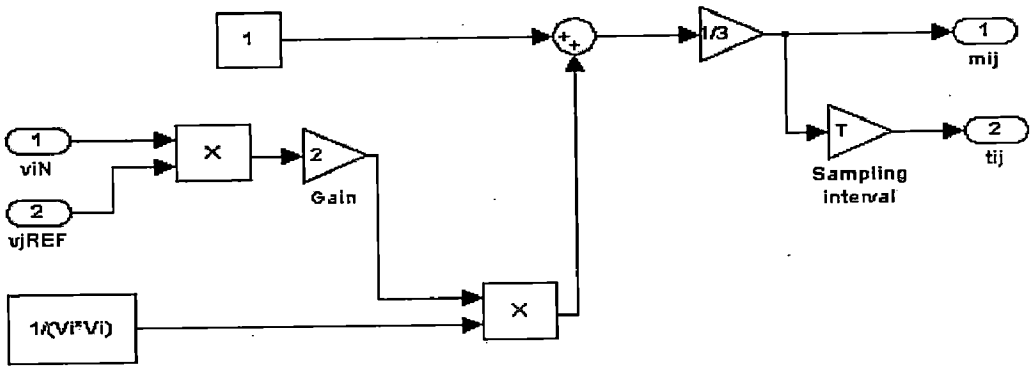

Figure 4.3: Generation of the duty cycle mij

4.2.3 Pulse Generation Scheme

The most important part of the simulation is the generation of switching functions of the bidirectional switches ($S_{ij}(t)$). These functions correspond to the gate drive signals

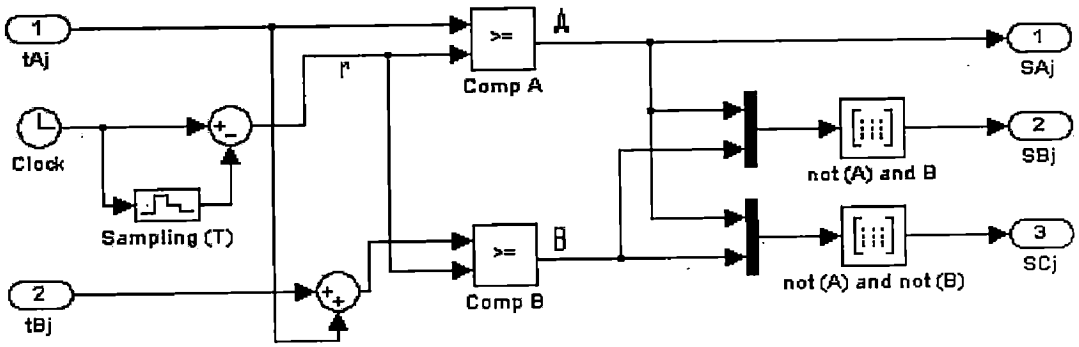

Figure 4.4: Pulse generation scheme for one output phase

of the power switches in the real converter. *Fig 4.4* presents the block diagram used to generate these functions in the case of jth output phase.This block diagram is more easily understood if we consider the variables and waveforms shown in *fig.4.5*, which corresponds to the following conditions: switching (sampling) time T=1 ms and conduction times t_{Aj}=0.4ms, t_{Bj}=0.2ms and t_{Cj}=0.4 ms. The variable r is ramp function with slope 1, starting from zero at the beginning of each sampling interval. This variable is compared with times t_{Aj} and $t_{Aj} + t_{Bj}$, using comparators CompA and CompB respectively. The output of comparator CompA is the required switching function S_{Aj}, which corresponds to a pulse of amplitude 1 with duration equal to t_{Aj}. The following logic decisions are used to generate the other switching functions:

$$S_{Bj} = \text{not (A) and B}$$

$$S_{Cj} = \text{not (A) and not (B)}$$

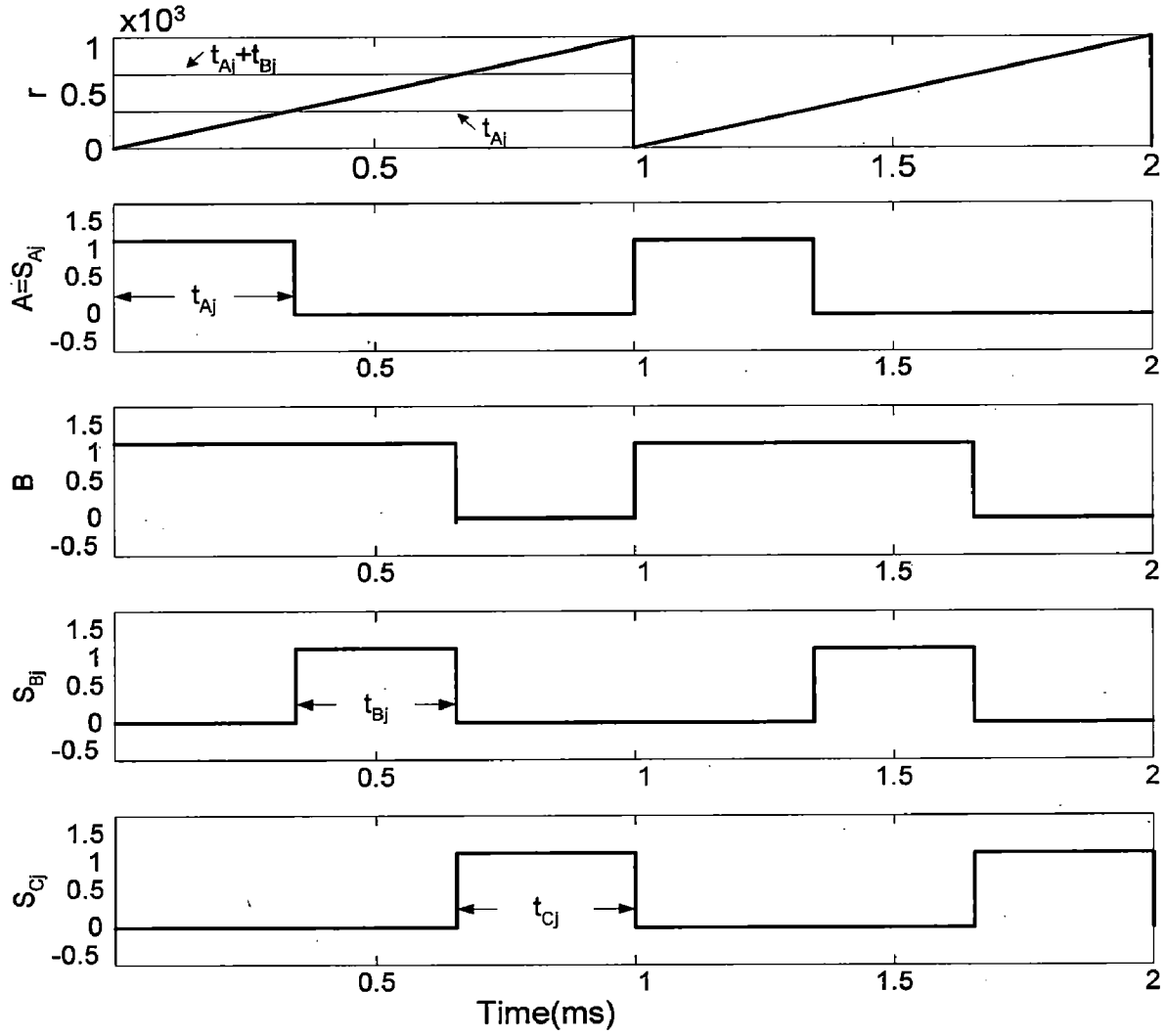

Figure 4.5: Variables used for the pulse generation of one output phase

4.3 Simulation Results

Simulation studies have been done for different cases with following parameters: Source Voltage 220V, 50Hz Load resistances R=10Ω and Load Inductance L=50 mH, switching frequency f_s=2000Hz.

Results of the unloaded matrix converter operated at Input voltage amplitude Vi=√2 × 220V, input frequency f_i=50Hz, output frequency f_o=100Hz, switching frequency f_s=2000Hz, voltage gain q=Vo/Vi=0.5 (this means that the reference has an amplitude equal to 0.5 ×√2 × 220V=155.56V and a frequency of 100 Hz), are presented in *figs 4.6-4.10. Fig 4.6* shows the output voltages with respect to source neutral V_{aN}, V_{bN} and V_{cN}. The FFT

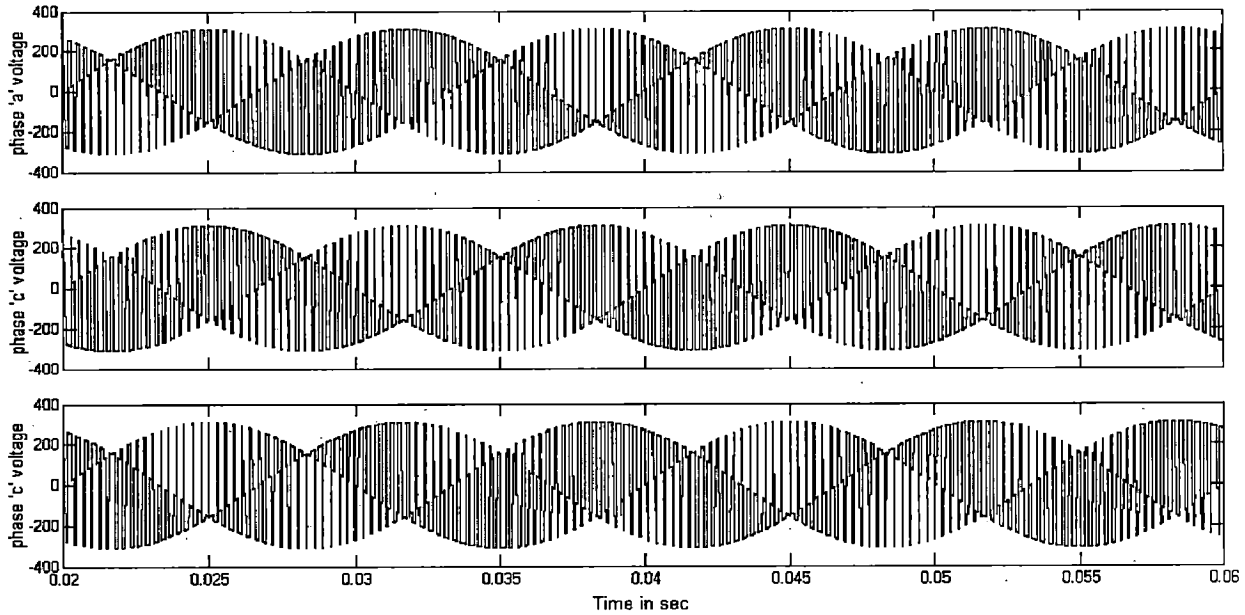

Figure 4.6: Simulation result of unloaded operation of a matrix converter at f_o=100Hz; Output voltages V_{aN}, V_{bN} and V_{cN}

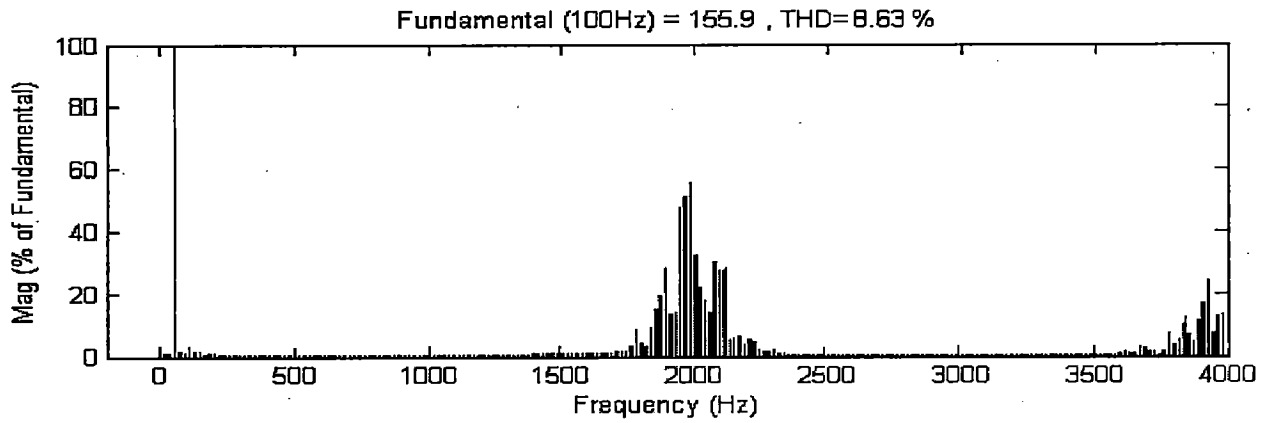

Figure 4.7: Simulation result of unloaded operation of a matrix converter at f_s=2000Hz f_o=100Hz; FFT of Output voltages V_{aN}

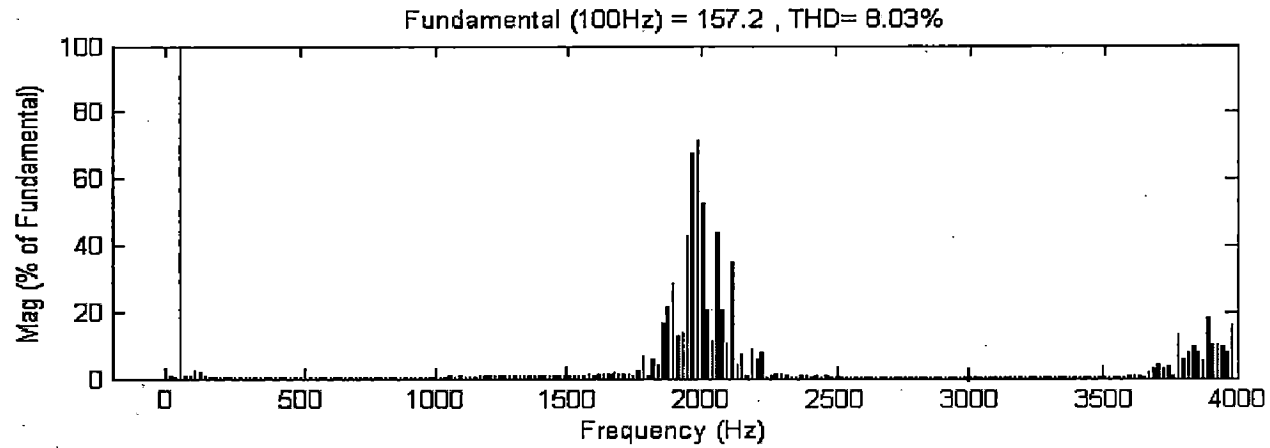

Figure 4.8: Simulation result of unloaded operation of a matrix converter at f_s=2000Hz f_o=100Hz; FFT of Output voltages V_{bN}

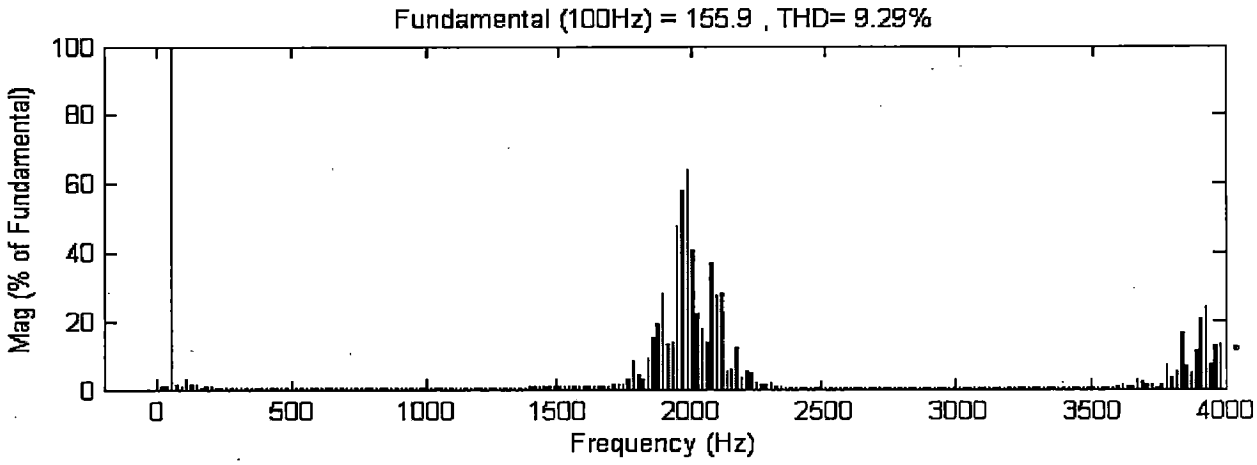

Figure 4.9: Simulation result of unloaded operation of a matrix converter at f_s=2000Hz f_o=100Hz; FFT of Output voltages V_{cN}

analysis of output voltage is shown in *Fig 4.7-4.9*; the results show that Total Harmonic Distortion is about 8%. The main Harmonics located at 100Hz and additional harmonics are around switching frequency. The duty cycle for all nine bidirectional switch are shown in *fig. 4.10.*

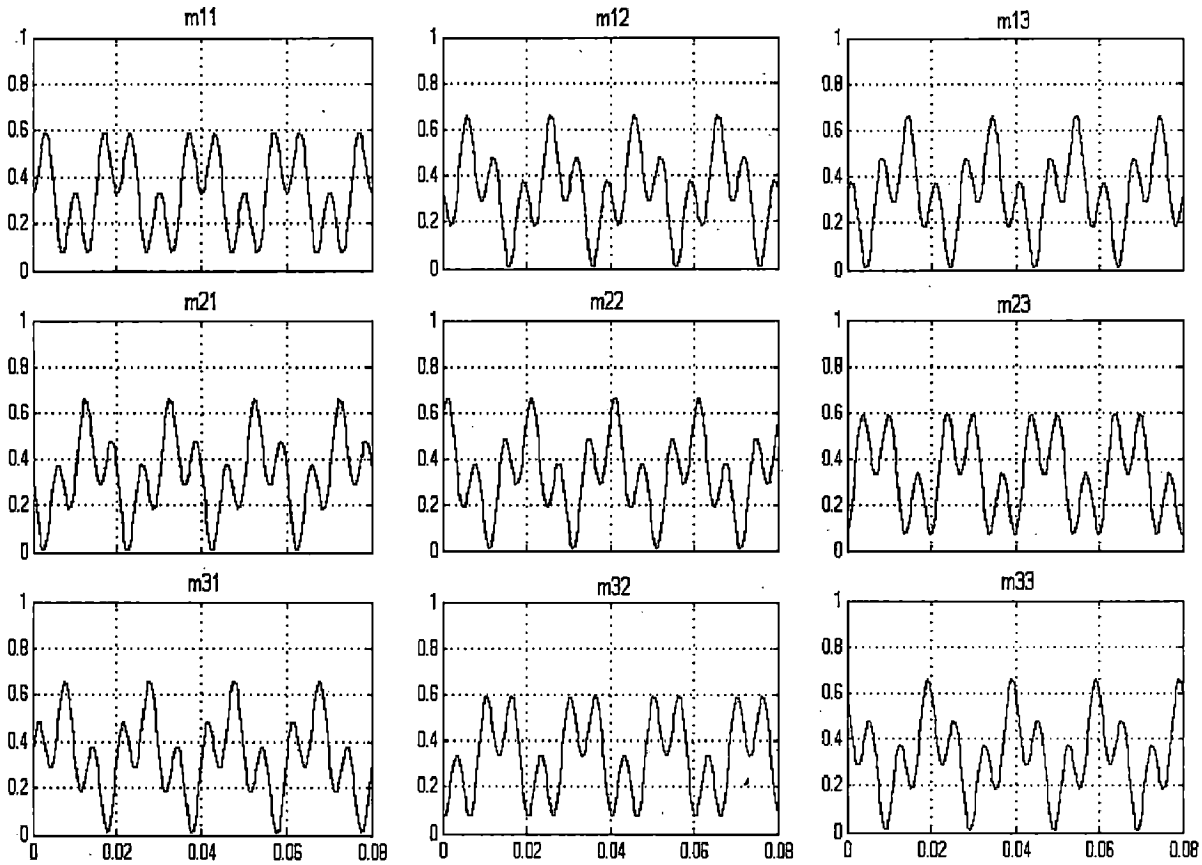

Figure 4.10: Simulation results of unloaded operation of a matrix converter at f_s=2000Hz f_o=100Hz; Calculated m-values

Simulation results of a matrix converter loaded with R-L load at $V_i=\sqrt{2} \times 220V$, $f_i=50Hz$, $f_o=100Hz$, $f_s=2000Hz$, voltage gain $q=Vo/Vi=0.5$, are presented in *Figs 4.11-4.13*. In general, the neutral of the load n is isolated from the neutral of source N. *Fig. 4.11* shows the output voltage for one phase of matrix converter with respect to load neutral n (V_{jn}). Output line to line voltage $V_{ab.}$ is shown in *fig 4.12*. The FFT analysis of output current is shown in *Fig 4.16*; the results show that total harmonic distortion (THD) is 1.28%. The main Harmonics located at 100Hz and additional harmonics are around switching frequency.

Load Specifications:

R-L load: R=10Ω, L=50mH

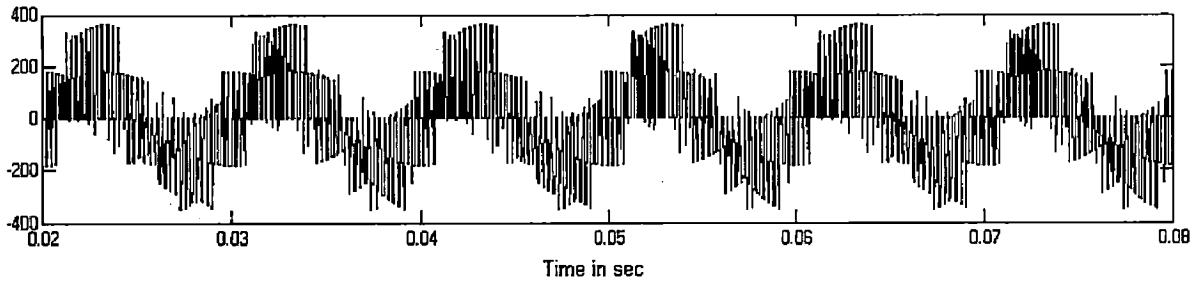

Figure 4.11: Simulation results of a matrix converter operated with R-L load at f_o=100Hz; Output voltage $V_{an.}$

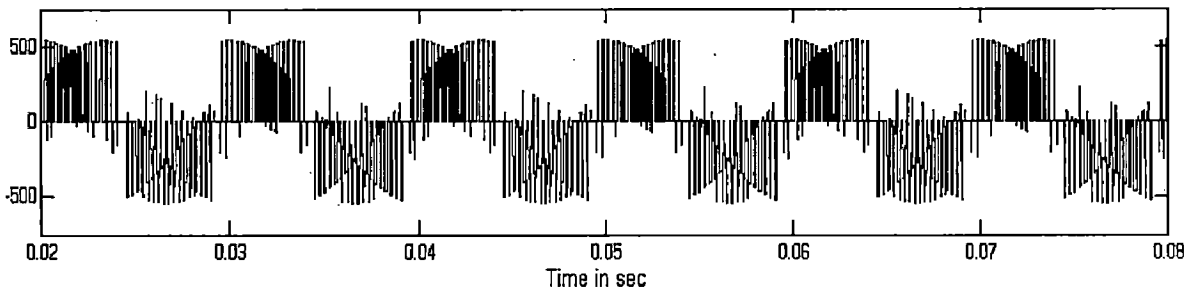

Figure 4.12: Simulation results of a matrix converter operated with R-L load at f_o=100Hz; Output line voltage $V_{ab.}$

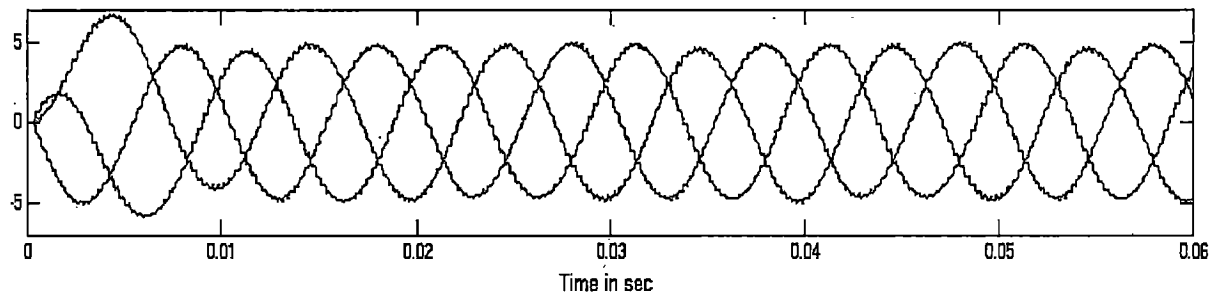

Figure 4.13: Simulation results of a matrix converter operated with R-L load at f_o=100Hz; Output current for all 3-phase.

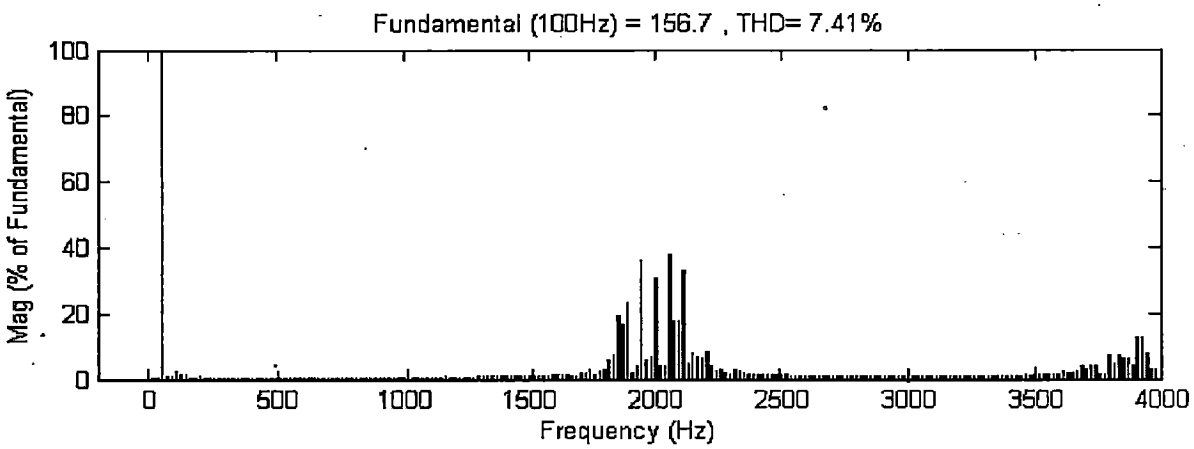

Figure 4.14: Simulation results of a matrix converter operated with R-L load at f_s=2000Hz; fo=100Hz; FFT of a Output phase voltage V_{an}.

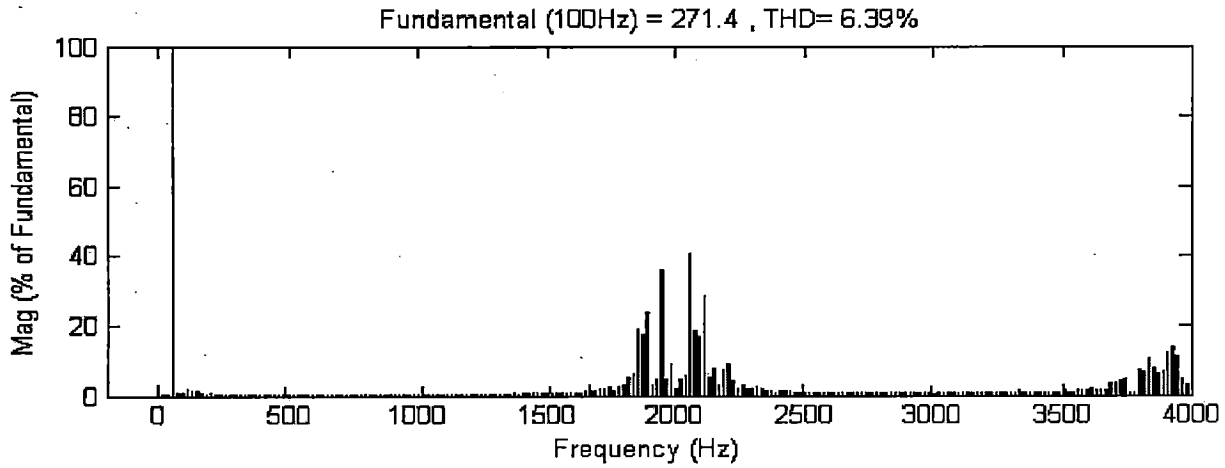

Figure 4.15: Simulation results of a matrix converter operated with R-L load at f_s=2000Hz, fo=100Hz; FFT of a Output line to line voltage V_{ab}.

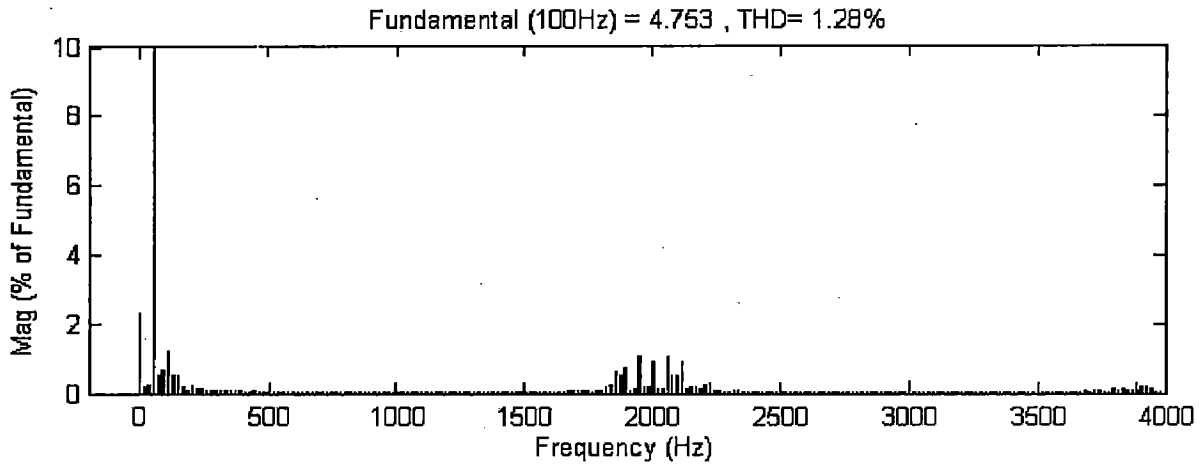

Figure 4.16: Simulation results of a matrix converter operated with R-L load at f_s=2000Hz, fo=100Hz; FFT of a Output line current of phase 'a'.

Simulation results of a matrix converter loaded with R-L load at Vi=$\sqrt{2}$ × 220V, fi=50Hz, f_o=25Hz, f_s=2000Hz, q=V_o/V_i=0.5, are presented in *Figs 4.17-4.22. Fig. 4.17*

shows the output voltage for one phase of matrix converter with respect to load neutral n (V_{jn}). The FFT analysis of output voltage is shown in *Fig 4.20*; the results show that Total Harmonic Distortion is 4.49%. Output line voltage V_{ab} and output current are shown in *fig 4.18* and *fig 4.19* respectively. Their FFT analysis are shown in *fig 4.21* and *fig 4.22* respectively. The main Harmonics located at 25Hz and additional harmonics are around switching frequency.

Load Specifications:

R-L load: R=10Ω, L=50mH

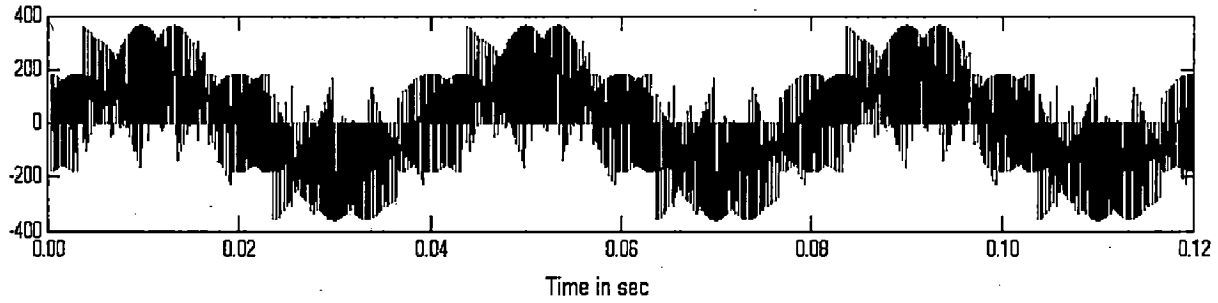

Figure 4.17: Simulation results of a matrix converter operated with R-L load at f_o=25Hz; Output voltage V_{an}.

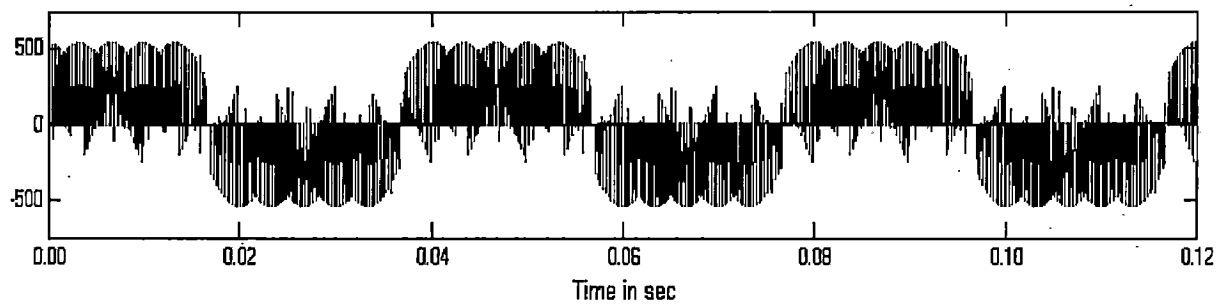

Figure 4.18: Simulation results of a matrix converter operated with R-L load at f_o=25Hz; Output line voltage V_{ab}.

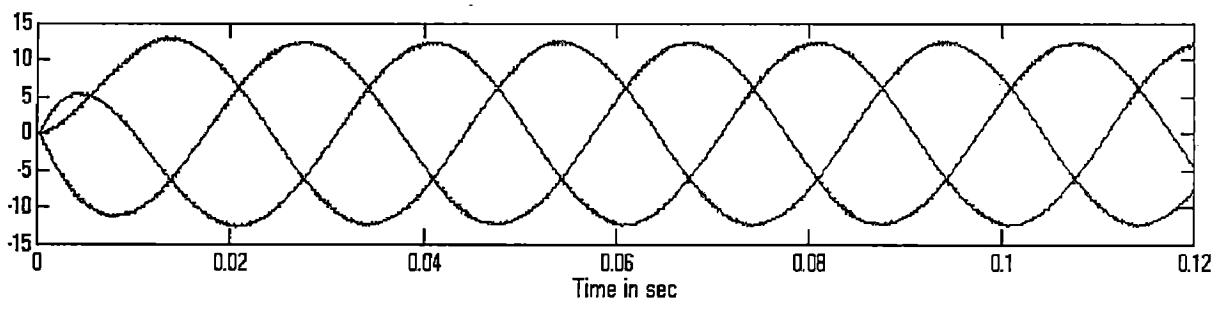

Figure 4.19: Simulation results of a matrix converter operated with R-L load at f_o=100Hz; Output line current for all 3-phase

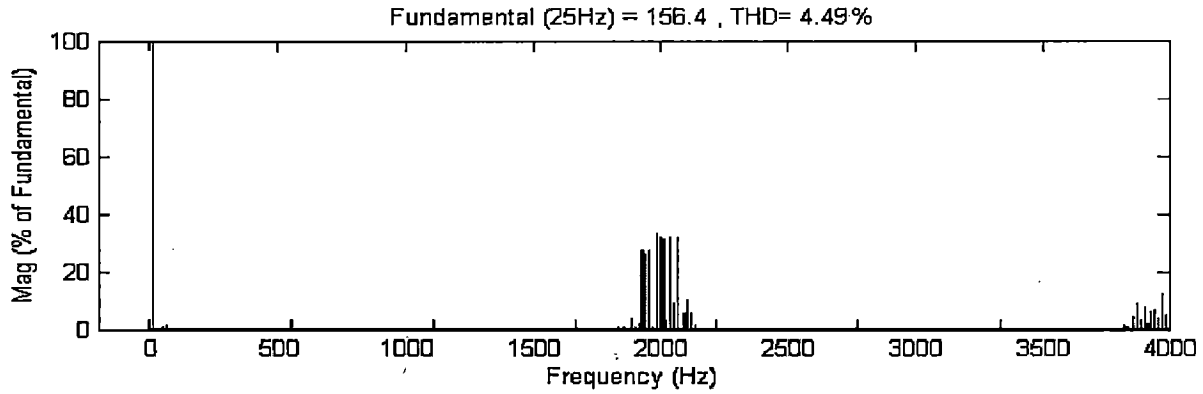

Figure 4.20: Simulation results of a matrix converter operated with R-L load at f_s=2000Hz, fo=25Hz; FFT of a Output phase voltage V_{an}.

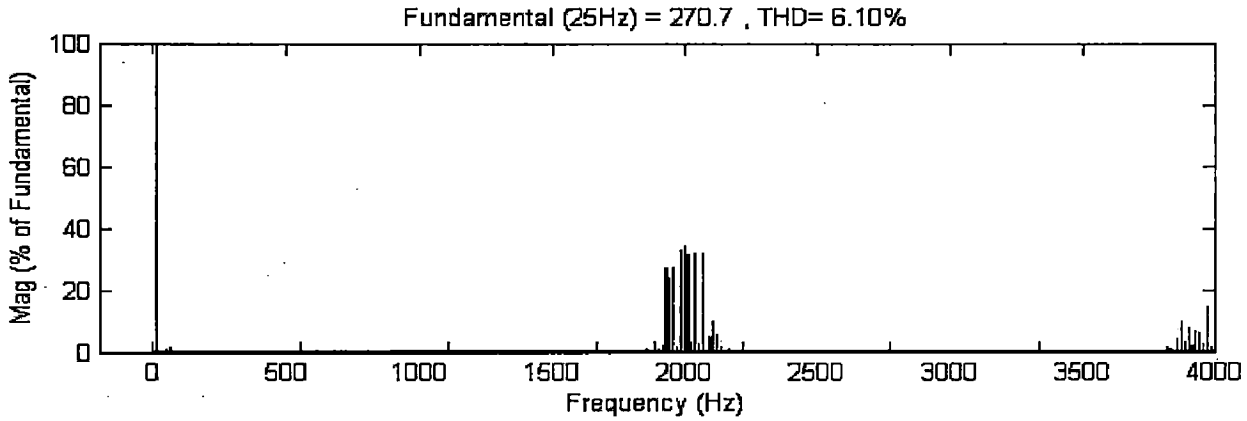

Figure 4.21: Simulation results of a matrix converter operated with R-L load at f_s=2000Hz, fo=25Hz ; FFT of a Output line to line voltage V_{ab}.

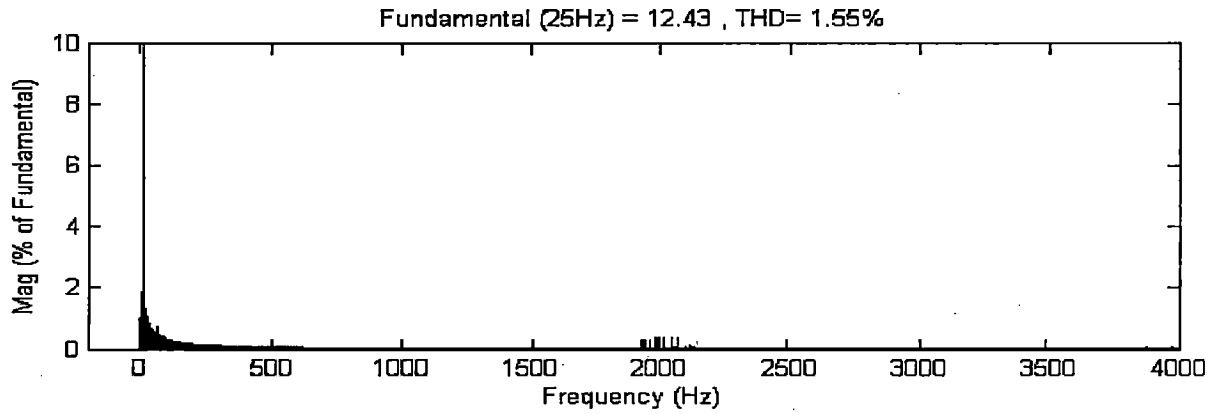

Figure 4.22: Simulation results of a matrix converter operated with R-L load at f_s=2000Hz, fo=25Hz; FFT of a Output line current of phase 'a'.

Fig. 4.23-4.24 illustrate the simulation results for a step change in output frequency. The frequency changes instantaneously from 50 Hz to 25Hz at t=40 ms. Matrix converter

loaded with R-L load (R=10Ω, L=50mH) at amplitude of input voltage $V_i=\sqrt{2} \times 220V$, $f_i=50Hz$, $f_s=2000Hz$, $q=V_o/V_i=0.5$.

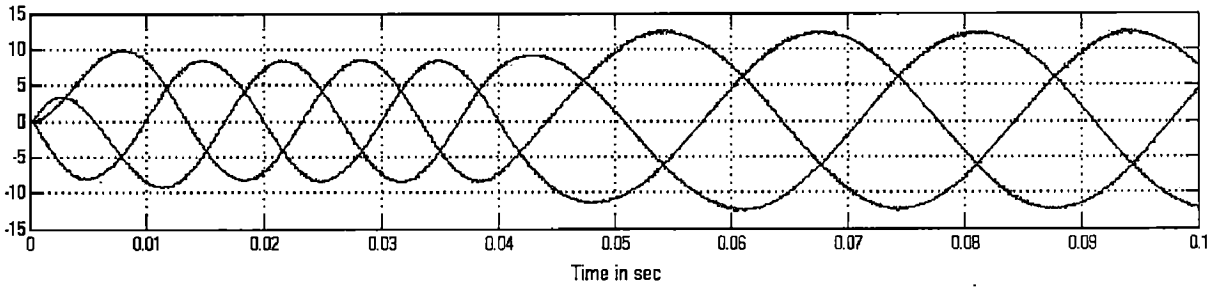

Figure 4.23: Simulation result of output line currents for step change in output frequency from 50Hz to 25Hz at t=40ms.

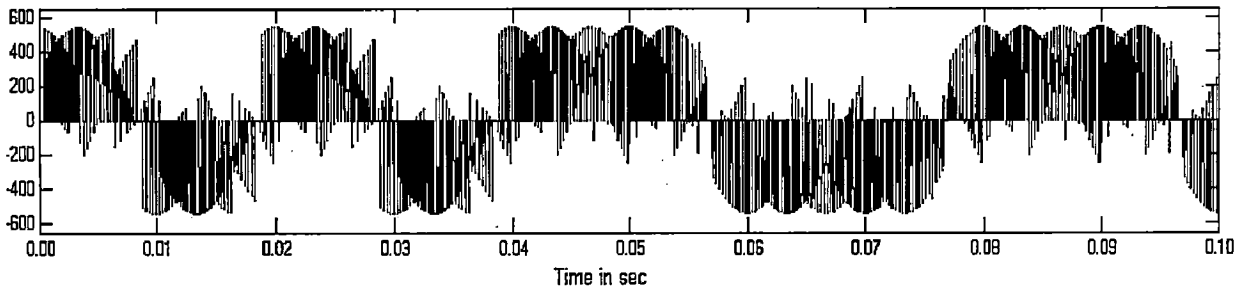

Figure 4.24: Simulation result of output line voltage V_{ab} for step change in output frequency from 50Hz to 25Hz at t=40ms.

Fig. 4.25 shows that the input current generated by the matrix converter has the form of several pulses with a high di/dt, making it necessary to introduce an input filter to avoid the generation of over voltages. The parameters of the converter for simulation are $Vi=\sqrt{2} \times 220V$, $f_i=50Hz$, $f_o=100Hz$, $f_s=2000Hz$, Load parameters R=10Ω, L=50mH, gain q=Vo/Vi=0.5, Filter Inductor=200μH, Filter capacitor=30μF. The frequency spectrum of *fig 4.25* confirms the presence of high order harmonics in input current with THD of about 69%. *Fig. 4.26* shows that the source current i_{sA} is free of high-frequency harmonics due to the action of the input filter, where the THD reduced to 10.58%.

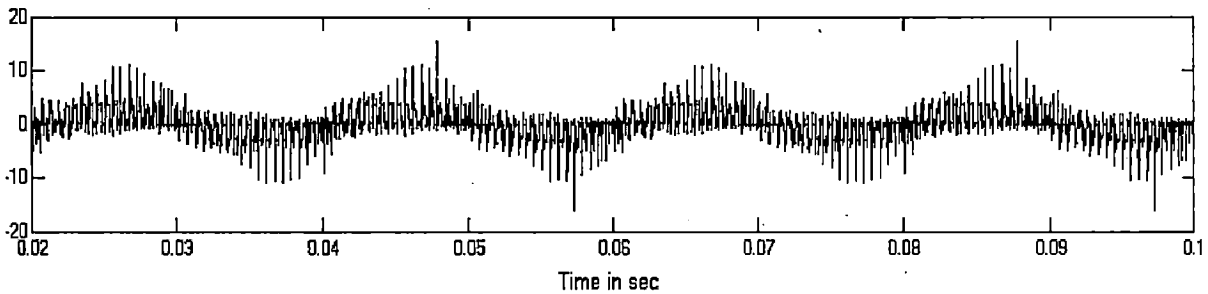

Figure 4.25: Input current before the inception of input filter (THD=69%).

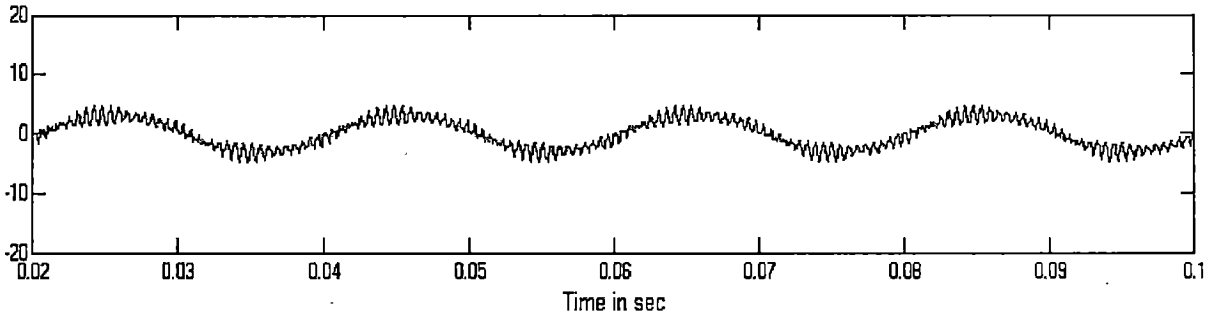

Figure 4.26 Input current after the inception of input filter (THD=10.58%).

Fig 4.27 shows the filtered input line current and input phase voltage of the matrix converter feeding R-L load. In this case, the converter operates at a 25-Hz output

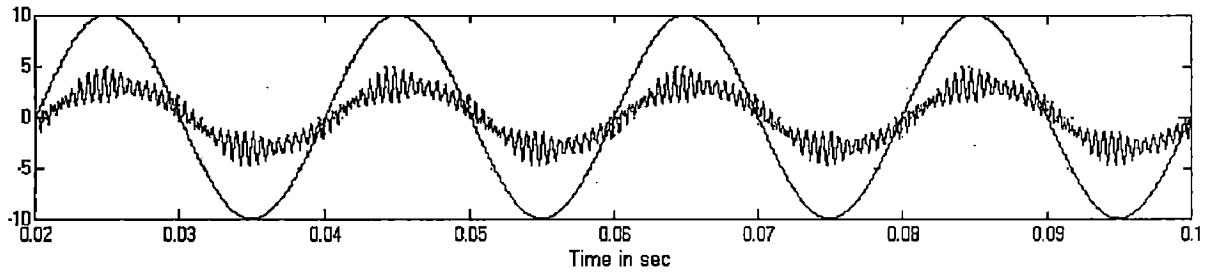

Figure 4.27: Simulation result of Input line current and input phase voltage with R-L load at f_s=2000Hz, fo=100Hz.

frequency with a 2 kHz switching frequency and a 220V phase voltage. As explained in chapter 3 the venturini modulation algorithm provides a unity input displacement factor at the input regardless of the load power factor. This is shown in *fig 4.27*, where the input current and voltage are in phase.

4.4 Conclusion

The simulation of the 3-phase to 3-phase matrix converter controlled with the Venturini modulation strategy been presented and clearly explained. Results are obtained for different output frequencies for matrix converter with R-L load. It was shown that THD of source current has reduced to 10.58% from 69% after inception input filter. Simulation studies carried out by suddenly changing output frequency.

System Development

This chapter describes the design of the hardware developed for the realization of 3-phase to 3-phase matrix converter. The protection of the MOSFETs has been discussed. All the hardware requirements have been discussed briefly in the following sections. PC interfacing with the hardware and data acquisition cards has been described briefly. Only pictorial representation of the above control techniques has been given trough flow charts.

5.1 Hardware development

The complete schematic diagram of 3-phase to 3-phase matrix converter is shown in *fig 5.1.* The system hardware can be divided in the following blocks:

- Power circuit
- Pulse amplification and isolation circuit
- Power supplies
- Circuit protection
- Zero crossing circuit
- AC voltage sensing circuit

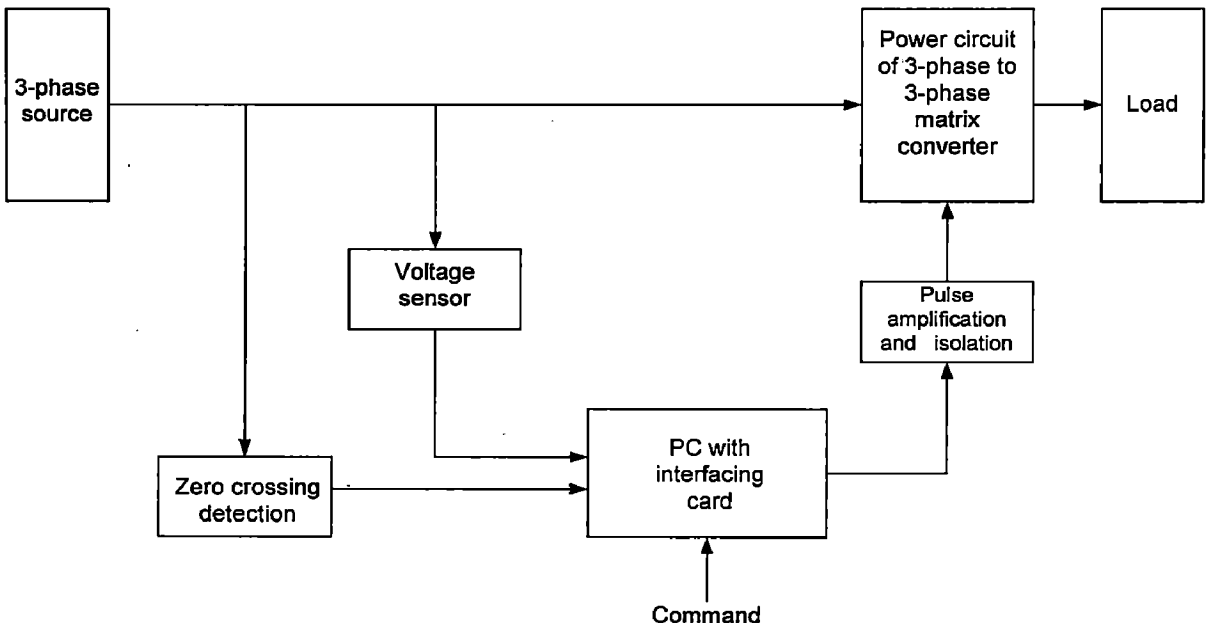

Figure 5.1: Complete scheme of 3-phase to 3-phase matrix converter

5.1.1 Power Circuit

Fig. 5.2 shows the power circuit of the 3-Phase to 3-phase matrix converter. The matrix converter requires a bi-directional switch capable of blocking voltage and conducting current in both directions. Unfortunately there is no such device currently available that fulfill the needs: so discrete devices need to be used to construct suitable bi-directional cells. Diode bridge bidirectional switch cell is used for the power circuit of 3-phase to 3-phase matrix converter. The number of Bi-directional switch required is nine in 3-phase to 3-phase matrix converter. MOSFET's are selected as power devices to use for developing 3-phase to 3-phase matrix converter. MOSFET switch is used in the circuit consists of an inbuilt anti parallel free wheeling diode. No forced commutation circuits are required for MOSFET because these are self commutated devices (they turn on when the gate signal is high and turn off when the gate signal is low). The data sheet of this MOSFET can be found in Appendix–B. These power devices are placed on heat sinks to dissipate the excessive heat generated by the switches. The heat sinks were made using aluminum sheet with thickness of 5mm.

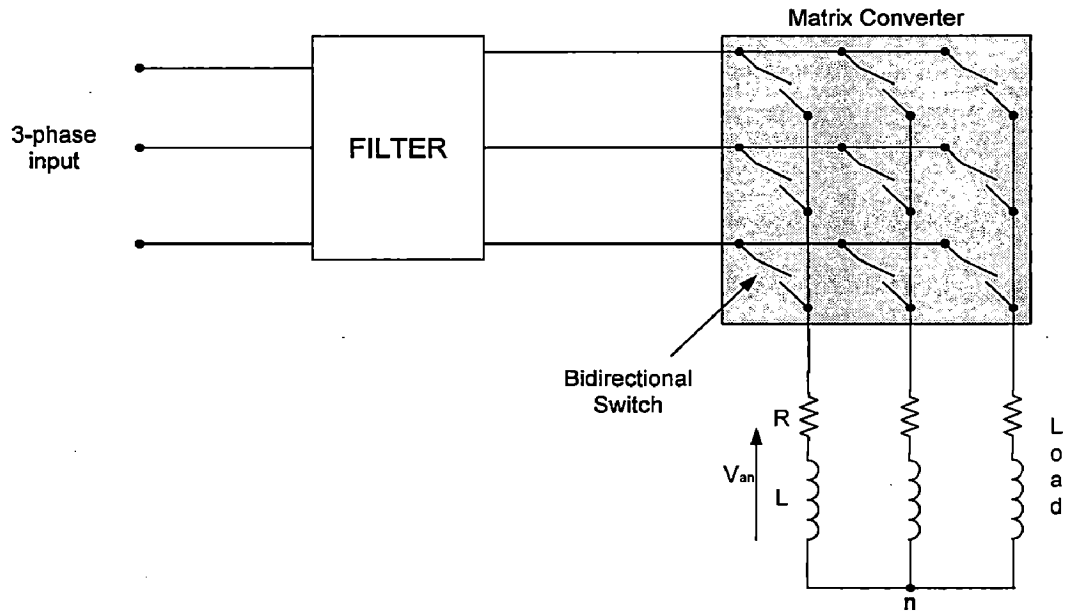

Figure 5.2: Basic power circuit of matrix converter

The load inductance restricts large di/dt through MOSFETs; hence only turnoff snubber is required for protection. An RCD (resistor, capacitor and diode) turn-off circuit is connected

to protect the circuit against high dv/dt and is protected against power voltage by connecting MOV (Metal Oxide Varistor).

5.1.1.1 Diode Bridge Bidirectional Switch cell

The diode bridge bidirectional switch cell arrangement consists of MOSFET (IRFP460) at the center of a single phase diode bridge arrangement as shown in *fig. 5.3*. Such nine bi-directional switch cell are required for 3-phase to 3-phase matrix converter. The main advantage is that both current directions are carried by the same switching device, therefore, only one gate driver is required per switch cell. Device losses are relatively high since there are three devices in each conduction path.

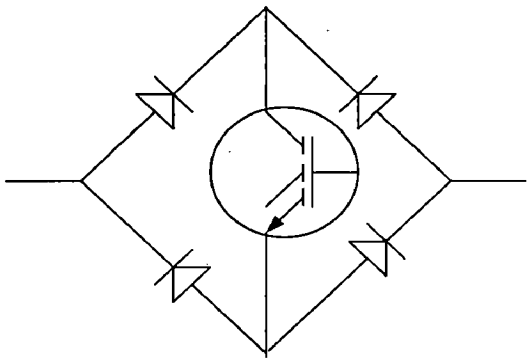

Figure 5.3: Diode bridge bidirectional switch cell

5.1.2 Snubber circuit

An RC snubber circuit has been used for the protection of the main switching device. Switching high currents in short time gives rise to voltage transients that could exceed the rating of MOSFET. Snubbers are therefore needed to protect the switch from transients. Snubber circuit for MOSFET is shown in *fig 5.4*. The diode prevents the discharging of capacitor via the switching device, which could damage the device owing to large discharge current. An additional protective device metal-oxide-Varistor (MOV) is used across each device to provide the protection against the over voltages. MOV acts as a back to back zener and bypasses the transient over voltages across the devices. The value of R is 3.3 kΩ, 5 W and C is 0.1 μF.

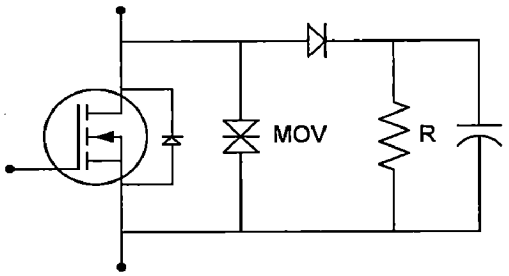

Figure 5.4: Snubber circuit for MOSFET protection

5.1.3 Pulse Amplification and Isolation Circuit

The pulse amplification and isolation circuit for MOSFET is shown in *fig 5.5*. The opto-coupler (MCT-2E) provides the necessary isolation between the low voltage isolation circuit and high voltage power circuit .The pulse amplification is provided by the output amplifier transistor 2N222. When the input gating pulse is at +5V level, the transistor saturates, the LED conducts and the light emitted by it falls on the base of phototransistor, thus forming its base drive. The output transistor thus receive no base drive and, therefore remains in cut-off state and a +12 v pulse (amplified) appears across it's collector terminal.

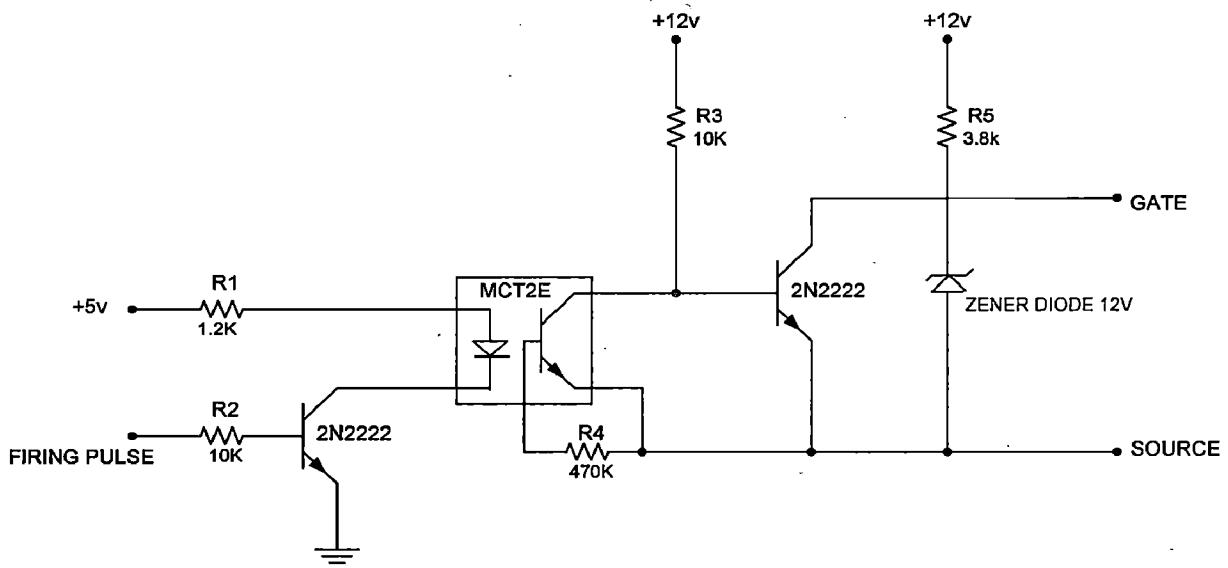

Figure 5.5: Pulse amplification and isolation Circuit

When the input gating pulse reaches the ground level (0V), the input switching transistor goes into the cut-off state and LED remains off, thus emitting no light and therefore a photo transistor of the opto-coupler receives no base drive and, therefore remains in cut-off state .A sufficient base drive now applies across the base of the output

amplifier transistor it goes into the saturation state and hence the output falls to ground level. Therefore circuit provides proper amplification and isolation. Further, since slightest spike above 20V can damage the MOSFET, a 12 V Zenor diode is connected across the output of isolation circuit. It clamps the triggering voltage at 12 V.

5.1.4 Power Supplies

DC regulated power supplies (+12v, -12v, +5v) are required for providing biasing

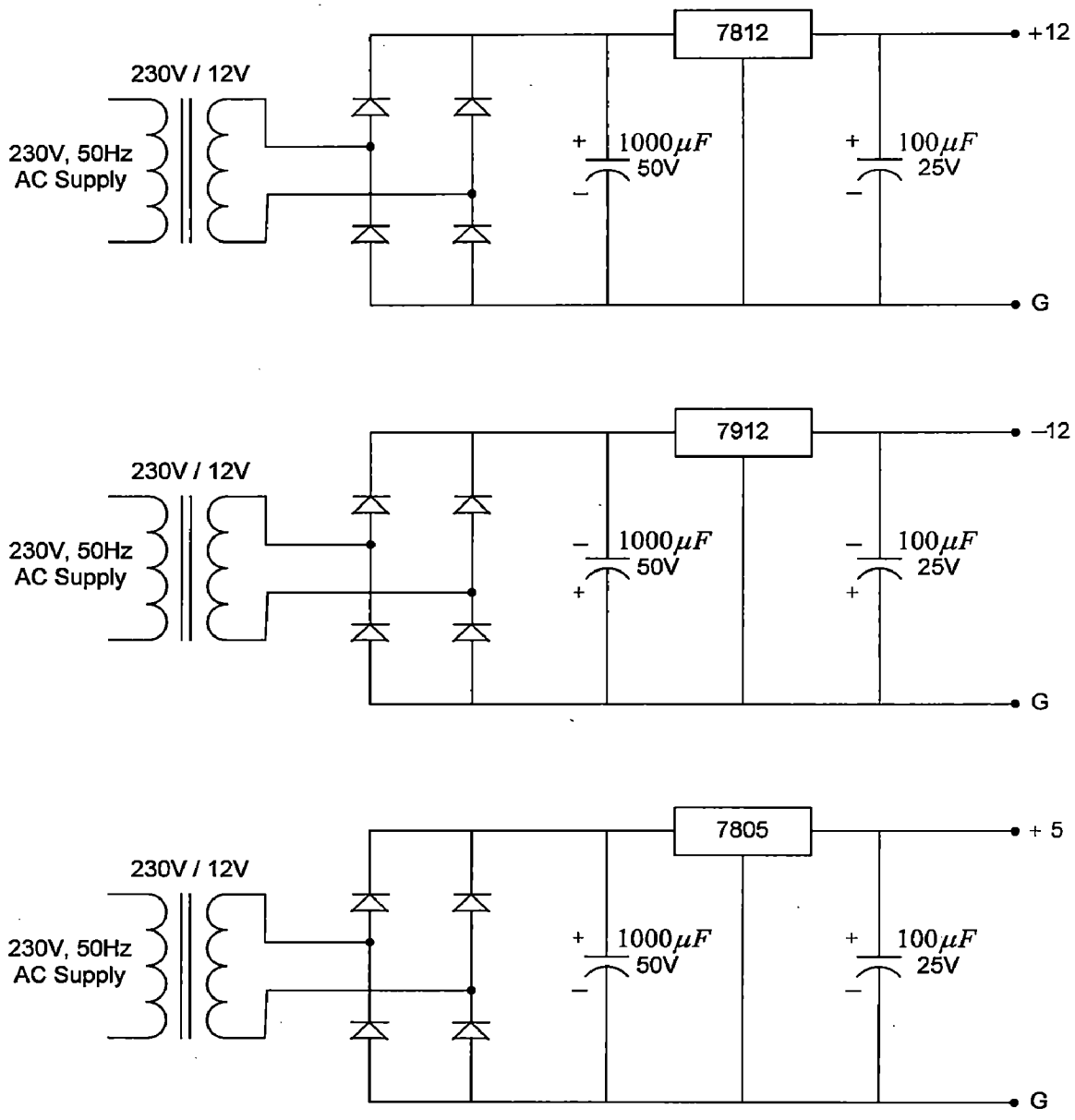

Figure 5.6: Circuit diagrams for IC regulated power supplies

100μf, 25V capacitor is connected at the output of the IC voltage regulator of each supply for obtaining the constant and ripple free DC voltage.

5.1.5 Zero Crossing Detection Circuit

A zero crossing detection circuit produces an output signal which changes state to indicate the occurrence of a positive-going zero crossing of an AC input signal. To synchronize the program with input frequency zero crossing interrupt is used. One phase is connected to the zero crossing detection circuit, which produce output pulse for rising edge of voltage from its zero. The zero crossing detection circuit offers the ability to sense zero crossings of AC input signals having a wide range of AC voltages. The zero crossing signal is connected to the interrupt line IR2 of VPC-IOT card.

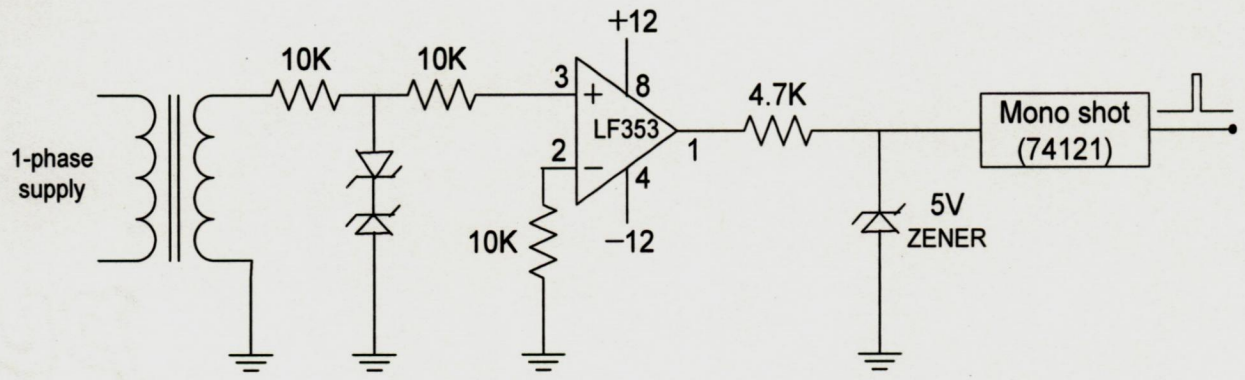

Figure 5.7: Zero crossing detection circuit

5.1.6 AC Voltage Sensing Circuit

The ac output voltage of the capacitor is sensed through isolation amplifier AD202 for the voltage control of the converter. AD202 provide the total galvanic isolation between input and output stages of the isolation amplifier through the use of internal transformer coupling. It gives a bi-polar output voltage +5v, adjustable gain range from 1v/v to 100v/v, +0.025% max non-linearity, 130db of CMR and 75mw of power consumption. Circuit diagram is shown in *fig 5.8*. In the shown figure output amplifier is made using op-amp which will be helpful in calibration. The transient response will deteriorate by using passive filter at the input side of AD202; but to reduce the ripples in measurement and control purpose it cannot be avoided.

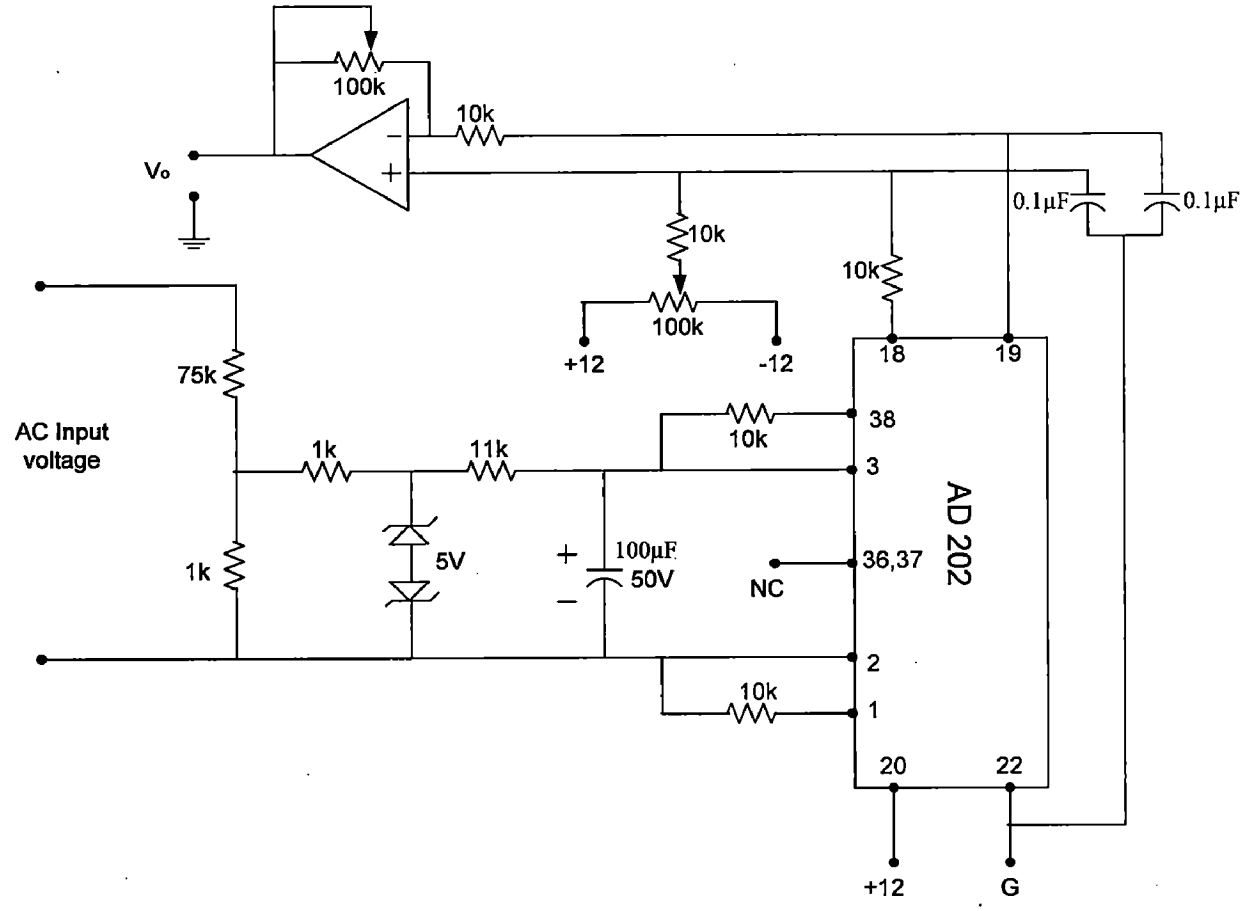

Figure 5.8: Circuit diagram used for AC voltage sensing

5.2 PC Interfacing and Control

For real-time application, the Venturini modulation method was implemented using PC compatible card. Pentium MMX Processor based PC with Digital input/output & Timer counter card (VPC-IOT) Vinytics Timer I/O card and ADC has been used for this application. VPC-IOT is a Programmable Input-Output interface card for IBM-PC/XT/AT or their compatibles. An interface card is employed for the output and timing of the PWM gating signal to the converter. The card contains 48 fully programmable input output lines, 3 independently programmable 16-bit counters. This card provides two 8255 each having three I/O ports A, B, C. Since there are 9 switches in 3-phase to 3-phase Matrix converter, three bits from each ports are being used as firing bits. The card has two timer chips 8253-1 and 8253-2. Each 8253 chip has three counters out of which TIMER2_0, TIMER2_1 and TIMER2_2 from 8253-2 have been used to control bidirectional switches of output Phase A, Phase B and Phase C respectively, and TIMER1_0 from 8253-1 for times out the

sampling period T_s. 2MHz clock from VPC-IOT card has been used as clock signal to all counters. Four bits from PORTC are being used as GATES of four counters. During each sampling interval the PC calculates nine switch duty cycles m_{ij} based on equation. 3.12 from chapter 3, while at the output port the timers time out the PWM gating signals. The calculated results are converted into integer time counts using the 2MHz clock frequency. These are used for next sampling period. At the beginning of each switching cycle, three timer pairs are loaded with T_{1j} (j=1, 2, 3) and TIMER1_0 with T_s. The timer countdown process begins with the outputs held low. When the timer finishes counting the corresponding outputs go high which changes PWM switching pattern. Subsequently, when TIMER1_0 finishes counting, it generates an interrupt signal to the PC that responds by loading timers with calculated integer counts and T_s, respectively, hence restarting the pulse output process.

The interrupt line IR4, IR5, IR7 connected to output of timer TIMER2_0, TIMER2_1, and TIMER2_2 for gating pulse generation. IR3 is connected to TIMER1_0, for interrupt at every sampling interval T_s. IR2 is connected to Zero crossing detection circuit. To avoid any damage to the ports, a buffer circuit has been fabricated (using 74245 buffers) and all firing bits are first buffered and then applied to the switching devices. The source code has been written in 'C' language.

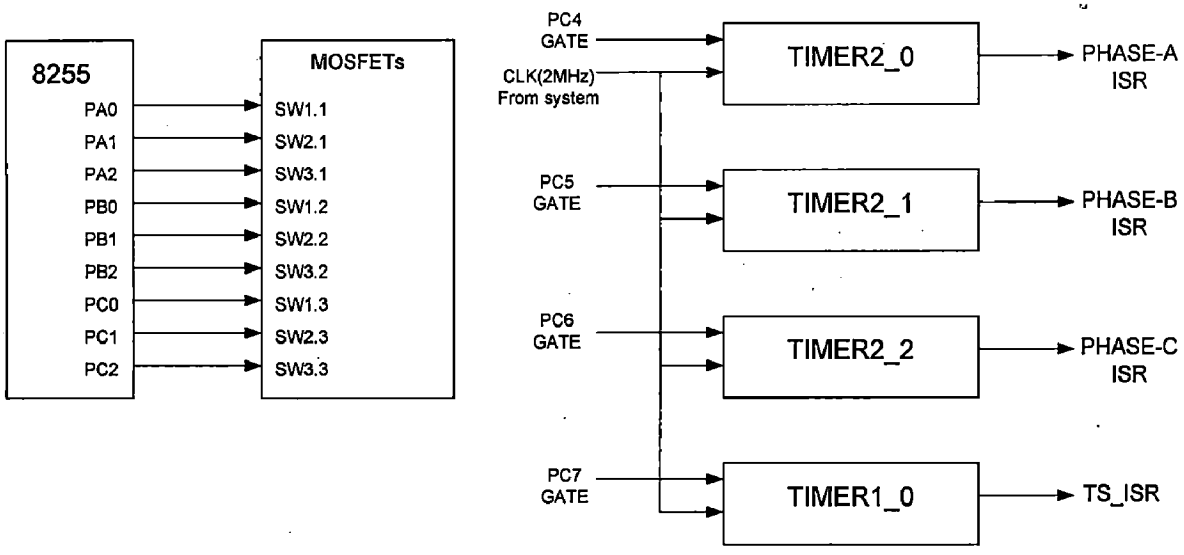

Figure 5.9: PC Interfacing to three phase to three phase matrix converter

5.3 Software Development

The Venturini control technique discussed in previous chapter was implemented through Pentium MMX processor based PC and Interfacing cards. Microprocessor based control reduces the complexity of the system hardware, increases the reliability and makes the control system fast.

The system hardware of the 3-phase to 3-phase matrix converter has been discussed in this chapter. For superior performance and fast response a suitable software is to be developed. The system software development consists of the main program of the system in open.. Only pictorial representation of the software is given through flow charts. The complete software has been developed using 'C' language.

5.4 Flow Chart

This software is based on two modules: the initialization module and the run module. The former is performed only once at the beginning. The second module is based on a waiting loop interrupted by the PWM underflow. When the interrupt flag is set, this is acknowledged and the corresponding Interrupt Service Routine (ISR) is served. The complete algorithm is computed within the PWM ISR. An overview of the software is given in the flow chart below:

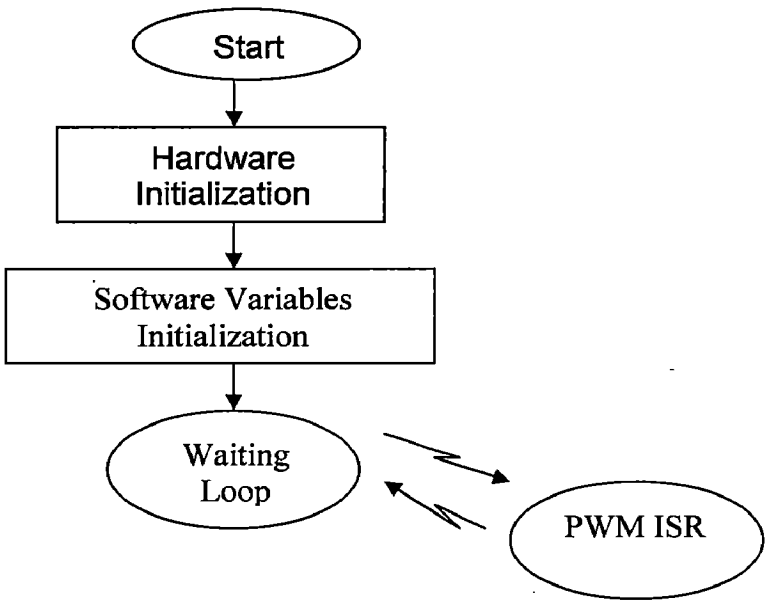

Main program

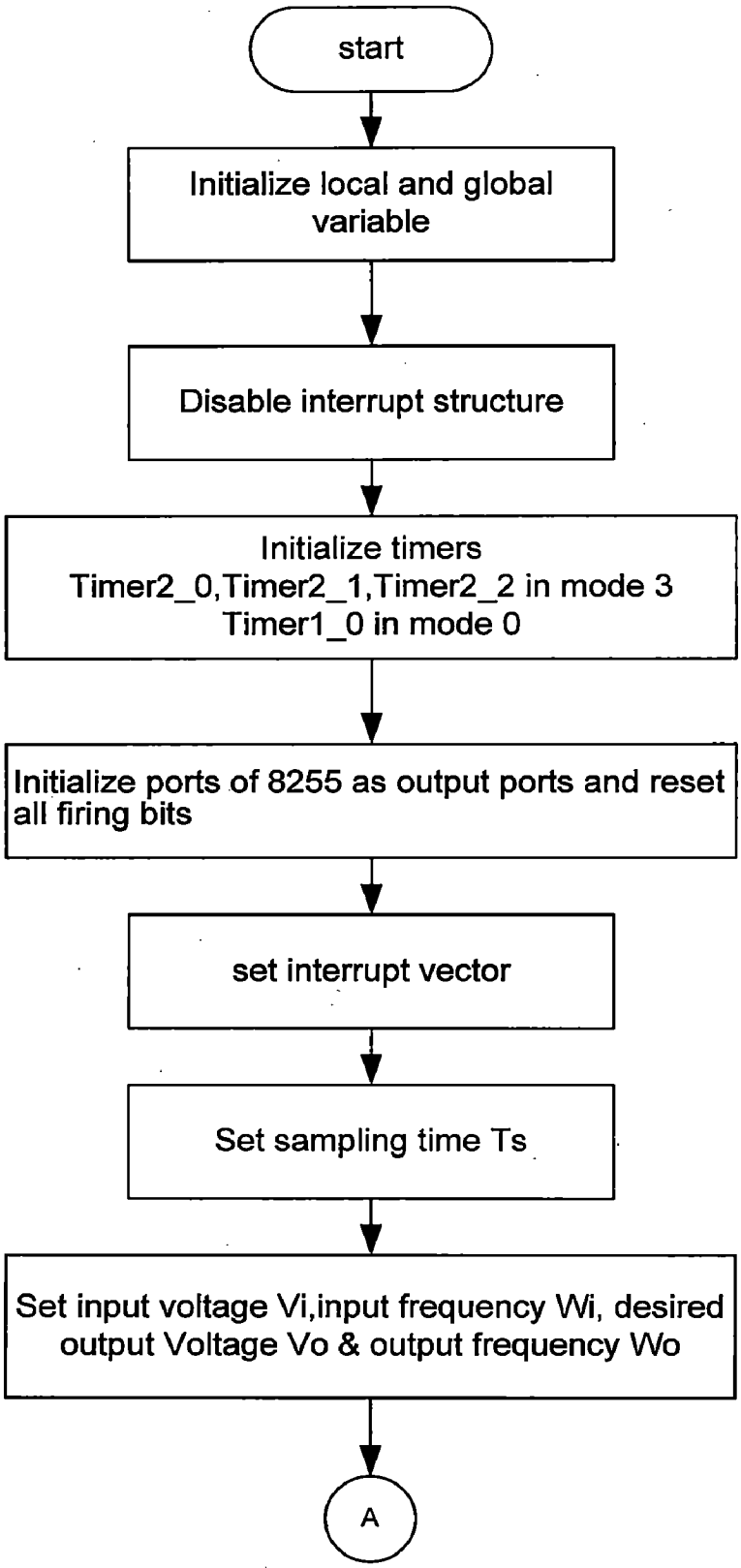

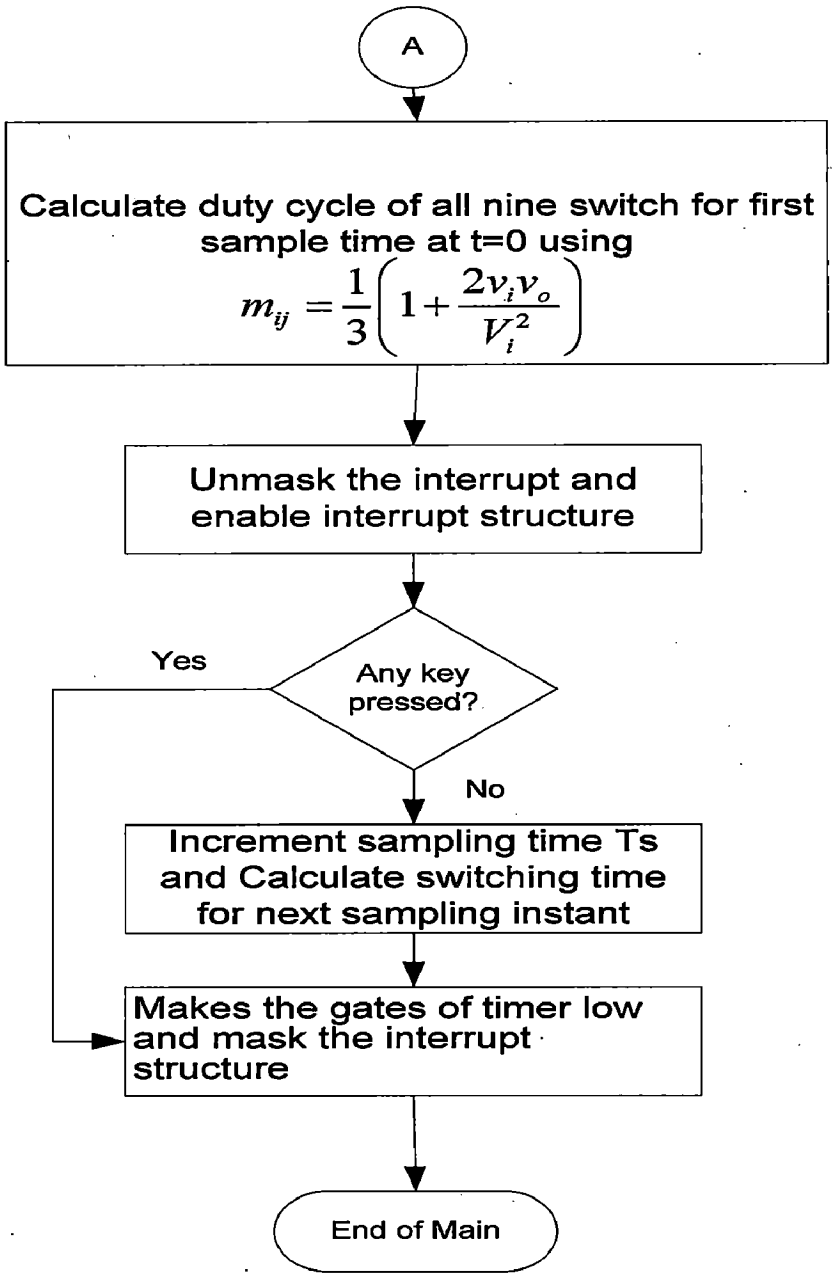
A
Calculate duty cycle of all nine switch for first sample time at t=0 using
$m_{ij} = \frac{1}{3}\left(1 + \frac{2v_i v_o}{V_i^2}\right)$
Unmask the interrupt and enable interrupt structure
Any key pressed?
Yes
No
Increment sampling time Ts and Calculate switching time for next sampling instant
Makes the gates of timer low and mask the interrupt structure
End of Main

ZC_ISR

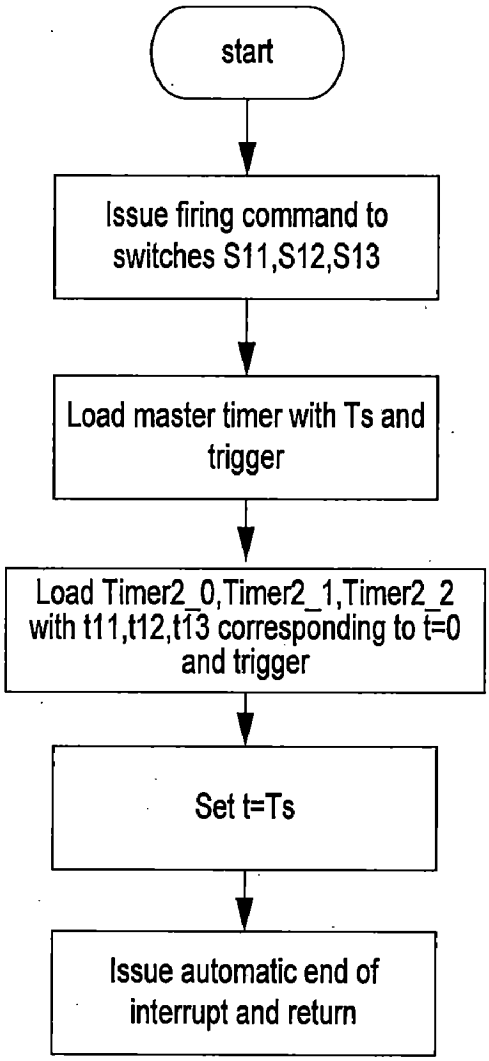
start
Issue firing command to switches S11,S12,S13
Load master timer with Ts and trigger
Load Timer2_0,Timer2_1,Timer2_2 with t11,t12,t13 corresponding to t=0 and trigger
Set t=Ts
Issue automatic end of interrupt and return

TS_ISR

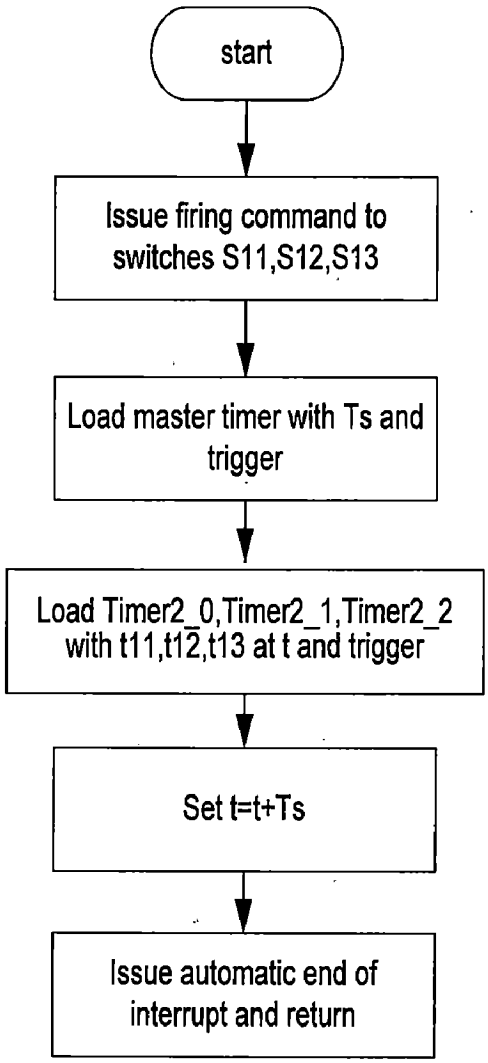
start
Issue firing command to switches S11,S12,S13
Load master timer with Ts and trigger
Load Timer2_0,Timer2_1,Timer2_2 with t11,t12,t13 at t and trigger
Set t=t+Ts
Issue automatic end of interrupt and return

PhaseA_ISR

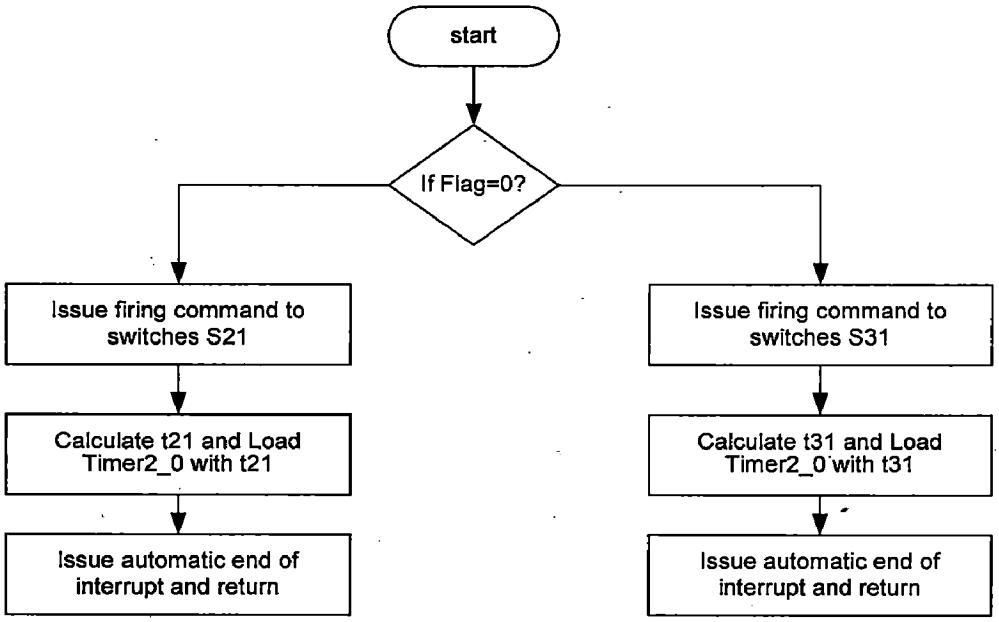

PhaseB_ISR

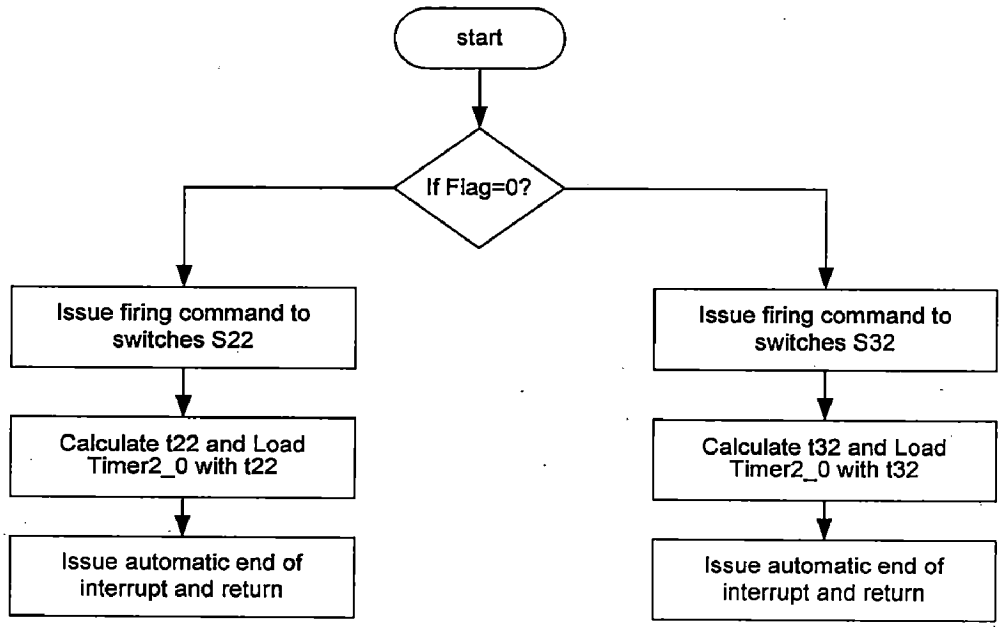

PhaseC_ISR

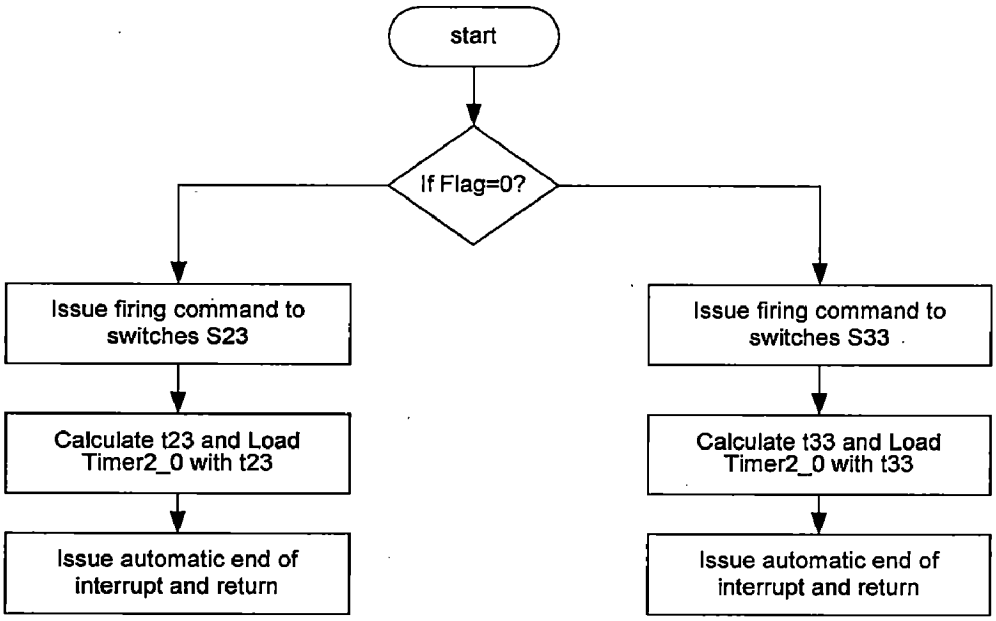

5.5 Conclusion

A prototype model of 3-phase to 3-phase matrix converter is developed in laboratory for experimental purpose. This chapter presents the hardware design, software flowcharts and PC interfacing for the prototype 3-phase to 3-phase matrix converter. The use PC along with interfacing cards for generating the firing pulses for matrix converter reduces the complexity of the system hardware.

Experimental Results

A prototype model of 3-phase to 3-phase Matrix converter is developed in the laboratory for experimentation purpose as shown in *fig 6.5* and *fig 6.6*. This experimental setup has been tested in open loop. The performance of 3-phase to 3-phase matrix converter with R-L load is investigated. This chapter presents the experimental results obtained from the prototype. Switching pulse and power circuit waveforms have been presented for different frequencies.

For real-time application, the venturini control method was implemented using a computer with interfacing card. An interface card is employed for the output and timing of the PWM gating signals to the converter. For venturini method four timers are used. Three of these are used for controlling the switches of output phases and fourth timer times out the sampling period Ts. The different parameters that have been selected for experimental purpose are; Input source voltage = 50V, Input frequency f_i= 50Hz, switching frequency f_s=2 kHz, voltage gain q=Vo/Vi=0.5, Load resistance R = 30Ω.

Fig 6.1 shows the master timer output Ts and Firing pulses for switch S11, S21 and S31 of the matrix converter at Switching frequency f_s = 2 kHz. In *Fig 6.1* Ts is sampling interval which is 0.5ms.

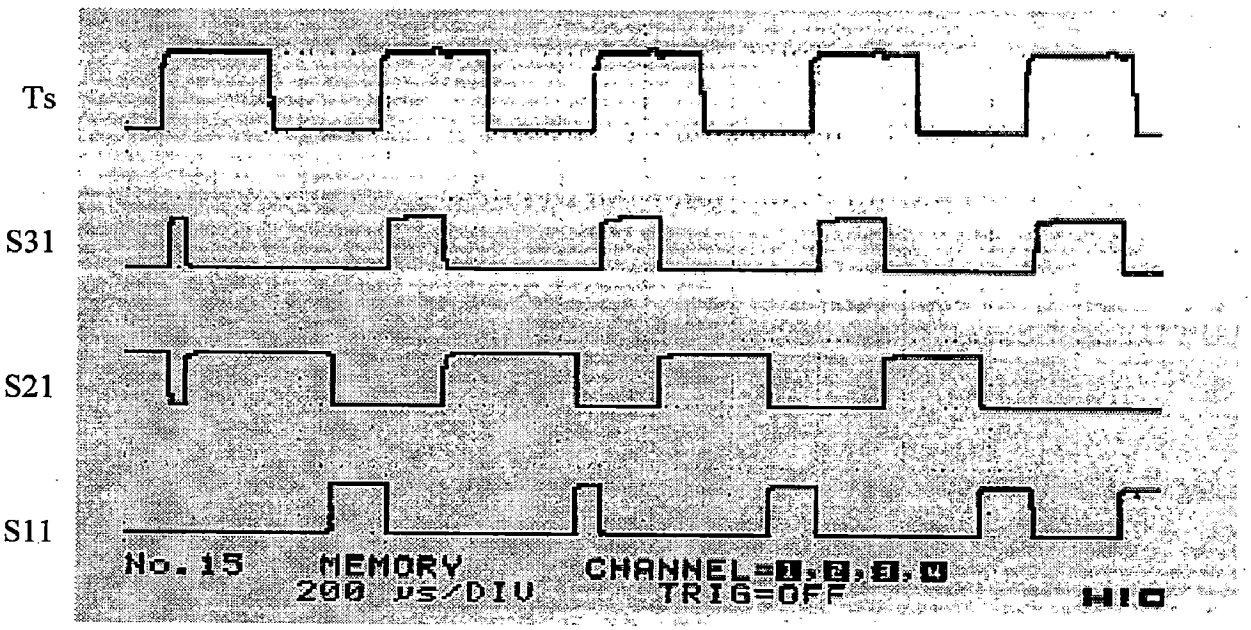

Figure 6.1: Firing Pulses to the Bidirectional switches S11, S21, S31.

Fig 6.2 shows the output phase voltage Van for output frequency fo=25Hz. Input source voltage = 50V, Input frequency f_i= 50Hz, switching frequency f_s=2 kHz, voltage gain q=Vo/Vi=0.5 (this means that the output voltage to 0.5×50V=25V and a frequency of 25 Hz), Load resistance R = 30Ω.

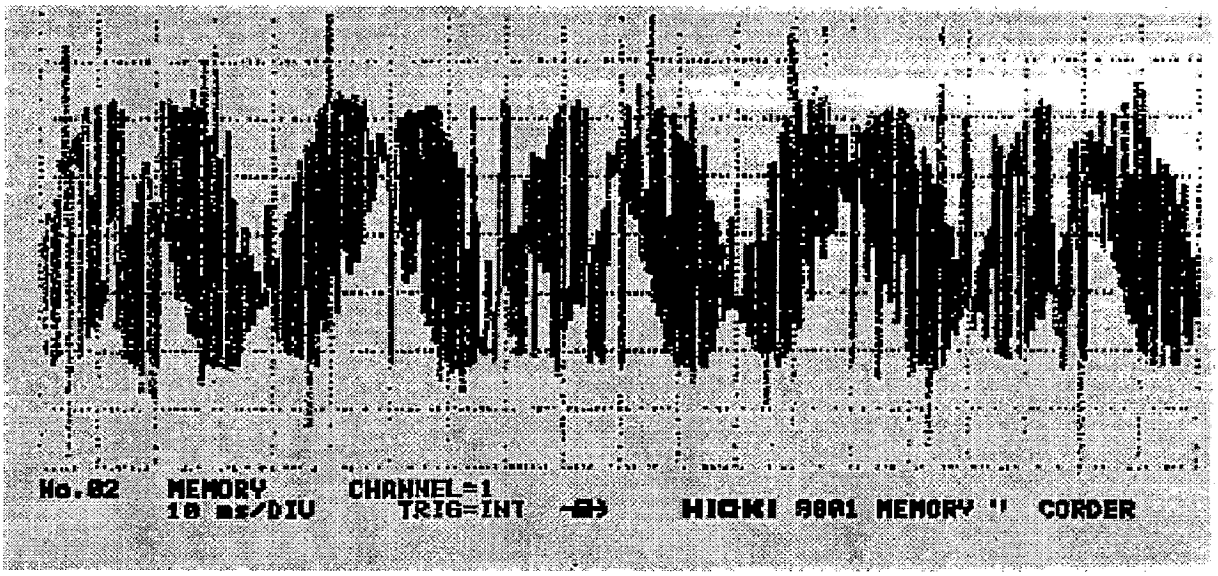

Figure 6.2: Output phase voltage V_{an} at a output frequency fo=25Hz

Fig 6.3 shows output phase voltage for one of the phase of 3-phase to 3-phase matrix converter with output frequency of 70 Hz and 50Hz respectively.

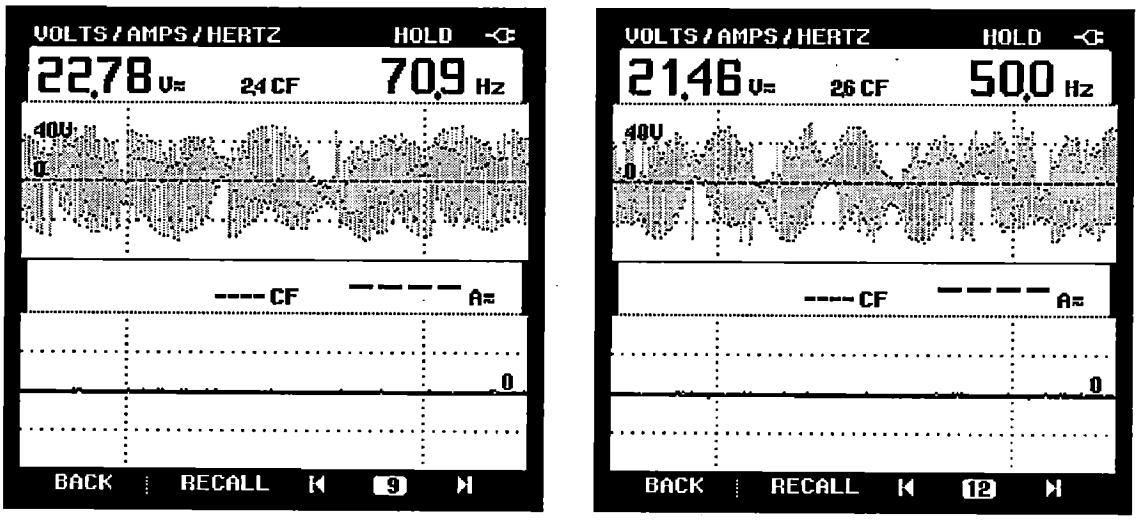

(a) (b)

Figure 6.3: (a) Output phase voltage V_{an} at a output frequency fo=70Hz
(b) Output phase voltage V_{an} at a output frequency fo=50Hz

Fig 6.4 shows output phase voltage for output frequency 25Hz and its FFT analysis. The different parameters that have been selected for experimental purpose are; Input source voltage = 50V, Input frequency f_i= 50Hz, switching frequency f_s=2 kHz, voltage gain q=Vo/Vi=0.5, Load resistance R = 30Ω. From result shown in *fig 6.4(b),* the THD is equal to 69.3% for the output phase voltage.

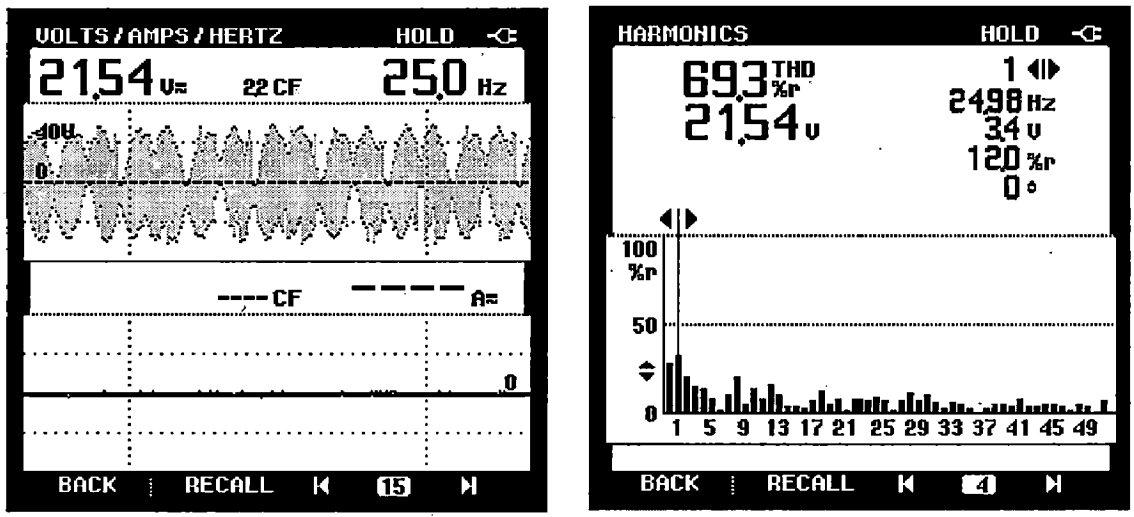

(a) (b)

Figure 6.4: (a) Output phase voltage V_{an} at output frequency fo=25Hz
(b) FFT analysis of output phase voltage at fo=25Hz

Conclusion

The experimental results are carried out on prototype 3-phase to 3-phase matrix converter developed in laboratory. Firing pulses for bi-directional switches and output phase voltage at different frequencies are presented. FFT analysis of output phase voltage gives THD to be 69.3% for output frequency of 25Hz.

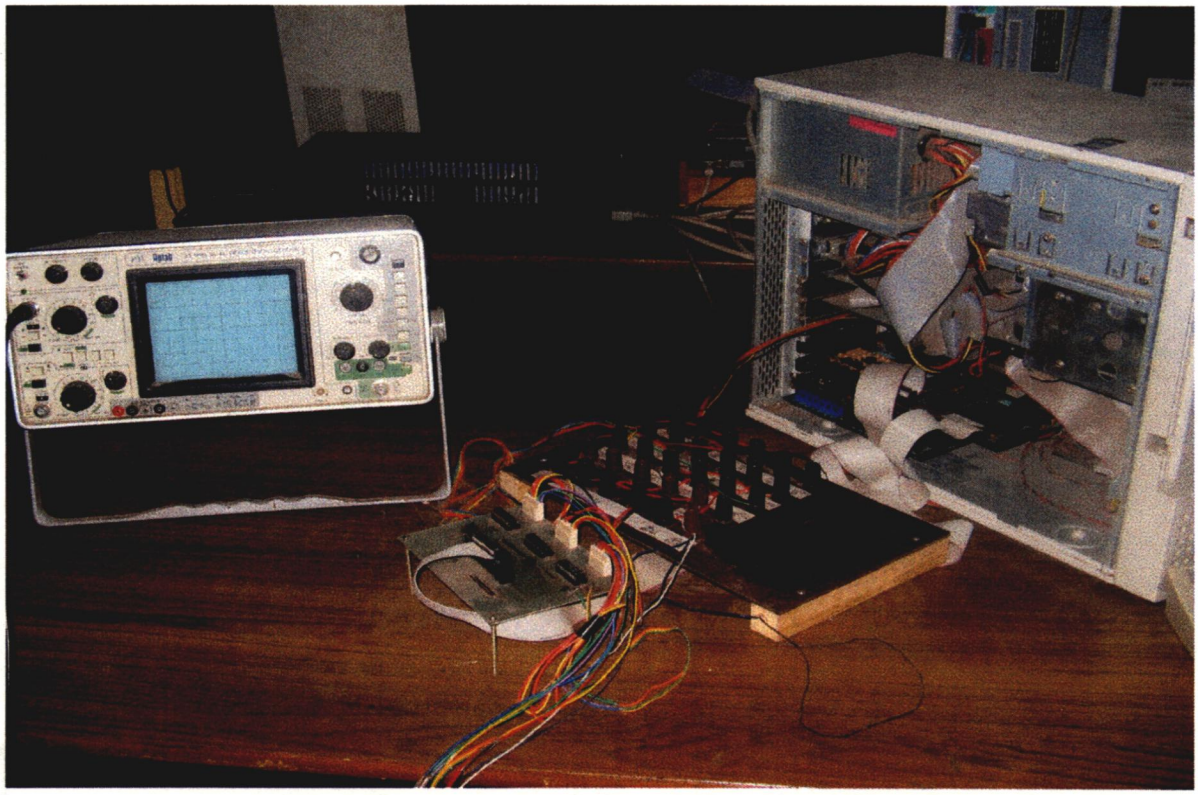

Figure 6.5: PC interfacing with hardware

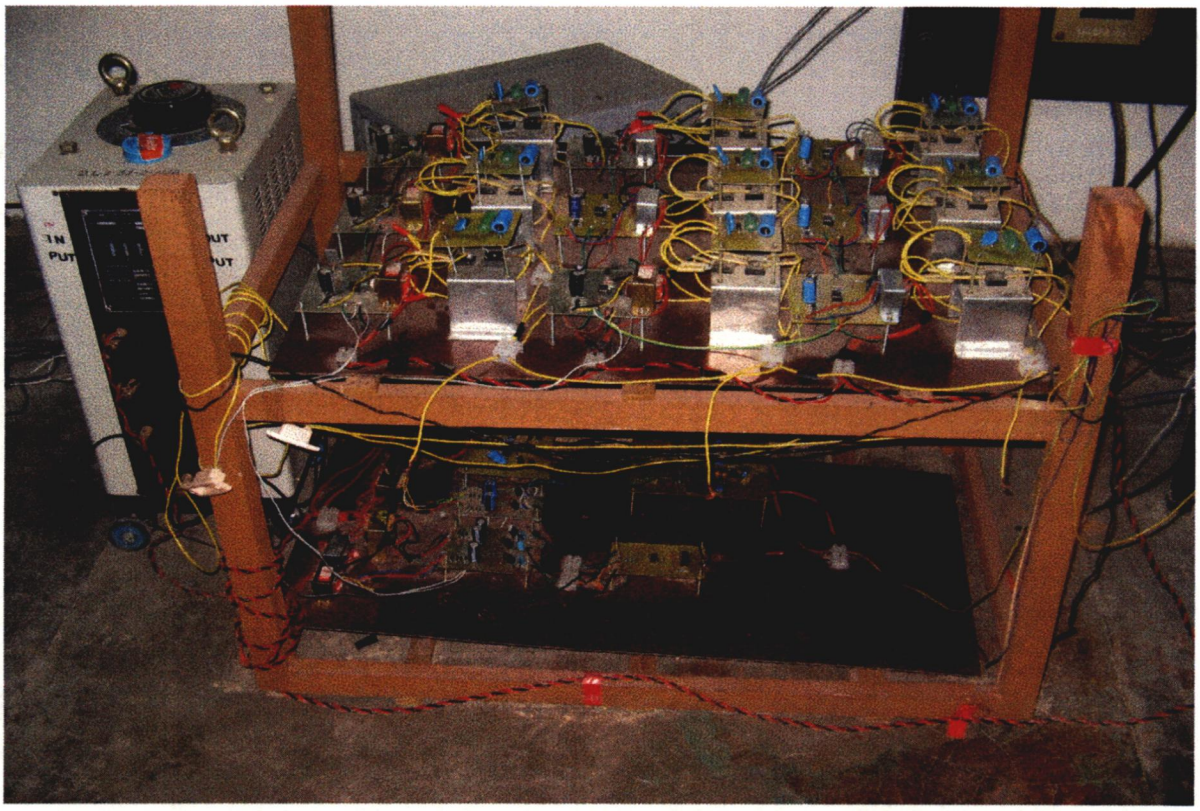

Figure 6.6: Module of 3-phase to 3-phase matrix converter

Conclusion and Future Scope

Conclusion

Matrix converter is a modern energy conversion device that has been developed over the last two decades. As the price of semiconductors continues to fall the matrix converter is also becoming a more attractive future alternative to the back-to-back inverter in applications where sinusoidal input currents or true bi-directional power flow are required. Furthermore, matrix converter allows a compact design due to the lack of dc-link capacitors for energy storage.

There are various control strategies used for matrix converter, some of these have been discussed. In this thesis Venturini modulation strategy has been implemented for 3-phase to 3-phase matrix converter and performance was tested using resistive load.

Simulation study is carried out on 3-phase to 3-phase matrix converter using venturini modulation method. Matrix converter loaded with R-L load. With switching frequency of 2 kHz and output frequency of 100Hz the THD of output phase voltage is 7.41% and output current THD is estimated to be 1.21% from FFT analysis. With same switching frequency and output frequency of 25Hz the THD to be equal to 4.49% for output phase voltage and output current THD is 1.55%. In simulation the output frequency is changed suddenly and results are recorded to know the performance. It was shown that THD of source current has reduced to 10.58% from 69% after inception input filter. It was also shown with the simulation results that the modulation algorithm provides a unity input displacement factor even when the load has an inductive characteristic.

Design of proposed Matrix converter is discussed and the performance is estimated in the simulation study. The next phase of thesis is to experimentally validate the results obtained from simulation study. The PWM control method was implemented on Pentium MMX Processor based PC using interfacing card. The software is written in 'C-Language'. The waveform of the PWM gating signals obtained experimentally has shown in present work. The power circuit waveforms have also been shown.

Future Scope

In this thesis, performance of the matrix converter was investigated using Venturini modulation method for different output frequencies. A conceptually different control technique based on the "fictitious dc link" idea was introduced by Rodriguez [5]. In this method, the switching is arranged so that each output line is switched between the most positive and most negative input lines using a pulse width modulation (PWM) technique, as conventionally used in standard voltage-source inverters (VSIs). This concept is also known as the "indirect transfer function" approach [6]. So same work can be implemented using space vector modulation (SVM). Huber *et al.* published the first of a series of papers [10]–[14] in which the principles of space-vector modulation (SPVM) were applied to the matrix converter modulation problem . These control techniques can be used to implement matrix converter.

The simultaneous commutation of controlled bidirectional switches used in matrix converters is very difficult to achieve without generating over current or over voltage spikes that can destroy the power semiconductors. This fact limited the practical implementation and negatively affected the interest in matrix converters. Fortunately, this major problem has been solved with the development of several multistep commutation strategies that allow safe operation of the switches. Burany [16] introduced the later-named "semi- soft current commutation" technique. So same work can be extended with such commutation techniques.

References

[1] L. Gyugi and B. Pelly, *Static Power Frequency Changers: Theory, Performance and Applications.* New York: Wiley, 1976

[2] V. Jones and B. Bose, "A frequency step-up cycloconverter using power transistors in inverse-series mode," *Int. J. Electron.*, vol. 41, no. 6, pp. 573–587, 1976.

[3] M. Venturini, ''A new sine wave in sine wave out conversion technique which eliminates reactive elements'', Proceedings of POWERCON 7, E3, pp. 1–15, 1980.

[4] M. Venturini and A. Alesina, ''The generalized transformer: A new bidirectional sinusoidal waveform frequency converter with continuously adjustable input power factor", Proceedings of IEEE PESC80, pp. 242–252, 1980.

[5] J. Rodriguez, ''A new control technique for AC–AC converters'', in proceedings of IFAC Control in Power Electronics and Electrical Drives Conference, Lausanne (Switzerland), 1983, pp. 203–208.

[6] J. Oyama, T. Higuchi, E. Yamada, T. Koga, and T. Lipo, "New control strategy for matrix converter," in *Proc. IEEE PESC'89*, 1989, pp. 360–367.

[7] P. D. Ziogas, S. I. Khan, and M. H. Rashid, "Some improved forced Commutated Cycloconverter structures," IEEE Trans. Ind. Electron., vol. 1A-21, pp. 1242-1253, Sept./Oct. 1985

[8] P. D. Ziogas, S. I. Khan, and M. H. Rashid, "Analysis and design of forced Commutated cycloconverter structures with improved transfer characteristics" IEEE Trans. Ind. Electron., vol. IE-33, pp.271-280, Aug.1986

[9] M. Braun and K. Hasse, "A direct frequency changer with control of input reactive power," in *Proc. IFAC Control in Power Electronics and Electrical Drives Conf.*, Lausanne, Switzerland, 1983, pp. 187–194

[10] L. Huber, D. Borojevic, and N. Burany, "Voltage space vector based PWM control of forced commutated cycloconvertors," in *Proc. IEEE IECON'89*, 1989, pp. 106– 111.

[11] L. Huber and D. Borojevic, "Space vector modulator for forced commutated cycloconverters," in *Conf. Rec. IEEE-IAS Annu. Meeting*, 1989, pp 871–876.

[12] L. Huber, D. Borojevic, and N. Burany, "Digital implementation of the space vector modulator for forced commutated cycloconverters," in Proc. IEE PEVD conf. 1990, pp. 63–65.

[13] L. Huber, D. Borojevic, and N. Burany, "Analysis design and implementation of the space-vector modulator for forced-commutated cycloconvertors," Proc. Inst. Elect. *Eng.*, pt. B, vol. 139, no. 2, pp. 103–113, Mar.1992.

[14] L. Huber and D. Borojevic, ''Space vector modulated three-phase to three-phase Matrix converter with input power factor correction", IEEE Transactions on IndustrialElectronics, 31, pp, 1234-1246,1995

[15] C. L. Neft and C. D. Schauder, "Theory and design of a 30-HP matrix converter," *IEEE Trans. Ind. Applicat.*, vol. 28, pp. 546–551, May/June 1992.

[16] N. Burany, "Safe control of four-quadrant switches," in *Conf. Rec.IEEE-IAS Annu. Meeting*, 1989, pp. 1190–1194.

[17] L. Empringham, P. Wheeler and J. Clare, "Intelligent commutation of matrix Converter bi-directional switch cells using novel gate drive techniques", in Proceeding of IEEE PESC98,1998, pp. 707-713.

[18] L.Empringham, P. Wheeler, and J. Clare,"Bi-directional switch current commutation for matrix converter applications," in *Proc. PEMatrix Converter Prague, Sept. 1998,* pp. 42–47.

[19] M. Ziegler and W. Hofmann, "Performance of a two steps commutated matrix converter for ac-variable-speed drives," in *Proc. EPE'99*, 1999, CD-ROM

[20] M. Ziegler and W. Hofmann, "Semi natural two steps commutation strategy for matrix converters," in *Proc. IEEE PESC'98*, 1998, pp.727–731.

[21] P. Nielsen, F. Blaabjerg, and J. Pedersen, "Novel solutions for protection of matrix converter to three phase induction machine," in *Conf. Rec. IEEE-IAS Annu. Meeting,*1997, pp. 1447–1454.

[22] J. Mahlein and M. Braun, "A matrix converter without diode clamped over-voltage protection," in *Proc. IPEMC 2000*, Beijing, China, pp. 817-822.

[23] C. Klumpner, P. Nielsen, I. Boldea, and F. Blaabjerg, "New steps toward a low cost power electronic building block for matrix converters," in *conf. Rec. IEEE IAS Annu. Meeting*, 2000, CD-ROM.

[24] J. Kang, H. Hara, A.M. Hava, E.Yamamoto, E. Watanabe, and T. Kume " The matrix converter drive performance under abnormal input voltage conditions" *IEEE Trans. on Power Electronics,* vol. 17, pp. 721-730, Sept. 2002.

[25] P. Wheeler, H. Zhang, and D. Grant, "A theoretical and practical consideration of optimized input filter design for a low loss matrix converter," in *Proc. IEE PEVD Conf.*, Sept. 1994, pp. 363–367.

[26] Watthanasarn C., Zhang L, D T W Liang, "Analysis and DSP based Implementation Modulation Algorithms for AC-AC Matrix converters", *Power Electronics Specialists Conference,1996. PESC '96 Record., 27th Annual IEEE* Volume 2, 23-27 June 1996 Page(s):1053-1058 Vol.2

[27] P.Wheeler, J.Rodri guez, J. Clare, L. Empringham and A. Weinstein, " Matrix Converters: A technology review", *IEEE Transactions on industrial Electronics,* 49, pp. 276-288,2002b.

[28] J.Rodriguez, E.silva, F.Blaabjerg, P.wheeler, " Matrix converter controlled with the Direct transfer function approach: analysis, modeling and simulation.", *International Journal of Electronics,* Vol. 92, No. 2, pp. 63-85, Feb. 2005.

List of Publications

[1] Mitesh Popat and Pramod Agrawal, "Matrix Converter: A New Breed of Converter", Proceedings of Second National Conference on Cutting Edge Technologies in Power Conversion and Industrial Drives, PCID-2006, at Bannari Amman Institute of Technology, Sathyamangalam, pp122-125,March 24 -25,2006.

[2] Mitesh Popat and Pramod Agrawal, " Modeling and Simulation of 3-phase to 3-phase Matrix Converter using Direct Transfer Function Approach", PRASTUTI-2006, at Banaras Hindu University, Varanasi, March 24 -26,2006.

Achievement

Secured First position in Electrical Engineering Category for the paper presentation contest PRASTUTI-2006 organized by IEE/IEEE/EES students' chapter of Institute of Technology, Banaras Hindu University, Varanasi.

Information of Data Acquisition Cards

The following two cards have been used for this application.

(1) **NUDAQ ACL-8316**: The ACL-8316 is a high performance, high speed, multi-function data acquisition card for IBM PC/XT/AT and compatible computers. The key features of this card are given below.

- 16 single-ended and 8 differential analog input channels
- An industrial standard 12-bit successive approximation converter (ADC574 or equivalent) to convert analog input. The maximum A/D sampling rate is 30 KHz in DMA mode.
- Switch selectable versatile analog input ranges.
  Bipolar: $\pm 1V, \pm 2V, \pm 5V, \pm 10V$
- Three A/D trigger modes: Software trigger
  Programmable pacer trigger
  External trigger pulse trigger
- The ability to transfer A/D converted data by program control interrupt handler routine, EOC interrupt, FIFI polling, FIFO or DMA transfer
- An INTEL 8253-5 Programmable Timer/Counter provides pacer output (trigger pulse) at the rate of 0.5 MHz to 35 minutes/pulse to the A/D. The timer time base is 2 MHz. One 16-bit counter channel is reserved for user configurable applications.
- Two 12-bit monolithic multiplying D/A output channels. An output range from 0 to ±10V can be created by using the onboard -10V reference
- 16 TTL compatible digital input, and 16 digital output channel.
- Auto scanning channel selection
- Up to 100KHz A/D sampling rates
- 3 independent programmable 16-bit down counter.

(2) **VYNITICS TIMER I/0 CARD:** The key features of this card are shown below.

- 48 programmable Input/Output using two 8255.
- Six channel of 16 Bit Timer/Counter.
- 8 optically isolated Input.
- 8 optically isolated Output.
- Jumper selectable I/0 addressing.
- Hardware clock selection for Timer/Counter.

Sample of Datasheets

International
IOR Rectifier

PD-9.512B

IRFP460

HEXFET® Power MOSFET

- Dynamic dv/dt Rating
- Repetitive Avalanche Rated
- Isolated Central Mounting Hole
- Fast Switching
- Ease of Paralleling
- Simple Drive Requirements

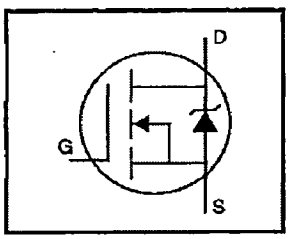

V_{DSS} = 500V

$R_{DS(on)}$ = 0.27Ω

I_D = 20A

Description

Third Generation HEXFETs from International Rectifier provide the designer with the best combination of fast switching, ruggedized device design, low on-resistance and cost-effectiveness.

The TO-247 package is preferred for commercial-industrial applications where higher power levels preclude the use of TO-220 devices. The TO-247 is similar but superior to the earlier TO-218 package because of its isolated mounting hole. It also provides greater creepage distance between pins to meet the requirements of most safety specifications.

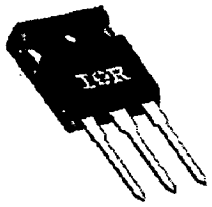

TO-247AC

DATA SHEETS

Absolute Maximum Ratings

	Parameter	Max.	Units
I_D @ T_C = 25°C	Continuous Drain Current, V_{GS} @ 10 V	20	A
I_D @ T_C = 100°C	Continuous Drain Current, V_{GS} @ 10 V	13	
I_{DM}	Pulsed Drain Current ①	80	
P_D @ T_C = 25°C	Power Dissipation	280	W
	Linear Derating Factor	2.2	W/°C
V_{GS}	Gate-to-Source Voltage	±20	V
E_{AS}	Single Pulse Avalanche Energy ②	960	mJ
I_{AR}	Avalanche Current ①	20	A
E_{AR}	Repetitive Avalanche Energy ①	28	mJ
dv/dt	Peak Diode Recovery dv/dt ③	3.5	V/ns
T_J T_{STG}	Operating Junction and Storage Temperature Range	-55 to +150	°C
	Soldering Temperature, for 10 seconds	300 (1.6mm from case)	
	Mounting Torque, 6-32 or M3 screw	10 lbf•in (1.1 N•m)	

Thermal Resistance

	Parameter	Min.	Typ.	Max.	Units
$R_{\theta JC}$	Junction-to-Case	—	—	0.45	°C/W
$R_{\theta CS}$	Case-to-Sink, Flat, Greased Surface	—	0.24	—	
$R_{\theta JA}$	Junction-to-Ambient	—	—	40	

DC COMPONENTS CO., LTD.

RECTIFIER SPECIALISTS

BR1005 THRU BR1010

TECHNICAL SPECIFICATIONS OF SINGLE-PHASE SILICON BRIDGE RECTIFIER

VOLTAGE RANGE - 50 to 1000 Volts *CURRENT - 10 Amperes*

FEATURES

* Surge overload rating: 200 Amperes peak
* Low forward voltage drop

MECHANICAL DATA

* Case: Molded plastic
* Epoxy: UL 94V-0 rate flame retardant
* Lead: MIL-STD-202, Method 208 guaranteed
* Polarity: Symbols molded or marked on body
* Mounting position: Any
* Weight: 6.9 grams

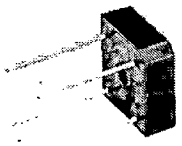

BR-8/10

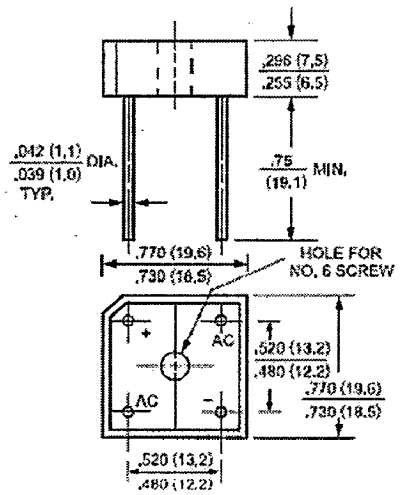

Dimensions in inches and (millimeters)

MAXIMUM RATINGS AND ELECTRICAL CHARACTERISTICS

Ratings at 25 °C ambient temperature unless otherwise specified.
Single phase, half wave, 60 Hz, resistive or inductive load.
For capacitive load, derate current by 20%.

		SYMBOL	BR1005	BR101	BR102	BR104	BR106	BR108	BR1010	UNITS
Maximum Recurrent Peak Reverse Voltage		V_{RRM}	50	100	200	400	600	800	1000	Volts
Maximum RMS Voltage		V_{RMS}	35	70	140	280	420	560	700	Volts
Maximum DC Blocking Voltage		V_{DC}	50	100	200	400	600	800	1000	Volts
Maximum Average Forward Rectified Output Current at Tc = 50°C		I_O	10							Amps
Peak Forward Surge Current 8.3 ms single half sine-wave superimposed on rated load (JEDEC Method)		I_{FSM}	200							Amps
Maximum Forward Voltage Drop per element at 5.0A DC		V_F	1.1							Volts
Maximum DC Reverse Current at Rated DC Blocking Voltage per element	@TA = 25°C	I_R	10							uAmps
	@Tc = 100°C		500							
I^2t Rating for Fusing (t<8.3ms)		I^2t	166							A^2Sec
Typical Junction Capacitance (Note1)		C_J	200							pF
Typical Thermal Resistance (Note 2)		RθJA	21							°C/W
Operating Temperature Range		T_J	-55 to + 125							°C
Storage Temperature Range		T_{STG}	-55 to + 150							°C

NOTES : 1.Measured at 1 MHz and applied reverse voltage of 4.0 volts

2. Thermal Resistance from Junction to Ambient and from junction to lead mounted on P.C.B. with 0.5 x 0.5" (13x13mm) copper pads.